

**INVESTIGATION OF COPPER WIRE-MEDIATED  
CONTROLLED/LIVING RADICAL POLYMERIZATION**

**Development of Greener Solvent Systems  
&  
Grafting *to* Cellulose via Thio-Bromo Click Reaction**

By

Oxana Shibaeva

A thesis submitted to the Graduate Program in Chemical Engineering  
in conformity with the requirements for the  
Degree of Master of Applied Science

Queen's University  
Kingston, Ontario, Canada

September, 2014

Copyright © Oxana Shibaeva, 2014

## Abstract

Copper wire mediated controlled living radical polymerization (CLRP) is a powerful tool that provides numerous opportunities for the development of new materials. It requires low catalyst loading and mild reaction conditions, but does involve use of organic solvents. There is a need for greener solvent systems to replace traditional volatile organic solvents without detrimentally affecting polymerization. The effects of greener solvents on control over polymerization and polymer characteristics were investigated with polyethylene glycol (PEG) and polypropylene glycol (PPG) for copper wire mediated CLRP. Polymerization of low molecular weight poly(methyl acrylate) (PMA) with bromine chain-end functionality was initiated by ethyl 2-bromoisobutyrate (EBiB). Two effective green solvent systems were established, 75-25 PEG-Ethanol and 75-25 PPG-Ethanol. Both provide good control over polymerization, livingness, narrow dispersity ( $\sim 1.1$ ), high retention of chain-end functionality ( $>90\%$ ), and can be recycled, which should be considered for an industrial scale implementation.

Furthermore, utilization of a bromine chain-end functionality of synthetic homopolymer (PMA) synthesized via copper wire mediated CLRP with EBiB was evaluated for grafting *to* cellulose substrates, microcrystalline cellulose and cellulose acetate. Cellulose was functionalized with thiol groups using ring opening reaction with ethylene sulfide. The grafting via thio-bromo click reaction was investigated, where grafting of EBiB was performed first to evaluate the reaction and then repeated with PMA. One-pot and two-pot reactions were performed. In one-pot reaction, functionalization of cellulose and grafting were performed in the same reaction solution to avoid exposure of thiols to oxygen. In a two-pot reaction, functionalized cellulose was purified before grafting. Nuclear Magnetic Resonance analysis showed that grafting of EBiB had low degree of substitution (DS) of 0.026 (1 unit per 39 AGU units), whereas grafting of polymer chains *to* cellulose substrate was not successful.

## **Co-Authorship**

This research was conducted independently by the author, under the supervision of Dr. Michael Cunningham and Dr. Pascale Champagne, both of whom reviewed this thesis.

## Acknowledgements

I would like to express my sincere gratitude to my research supervisors, Dr. Michael F. Cunningham and Dr. Pascale Champagne, for their continuing support, motivation, guidance and for providing opportunities to develop and learn. I am grateful to Queen's University, and many staff members of the Department of Chemistry, Chemical Engineering and Civil Engineering Departments. Particularly, I would like to thank James McLellan, Lynn O'Malley, Barb Lawson, Steven Hodgson, Kelly Sedore, Laurie Phillips, Kalam Mir, Dr. Robin Hutchinson, Dr. Carlos Escobedo, Dr. Philip Jessop, Dr. Ralph Whitney, Dawn Free, and Colette Steer for their advice and hard work in contributing to an environment I was proud to be a part of. I would like to acknowledge the financial support of Queen's University, Canada Research Chairs, Ontario Research Chair in Green Chemistry and Engineering (Dr. Michael F. Cunningham), Early Researcher Award and Canada Research Chair in Bioresources Engineering (Dr. Pascale Champagne,) Ontario Ministry of the Environment, and Ministry of Research and Innovation.

I thank many student colleagues for creating a stimulating and warm social atmosphere. I am grateful to Calista Preusser, Weiwei Yang, Jason Donaldson, Kevin Payne, Eric Peterson, Eric Edwards, Jennifer Li, Sean George, Stuart Young, Stu Bacon, Praphulla Tewary, Vitaliy Kapishon, Lydia Fütterer, Rachel Champagne Hartley, Abbas Rezaei Shirin-Abadi, Ali Darabi, Ryan Roeder and Hai-Dong Wang for their academic assistance and stretching my mind with lively discussions. I would like to thank my close friend and a fumehood mate, Haixia Jin, for sharing the tough days, the fun days and the vastly complex graduate life emotions along the way. I am truly lucky to have met so many incredible people.

Through many extracurricular activities in the last two years I have met amazing people who inspired me with their creativity and interdisciplinary knowledge. I am thankful to all WatIF creators and co-volunteers, particularly Dr. Geoffrey Hall, Dr. Kent S. Novakowski, Donya Danesh, Sarah Thompson, Dan Lamhonwah, Alexandra Elias, Erin Murphy-Mills, Rudy Schueder, MacKenzie Waller, and Gillian

Mullan-Boudreau. I would also like to thank everyone who is involved in building NESSE, specifically Dr. Jennifer Dodson, Dr. Cliff Cross, Laura Hoch, ACS Green Chemistry Institute and Dr. Mary Kirchhoff.

I would like to thank my parents for all of their support throughout my life, without them I would not be here. Finally, I am grateful to my wonderful husband, best friend and soul mate, Sergei Shibaev, for endless love, encouragement and inspiration, for giving me wings and showing that anything is possible.

*“Look up at the stars and not down at your feet. Try to make sense of what you see, and wonder about what makes the universe exist. Be curious.”*

*— Stephen Hawking*

*“Our population and our use of the finite resources of planet Earth are growing exponentially, along with our technical ability to change the environment for good or ill.”*

*— Stephen Hawking*

*“Learn from yesterday, live for today, hope for tomorrow. The important thing is to not stop questioning.”*

*— Albert Einstein*

*“I started my life with a single absolute: that the world was mine to shape in the image of my highest values and never to be given up to a lesser standard, no matter how long or hard the struggle.”*

*— Ayn Rand, “Atlas Shrugged”*

## Table of Contents

Abstract.....	ii
Co-Authorship.....	iii
Acknowledgements.....	iv
List of Figures.....	viii
List of Tables.....	xi
List of Abbreviations.....	xii
List of Symbols.....	xiii
Chapter 1 . Introduction.....	1
1.1 Background Information.....	1
1.2 Thesis Objectives.....	2
1.3 Thesis Outline.....	3
Chapter 2 . Literature Review: Effect of Solvent Selection on Copper Wire Mediated Controlled/Living Radical Polymerization.....	4
2.1 Introduction.....	4
2.2 Controlled/Living Radical Polymerization.....	4
2.2.1 ATRP Kinetic Mechanism.....	5
2.2.2 SET-LRP Mechanistic Assumptions.....	6
2.2.3 SARA-ATRP Mechanistic Assumptions.....	8
2.3 Solvent effects on copper wire mediated CLRP.....	8
2.3.1 Solvent effects on SET-LRP.....	9
2.3.2 Solvent effect on SARA-ATRP.....	17
2.4 Conclusion.....	22
Chapter 3 . Development of Greener Solvent Systems for Copper Wire Mediated Controlled/Living Radical Polymerization of Methyl Acrylate.....	24
Abstract.....	24
3.1 Introduction.....	24
3.2 Experimental.....	28
3.2.1 Materials.....	28
3.2.2 Characterization.....	29
3.2.3 Typical polymerization procedure.....	29
3.3 Results and Discussion.....	30

3.3.1 Polymerization of MA in DMSO.....	32
3.3.2 Polymerization of MA in PEG and its binary mixtures .....	36
3.3.2.1 Polymerization of MA in PEG-DMSO mixtures .....	39
3.3.2.2 Polymerization of MA in PEG-Ethanol mixtures .....	42
3.3.2.3 5K, 10K and 25K PMA synthesized in 50% 90-10 PEG-Ethanol system.....	43
3.3.2.4 5K, 10K and 25K PMA synthesized in 33% 75-25 PEG-Ethanol system.....	45
3.3.3 Polymerization of MA in PPG and its binary mixtures .....	47
3.3.3.1 Polymerization of MA in PPG-DMSO mixtures .....	50
3.3.3.2 Polymerization of MA in 33% 75-25 PPG-Ethanol mixtures.....	52
3.4 Conclusion & Recommendations.....	53
Chapter 4 . ‘Grafting- <i>to</i> ’ Cellulose using Thio-Bromo Click Reaction by Utilizing Bromine Chain-End Functionality of PMA Synthesized via Copper Wire Mediated Controlled Living Radical Polymerization .....	56
Abstract.....	56
4.1 Introduction.....	56
4.2 Experimental .....	61
4.2.1 Materials .....	61
4.2.2 Characterization .....	61
4.2.1 Procedure .....	62
4.2.1.1 Synthesis of PMA grafts with bromine chain-end functionality.....	62
4.2.1.2 Example of one-pot ‘Grafting to’ procedure.....	63
4.2.1.3 Example of the procedure of the ‘Grafting to’ via a two-pot process.....	64
4.3 Results and Discussion .....	64
4.4 Conclusions & Recommendations .....	78
Chapter 5 . Conclusion & Recommendations .....	80

## List of Figures

Figure 2-1. ATRP mechanism <sup>17</sup> .....	6
Figure 2-2. Mechanism of SET-LRP <sup>5</sup> .....	7
Figure 2-3. Mechanism of SARA-ATRP <sup>16</sup> .....	8
Figure 2-4. PMA polymerization in mixtures of DMSO (■) and acetonitrile (●) <sup>25</sup> .....	12
Figure 2-5. Measured and Predicted (represented by the line) Log ( $K_{ATRP}$ ) values. <sup>19</sup> .....	19
Figure 2-6. a) log $k_{act}$ vs. $\pi^*$ b) log $k_{act}$ calculated vs. experimental <sup>34</sup> .....	19
Figure 3-1. Kamlet-Taft plot for common organic aprotic solvents <sup>9</sup> .....	26
Figure 3-2. Kamlet-Taft plot of select greener solvents <sup>9</sup> .....	26
Figure 3-3. 400Hz <sup>1</sup> H NMR spectra (CDCl <sub>3</sub> ) of PMA from polymerization catalyzed with copper wire/Me <sub>6</sub> -TREN and initiated with EBiB used for monomer conversion measurement .....	31
Figure 3-4. 400Hz <sup>1</sup> H NMR spectrum (CDCl <sub>3</sub> ) of PMA from polymerization catalyzed with copper wire/Me <sub>6</sub> -TREN and initiated with EBiB. ....	32
Figure 3-5. Polymerization mixtures of MA [50]:[1]:[0.2] in DMSO 33% v/v (84) and 50% v/v (85) at 30°C.....	33
Figure 3-6. Conversion and normalized conversion vs. time for MA [50]:[1]:[0.2] polymerized in DMSO, 33% v/v (84) and 50% v/v (85), at 30°C .....	33
Figure 3-7. Evolution of a) number-average molecular weight ( $M_n$ , filled symbols) and dispersity ( $M_w/M_n$ , open symbols) vs. theoretical molecular weight ( $M_{th}$ ), and b) Molecular weight distribution of PMA [50]:[1]:[0.2] synthesized in DMSO, 33% v/v (84) and 50% v/v (85), at 30°C.....	34
Figure 3-8. Conversion and normalized conversion vs. time for MA [50]:[1]:[0.2] polymerized in DMSO, 33% v/v, at 30°C (84) and 50°C (47) .....	36
Figure 3-9. Polymerization mixtures of MA [50]:[1]:[0.2] in PEG 33% v/v (96) and 50% v/v (75) at 30°C .....	37
Figure 3-10. Conversion and normalized conversion vs. time for MA [50]:[1]:[0.2] polymerized in PEG, 33% v/v (96) and 50% v/v (75), at 30°C .....	37
Figure 3-11. Evolution of number-average molecular weight ( $M_n$ , filled symbols) and dispersity ( $M_w/M_n$ , open symbols) vs. theoretical molecular weight ( $M_{th}$ ) of PMA [50]:[1]:[0.2] synthesized in PEG, 33% v/v (96) and 50% v/v (75), at 30°C .....	38
Figure 3-12. Molecular weight distribution of PMA [50]:[1]:[0.2] synthesized in PEG, 33% v/v (96) and 50% v/v (75), at 30°C.....	38



Figure 3-13. Normalized conversion vs. time for MA [50]:[1]:[0.2] polymerized in binary mixtures of PEG-DMSO, 33% v/v (70, 88) and 50% v/v (71, 89), at 30°C.....	40
Figure 3-14 Dispersity ( $M_w/M_n$ ) vs. conversion for PMA [50]:[1]:[0.2] synthesized in binary mixtures of PEG-DMSO, 33% v/v (70, 88) and 50% v/v (71, 89), at 30°C.....	40
Figure 3-15. Normalized conversion vs. time for MA polymerized in PEG based solvent systems, 33% v/v, at 30°C (96, 70) and 50°C (41, 45, 46) .....	41
Figure 3-16. Polymerization mixtures of MA in PEG-Ethanol 33% v/v (81, 86) and 50% v/v (83, 87).....	42
Figure 3-17. Normalized conversion vs. time for MA [50]:[1]:[0.2] polymerized in binary mixtures of PEG-Ethanol, 33% v/v (81, 86) and 50% v/v (83, 87), at 30°C.....	43
Figure 3-18. Molecular weight distribution of 5K (104), 10K (105) and 25K (106) PMA synthesized in 50% 90-10 PEG-Ethanol, at 30°C.....	44
Figure 3-19. Polymerization mixtures of MA in 50% 90-10 PEG-Ethanol at 30°C; 5K(104), 10K(105) and 25K(106).....	44
Figure 3-20. Conversion and normalized conversion vs. time for 5K (104), 10K(105) and 25K(106) PMA synthesized in 50% 90-10 PEG-Ethanol at 30°C .....	45
Figure 3-21. Polymerization mixtures of MA in 33% 75-25PEG-Ethanol, 5K(109), 10K(110) and 25K(111).....	46
Figure 3-22. Conversion and normalized conversion vs. time for 5K(109), 10K(110) and 25K(111) PMA synthesized in 33% 75-25 PEG-Ethanol at 30°C .....	46
Figure 3-23. Molecular weight distribution of 5K (109), 10K (110) and 25K (111) PMA synthesized in 33% 75-25 PEG-Ethanol, at 30°C.....	47
Figure 3-24. Polymerization mixtures of MA [50]:[1]:[0.2] in PPG, 33% v/v (92) and 50% v/v (93), at 30°C.....	48
Figure 3-25. Molecular weight distribution of PMA [50]:[1]:[0.2] synthesized in PPG, 33% v/v (92) and 50% v/v (93), at 30°C.....	48
Figure 3-26. Conversion and normalized conversion vs. time for MA [50]:[1]:[0.2] polymerized in PPG, 33% v/v (92) and 50% v/v (93), at 30°C.....	49
Figure 3-27. Expanded view of Figure 3-26, normalized conversion vs. time MA [50]:[1]:[0.2] polymerized in PPG, 33% v/v (92) and 50% v/v (93), at 30°C.....	49
Figure 3-28. Polymerization mixtures of MA in PPG-DMSO systems: 33% v/v 75-25 (94), 50% v/v 75-25 (95), 50% v/v 90-10 (112), and 50% v/v 95-5 (103) .....	50
Figure 3-29. Molecular weight distribution of PMA synthesized in PPG-DMSO systems: 33% v/v 75-25 (94), 50% v/v 75-25 (95), 50% v/v 90-10 (112), and 50% v/v 95-5 (103).....	51

Figure 3-30. Normalized conversion vs. time for MA polymerized at 30°C in PPG-DMSO systems: 33% v/v 75-25 (94), 50% v/v 75-25 (95), and 50% v/v 90-10 (112).....	51
Figure 3-31. Polymerization mixtures of 4K (97) and 10K (99) PMA in 33% v/v 75-25PPG-Ethanol.....	52
Figure 3-32. Molecular weight distribution of 4K (97) and 10K (99) PMA synthesized in 33% v/v 75-25 PPG-Ethanol at 30°C.....	52
Figure 3-33. Conversion and normalized conversion vs. time for 4K (97) and 10K (99) PMA synthesized in 33% v/v 75-25 PPG-Ethanol at 30°C.....	53
Figure 4-1. Cellulose Structure .....	57
Figure 4-2. Cellulose Acetate.....	57
Figure 4-3. Grafting <i>from</i> and Grafting <i>to</i> scheme .....	58
Figure 4-4. Grafting <i>to</i> scheme .....	60
Figure 4-5. Molecular weight distribution of PMA grafts during synthesis and of the final polymer.....	65
Figure 4-6. Chain-end functionality determination using 400Hz <sup>1</sup> H NMR of PMA grafts synthesized via CLRP catalyzed by wire copper wire/Me <sub>6</sub> -TREN and initiated with EBiB .....	66
Figure 4-7. An examples of <sup>1</sup> H NMR of unmodified Cellulose Acetate in acetone-d <sub>6</sub> .....	67
Figure 4-8. An example of HSQC NMR of unmodified Cellulose Acetate in acetone-d <sub>6</sub> .....	67
Figure 4-9. <sup>1</sup> H NMR of Cellulose Acetate grafted with EBiB (111-1) in acetone-d <sub>6</sub> .....	69
Figure 4-10. HSQC NMR of Cellulose Acetate grafted with EBiB (111-1) in acetone-d <sub>6</sub> .....	69
Figure 4-11. Molecular weight distribution of PMA following the grafting procedure <i>to</i> CA.....	72
Figure 4-12. HSQC NMR of PMA grafts in acetone-d <sub>6</sub> synthesized via CLRP catalyzed by wire copper wire/Me <sub>6</sub> -TREN and initiated with EBiB .....	73
Figure 4-13. <sup>1</sup> H-NMR of 102-3 PMA analysis following the grafting <i>to</i> cellulose acetate procedure.....	74
Figure 4-14. HSQC NMR of 102-3 PMA analysis following the grafting <i>to</i> cellulose acetate procedure.	74
Figure 4-15. Molecular weight distribution of PMA following the grafting procedure <i>to</i> MCC .....	77

## List of Tables

Table 2-1. Values of $K_{dis}$ measured in the absence of complexing agents in different solvents <sup>21</sup> .....	11
Table 2-2. SET-LRP of MA in binary mixtures of organic solvents at 25°C <sup>22</sup> , $[M]_0/[I]/[L]=222/1/0.1$ .....	13
Table 2-3. Normalized Dimroth-Reichardt solvent parameters, <b>ETN</b> , of select solvents <sup>22</sup> .....	14
Table 3-1. Polymerization of MA [50]:[1]:[0.2] in DMSO, 33% v/v (84) and 50% v/v (85), at 30°C.....	33
Table 3-2. Effect of increased temperature on polymerization of MA [50]:[1]:[0.2] in DMSO, 33% v/v, at 30°C (84) and 50°C (47).....	35
Table 3-3. Polymerization of MA [50]:[1]:[0.2] in PEG, 33% v/v (96) and 50% v/v (75), at 30°C.....	36
Table 3-4. Polymerization of MA [50]:[1]:[0.2] in binary PEG-DMSO mixtures, 33% v/v (70, 88) and 50% v/v (71, 89), at 30°C.....	39
Table 3-5. Effect of temperature increase on polymerization of MA in PEG based solvent systems .....	41
Table 3-6. Polymerization of MA [50]:[1]:[0.2] in binary PEG-Ethanol mixtures, 33%v/v (81, 86) and 50%v/v (83, 87), at 30°C.....	42
Table 3-7. Synthesis of 5K (104), 10K (105) and 25K (106) PMA in 50% 90-10 PEG-Ethanol mixtures, at 30°C.....	43
Table 3-8. Synthesis of 5K (109), 10K (110) and 25K (111) PMA in 33% 75-25 PEG-Ethanol mixtures, and 25K in pure PEG at 30°C .....	46
Table 3-9. Polymerization of MA [50]:[1]:[0.2] in PPG, 33% v/v (92) and 50% v/v (93) at 30°C.....	48
Table 3-10. Polymerization of MA in binary PPG-DMSO mixtures, 33% v/v (94) and 50% v/v (95, 112, 103), at 30°C .....	50
Table 3-11. Synthesis of 4K (97) and 10K (99) PMA in 33% 75-25 PPG-Ethanol mixtures, at 30°C.....	52
Table 4-1. PMA grafts characteristics.....	65
Table 4-2. List of experimental conditions of the grafting <i>to</i> cellulose acetate experiments.....	70
Table 4-3. Gravimetric analysis of cellulose acetate and PMA following the grafting <i>to</i> procedure .....	71
Table 4-4. Results of GPC and NMR analysis of PMA following the grafting procedure <i>to</i> CA .....	71
Table 4-5. List of experimental conditions of grafting <i>to</i> microcrystalline cellulose .....	75
Table 4-6. Gravimetric analysis of MCC and PMA following the grafting <i>to</i> procedure .....	76
Table 4-7. Results of GPC and NMR analysis of PMA following the grafting procedure <i>to</i> MCC.....	76

## List of Abbreviations

AGU	Anhydroglucose unit
ATRP	Atom transfer radical polymerization
ARGET	Activator regenerated by electron transfer
CELL	Cellulose
CA	Cellulose acetate
$\text{CDCl}_3$	Chloroform-d
CLRP	Controlled living radical polymerization
CRT	Catalytic radical termination
DMAC	Dimethylacetamide
DMF	N,N-Dimethyl formamide
DMSO	Dimethyl sulfoxide
DP	Degree of polymerization
DS	Degree of substitution
EBiB	Ethyl $\alpha$ -bromoisobutyrate
EC	Ethylene carbonate
ES	Ethylene sulfide
GPC	Gel permeation chromatography
HSQC	Heteronuclear single quantum coherence
ICAR-ATRP	Initiators for continuous activator regeneration ATRP
IE	Initiator efficiency
ISSET	Inner-sphere electron transfer
MA	Methyl acrylate
MAA	Methacrylic acid
MCC	Microcrystalline cellulose
MeOH	Methanol
$\text{Me}_6\text{-TREN}$	Tris[2-(dimethylamino)ethyl] amine
MMA	Methyl methacrylate
NMR	Nuclear magnetic resonance
NMP	N-Methyl-2-pyrrolidone
OSET	Outer-sphere electron transfer
$\bar{D}$	Dispersity, $M_w/M_n$
PEG	Polyethylene glycol
PMA	Poly(methyl acrylate)
PPG	Polypropylene glycol
PRE	Persistent radical effect
PTC	Phase transfer catalyst
SARA-ATRP	Supplemental activator and reducing agent ATRP
SET-LRP	Single-electron transfer living radical polymerization
THF	Tetrahydrofuran
TMS	Tetramethylsilane

## List of Symbols

$\%f$	Fraction of chains capped with the desired chemical group
$\alpha$	Mark-Houwink parameter
$\beta$	Basicity
$\delta$	Chemical shift, NMR
$E_T^N$	Normalized Dimroth-Reichardt Solvent Polarity Parameter
$[I]$	Initiator concentration
$K$	Mark-Houwink parameter
$k_{act}$	Activation rate constant
$k_{app}$	Apparent polymerization rate
$K_{ATRP}$	ATRP equilibrium constant; ratio of $k_{act}/k_{deact}$
$k_{comp}$	Comproportionation rate constant
$K_{dis}$	Disproportionation constant
$k_{deact}$	Deactivation rate constant
$k_p$	Propagation rate constant
$k_t$	Termination rate constant
$[L]$	Concentration of ligand
$[M]$	Monomer concentration
$M_n$	Number-average molecular weight
$M_p$	Peak molecular weight
$M_t$	Transition metal
$M_w$	Weight-average molecular weight
$MW$	Molecular Weight
$M_{th}$	Theoretical molecular weight
$\pi^*$	Dipolarity/polarizability
$v/v\%$	Volume percent concentration

# Chapter 1.

## Introduction

### 1.1 Background Information

Controlled living radical polymerization (CLRP) is a powerful tool that can be used to develop new polymeric materials with tailored properties. It allows for precise control over macromolecular structure, molecular weight, dispersity, and chain-end group functionality.<sup>1,2</sup> One of the variations of this technique is copper wire mediated CLRP, termed single-electron transfer living radical polymerization (SET-LRP)<sup>3-6</sup> or supplemental activator and reducing agent atom transfer radical polymerization (SARA-ATRP).<sup>7,8</sup> It provides excellent control over polymerization and polymer characteristics, while requiring only low catalyst loading and mild reaction conditions.<sup>3,5,6</sup> Full potential and large scale implementation of this polymerization method are yet to be realized. There are vast opportunities for further improvement and utilization of this powerful technique to meet the demand for new materials, while meeting environmental requirements.

One of the improvement opportunities for copper wire mediated CLRP is establishing greener solvent systems, which may make it more attractive for industrial applications in terms of cost and environmental friendliness. Solvents can have significant effects on control and livingness of polymerization, dispersity, monomer conversion and chain-end functionality of the polymer. These effects are discussed in detail in Chapter 2. Factors such as polarity, disproportionation constant, viscosity, solubility, ability to solvate and coordinate catalyst were found to contribute to the characteristics of polymerization. The number of green solvents has been steadily growing, and their use is continuously evaluated for various applications. In Chapter 3, two of these greener solvents, polyethylene glycol and polypropylene glycol,<sup>9</sup> were

studied and their effect on polymerization kinetics of copper wire mediated CLRP carefully considered.

Polymers produced with copper wire mediated CLRP can contain predetermined chain-end functionality that can be used for post-polymerization modification method to create new materials, such as copolymers that combine natural renewable polymers with synthetic polymers. Grafting of well-defined polymer chains *to* cellulose is an example of a graft copolymerization technique, which can be used to control and tailor properties of the new composited. Cellulose is the most abundant renewable polymer in the world, with numerous interesting properties, and it needs to be modified to utilize these properties for highly technical applications, such as sensors, drug delivery, stimuli-responsive materials, etc.<sup>10</sup> Chapter 4 evaluates a thio-bromo click reaction<sup>11</sup> as a grafting scheme of low molecular weight poly(methyl acrylate) with bromine chain-ends to the imparted thiol groups on cellulose backbone.

## **1.2 Thesis Objectives**

This thesis investigates further improvement and utilization of the efficient polymerization technique, copper wire mediated CLRP. First, the effects of greener solvent systems are studied for polymerization of methyl acrylate in PEG and PPG, and binary mixtures of PEG-DMSO, PEG-Ethanol, PPG-DMSO and PPG-Ethanol. The control over polymerization, livingness characteristics, final polymer chain-end functionality and narrowness of dispersity are the key chosen parameters for evaluating these effects. The second objective is to evaluate grafting *to* cellulose substrates of well-defined polymer grafts, a post-polymerization modification technique. The goal is to utilize a bromine chain-end functionality of a poly(methyl acrylate) synthesized with copper wire mediated CLRP for grafting *to* cellulose substrates. Functionalization of microcrystalline cellulose and cellulose acetate with ethylene sulfide to

obtain thiol functionality and a recently established facile thio-bromo click reaction are investigated for the grafting *to* mechanism.

### 1.3 Thesis Outline

The literature review in Chapter 2 of this thesis discusses in detail the two debated mechanistic assumptions of copper wire mediated CLRP, SET-LRP and SARA-ATRP. An overview of both perspectives is given on the effects of solvent selection and specific solvent properties on the kinetics of copper wire mediated CLRP and characteristics of a synthesized polymer. Chapter 3 focuses on investigation of greener solvent systems, based on polyethylene glycol and polypropylene glycol, for the copper wire mediated CLRP. Low molecular weight poly(methyl acrylate) with bromine chain-end functionality is used as a model polymer. The effects on polymerization rates, livingness characteristics, molecular weight, dispersity, and chain-end functionality are evaluated.

In Chapter 4 the retained bromine chain-end functionality of poly(methyl acrylate) synthesized using copper wire mediated CLRP is utilized for grafting *to* cellulose substrates, cellulose acetate and microcrystalline cellulose. The thio-bromo click reaction was investigated as a grafting scheme, where cellulose is first functionalized with thiol groups using ethylene sulfide and then polymer grafts are attached by reacting thiol groups on the cellulose backbone with bromine chain-ends of the polymer. One-pot and two-pot reaction systems were studied, to reduce the number of steps in the procedure and to minimize an exposure of easily oxidized thiol groups to oxygen. The obtained results and some recommendations are summarized in Chapter 5.



## Chapter 2.

### Literature Review: Effect of Solvent Selection on Copper Wire

### Mediated Controlled/Living Radical Polymerization

#### 2.1 Introduction

To fully understand the effects of a solvent selection on copper wire mediated controlled living radical polymerization (CLR), its kinetic mechanism needs to be understood well. There are two debated versions of this mechanism, and hence competing explanations of why some solvents perform better than the others. The following literature review introduces the general mechanism of the transition metal catalyzed CLR, and proceeds with the detailed explanation of the two different mechanistic assumptions, SET-LRP and SARA-ATRP, for the heterogeneous copper mediated CLR. Then, the studies focused on the solvent effects are reviewed separately for both methods, since the approach to the evaluation and explanation of these effects is significantly different.

#### 2.2 Controlled/Living Radical Polymerization

Since 1995 controlled/living radical polymerization (CLR) has attracted considerable attention as an approach capable of providing good control over a macromolecular structure of polymers, molecular weight, dispersity ( $M_w/M_n$ ), and polymer chain-end functionality.<sup>1,2</sup> In a well-controlled polymerization, the rate of propagation is constant throughout the polymerization, implying a constant number of living radicals, where the molecular weight of polymer increases in a linear manner. The predominant chain deactivation mechanism in a CLR is considered to be a fast and reversible termination of propagating chains.<sup>2</sup> Livingness of polymerization is characterized by an effective preservation of the chain-end fidelity, meaning the polymerization can be reinitiated or chain-end functionality can be utilized for subsequent reactions. To attain a

good control and livingness, the polymerization system requires a low concentration of growing radicals (to reduce possibility of bimolecular termination) that are reversibly deactivated forming dormant persistent radicals.<sup>1,2</sup>

To date, a great deal of progress has been made in the development of the transition metal-mediated CLRP termed atom-transfer radical polymerization (ATRP).<sup>1,2,12,13</sup> There are several variations of ATRP that utilize copper-based catalyst systems, which include activator regenerated by electron transfer (ARGET) ATRP<sup>14</sup>, initiators for continuous activator regeneration (ICAR) ATRP<sup>15</sup>, single-electron transfer living radical polymerization (SET-LRP)<sup>3-6</sup> and supplemental activator and reducing agent (SARA) ATRP.<sup>7,8</sup> ICAR and ARGET are commonly homogeneous systems, whereas SET-LRP and SARA-ATRP are heterogeneous systems utilizing copper powder or wire.<sup>16</sup> An advantage of using a heterogeneous system is the ease of catalyst removal and recycling, and therefore increased interest for industrial applications.

SET-LRP and SARA-ATRP present two debated kinetic mechanisms that use exactly the same components (ligand, catalyst, solvent), but are different in the fundamental mechanistic assumptions. The role of  $\text{Cu}^0$ ,  $\text{Cu}^{\text{I}}$  and  $\text{Cu}^{\text{II}}$  complexes in the ATRP has been debated in the literature for nearly a decade; primarily in terms of whether  $\text{Cu}^{\text{I}}$  or  $\text{Cu}^0$  are the main activator species in the heterogeneous copper-mediated CLRP, and whether  $\text{Cu}^{\text{I}}$  disproportionates into “nascent”  $\text{Cu}^0$  and  $\text{Cu}^{\text{II}}$  or it is formed by comproportionation of  $\text{Cu}^0$  and  $\text{Cu}^{\text{II}}$ .<sup>16</sup>

### **2.2.1 ATRP Kinetic Mechanism**

The general ATRP mechanism (Figure 2-1) is governed by the activator-deactivator equilibrium, where a transition metal complexed with a ligand in a lower oxidation state activates an alkyl halide, generating a radical and a higher oxidation state metal complex. A radical propagates with a monomer before reacting with a higher oxidation state metal complex to return to an alkyl halide, forming a dormant chain. The deactivation must be fast to suppress the rate of

irreversible termination, and fast activation is necessary for an effective propagation rate to ensure all chains grow almost simultaneously with a narrow molecular weight distribution.

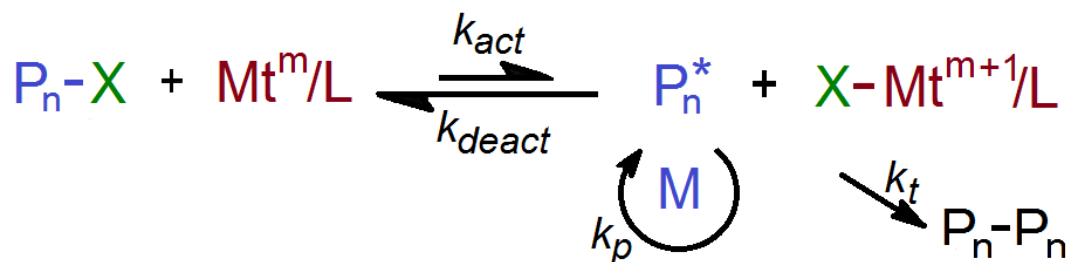


Figure 2-1. ATRP mechanism<sup>17</sup>

ATRP is subject to a persistent radical effect (PRE); buildup of a deactivator complex  $Mt^{II}$  (“persistent radical”) caused by unavoidable termination reactions, decreased rate of polymerization and suppressed rate of termination.<sup>17</sup> There are a number of reducing agents that can be used to reduce the  $Mt^{II}$  complex to  $Mt^I$ , such as glucose, ascorbic acid, hydrazine, sulfites, and zerovalent metals, including  $Cu^0$ .<sup>16</sup> ATRP is a complex polymerization system, where kinetics and thermodynamics are dependent on all of the system’s components: ligand, monomer, initiator, catalyst, temperature and solvent.<sup>18,19</sup>

### 2.2.2 SET-LRP Mechanistic Assumptions

In 2006, Percec *et al.* reported on the SET-LRP mechanism, stating that it was capable of ultra-fast synthesis of high molecular weight poly(methyl acrylate), poly(methyl methacrylate) and poly(vinyl chloride) with low catalyst loading (copper powder or wire) and mild reaction conditions.<sup>5</sup> SET-LRP demonstrated robustness, absence of PRE, immortality and excellent control over MW, narrow dispersity, constant rate of polymerization and nearly perfect chain-end functionality even at 100% monomer conversion.<sup>3,5,6</sup>

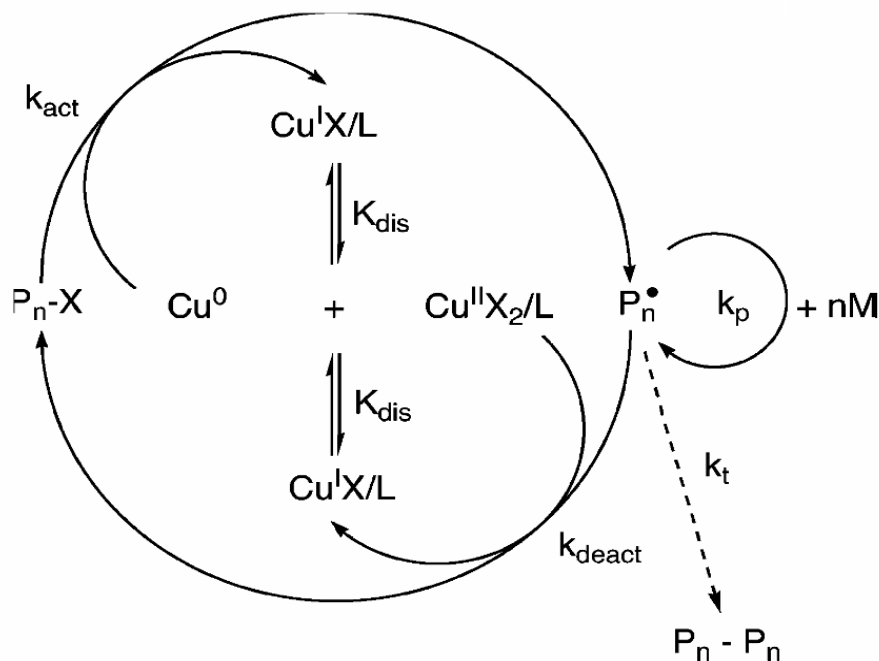


Figure 2-2. Mechanism of SET-LRP<sup>5</sup>

In SET-LRP (Figure 2-2) it is assumed that  $\text{Cu}^0$  activates an alkyl halide, forming a propagating radical and  $\text{Cu}^{\text{I}}$  complexed with a ligand ( $\text{Cu}^{\text{I}}\text{X}/\text{L}$ ) that spontaneously disproportionates into deactivating species  $\text{Cu}^{\text{II}}\text{X}_2/\text{L}$  and activating species  $\text{Cu}^0$ . It is assumed that dormant chains are activated through the heterolytic cleavage of the carbon halide bond by a  $\text{Cu}^0$  catalyzed outer-sphere electron transfer (OSET) process, and propagating macroradicals are reversibly deactivated by  $\text{Cu}^{\text{II}}\text{Br}_2/\text{N}$ -Ligand complex. Fast polymerization is due to a fast reaction between an alkyl halide and a “nascent”  $\text{Cu}^0$ , and  $\text{Cu}^0$  is presumed to control initiation, reactivation of dormant species and reversible termination. A critical element of the SET-LRP mechanism is the establishment of the appropriate balance between a “nascent”  $\text{Cu}^0$  and  $\text{Cu}^{\text{II}}$  species obtained from the disproportionation of the formed  $\text{Cu}^{\text{I}}$ .<sup>5,6</sup> This complex system is sensitive to various parameters, such as solvent polarity, solvent disproportionation constant, ligand structure and concentration, monomer solvation, reaction temperature and initiator selection, but the key to this mechanism is that the conditions must promote the disproportionation of  $\text{Cu}^{\text{I}}\text{X}/\text{L}$  into  $\text{Cu}^0$  and  $\text{Cu}^{\text{II}}\text{X}_2/\text{L}$ .<sup>5</sup>

### 2.2.3 SARA-ATRP Mechanistic Assumptions

Another proposed mechanism for the heterogeneous copper-mediated CLRP is SARA-ATRP (Figure 2-3).<sup>7,8,16</sup>

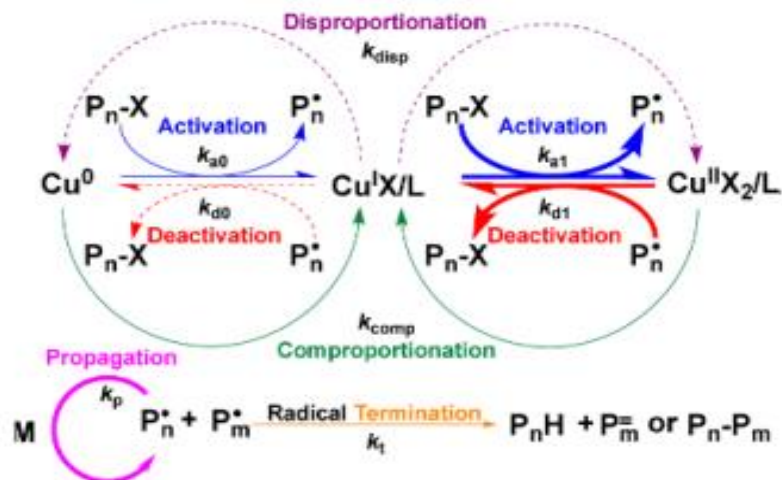


Figure 2-3. Mechanism of SARA-ATRP<sup>16</sup>

In SARA-ATRP, a  $\text{Cu}^{\text{I}}$  complex is assumed to be the main activator of an alkyl halide, where  $\text{Cu}^0$  acts as a supplemental activator and a reducing agent of a  $\text{Cu}^{\text{II}}$  complex to  $\text{Cu}^{\text{I}}$ . The process is governed by an inner-sphere electron transfer (ISET), where the role of  $\text{Cu}^0$  is to continuously supply activating species ( $\text{Cu}^{\text{I}}$ ) and radicals by supplemental activation and comproportionation, to compensate for the  $\text{Cu}^{\text{I}}$  lost due to unavoidable radical termination reactions and persistent radical effect. Rates of deactivation by  $\text{Cu}^{\text{II}}$  and activation by  $\text{Cu}^{\text{I}}$  complexes are considered to be responsible for regulating the ATRP equilibrium in this mechanism. Konkolewicz *et al.* demonstrated that activation of alkyl halides by  $\text{Cu}^{\text{I}}$  is significantly faster than by  $\text{Cu}^0$ , and comproportionation and disproportionation are slow processes, asserting that  $\text{Cu}^{\text{I}}$  not  $\text{Cu}^0$  are the main activating species.<sup>16</sup>

### 2.3 Solvent effects on copper wire mediated CLRP

Heterogeneous copper mediated CLRP of hydrophobic polymers has been extensively studied in a wide range of solvents, such as dimethyl sulfoxide (DMSO), dimethylformamide

(DMF), alcohols, ethylene carbonate (EC), other dipolar aprotic solvents and their binary mixtures. This section discusses the reported effects of these solvents on kinetics and the resulting polymers for both, SET-LRP and SARA-ATRP, mechanisms. The explanations for observed solvent effects are significantly different for each of these approaches, and therefore are reviewed separately for clarity. The effects on SET-LRP is typically categorized by evaluating dispersity, chain-end fidelity, and polymerization rate ( $k_{app}$ ), whereas for SARA-ATRP, the  $K_{ATRP}$  equilibrium constant, rates of activation ( $k_{act}$ ), deactivation ( $k_{deact}$ ) and more recently comproportionation of  $\text{Cu}^0$  and  $\text{Cu}^{\text{II}}$  ( $k_{comp}$ ) are considered to be the guiding factors for the extent of control of polymerization.

### 2.3.1 Solvent effects on SET-LRP

In the SET-LRP mechanism a spontaneous disproportionation of  $\text{Cu}^{\text{I}}$  into  $\text{Cu}^0$  and  $\text{Cu}^{\text{II}}$  species is assumed to be a key process contributing to a well-controlled LRP that establishes reactivity and prevents bimolecular termination.<sup>20</sup> Since the establishment of the SET-LRP, groups evaluating the effects of different solvents have found that the relationship between polymerization kinetics and solvent systems was not easily predictable. Factors such as polarity, disproportionation constant, viscosity, solubility of growing polymer chains, ability to solvate and coordinate copper complexes, and perhaps the nature of “nascent”  $\text{Cu}^0$  have been reported to affect SET-LRP kinetics.<sup>21-23</sup> A better understanding of this dependency on solvent properties could be a valuable guiding tool for the selection of an appropriate solvent system for a particular monomer.

To determine the extent of control and livingness of SET-LRP there are a number of parameters that are typically assessed: a)  $\ln([\text{M}]_0/[\text{M}])$  versus time plot, where the slope of the line is the apparent polymerization rate,  $k_{app}$ , and the linearity indicates a constant concentration of active species throughout polymerization, a living behavior; b) linear increase of molecular

weight ( $M_n$ ) with conversion; c) chain-end functionality, fraction of chains effectively capped with halogen atom; and d) dispersity ( $\bar{D}$ ), narrowing with conversion.<sup>24</sup>

In 2006 Percec *et al.* reported that DMSO was an excellent solvent for copper wire-mediated CLRP that facilitated fast, well-controlled and living polymerization of acrylates, methacrylate and vinyl chloride at 25°C, with nearly 100% chain-end functionality retained. These remarkable results were attributed to the ability of DMSO to promote  $\text{Cu}^{\text{I}}$  disproportionation.<sup>5</sup> Alcohols showed a higher propensity for disproportionation of  $\text{Cu}^{\text{I}}$  than DMSO, and were expected to be excellent solvents for SET-LRP as well. The polymerization kinetics of poly(methyl acrylate) (PMA) were consequently evaluated for methanol, ethanol (95%), 1-propanol, and tert-butanol alcohols.<sup>21</sup> For all reactions, data showed a linear dependence of  $\ln([M]_0/[M])$  on time, indicating a first-order propagation rate of growing radicals and decrease in monomer concentration. Molecular weight increased linearly and dispersity narrowed with conversion. Interestingly, polymerization rates decreased with the increasing hydrophobicity of the alcohol, which may have induced slower disproportionation. Conversion was limited in tert-butanol to 82% and in propanol to 80%, with broader dispersity, over 1.3.<sup>21</sup>

Even though methanol has a higher disproportionation constant than ethanol as seen in Table 2-1, a faster polymerization rate was observed in ethanol, possibly because the ethanol used contained 5% v/v water.<sup>21</sup> Based on this observation, binary mixtures of alcohols with water were evaluated further. Water has the highest disproportionation constant, and it was expected that addition of small amounts of it to alcohols would increase polymerization rates by affecting copper disproportionation. Indeed, with 5% volume of water added to alcohols an acceleration in polymerization rates was obtained, dispersity improved as well, indicating an improved living character of polymerization. Increasing the amount of water in excess of 5% volume resulted in PMA precipitating at low conversions. Chain-end functionality was not disclosed.<sup>21</sup>

**Table 2-1. Values of  $K_{dis}$  measured in the absence of complexing agents in different solvents<sup>21</sup>**

<b>Solvent</b>	<b><math>K_{dis}</math></b>	<b><math>\text{Log}(K_{dis})</math></b>
Water	$0.54 \times 10^6 - 5.8 \times 10^7$	5.95 – 7.74
Methanol	$6.3 \times 10^3$	3.8
Ethanol	3.6	0.56
DMSO	1.52 - 4.4	0.18 – 0.64
Acetone	0.03	-1.5
Acetonitrile	$6.3 \times 10^{-21}$	-20.2

In pure DMSO a  $\text{Cu}^{\text{I}}$  complex was found to be stable relative to  $\text{Cu}^{\text{II}}$  and metallic  $\text{Cu}^0$  due to its strong solvation, but in the presence of  $\text{Me}_6\text{-TREN}$  ligand the disproportionation of  $\text{Cu}^{\text{I}}$  was favored, stabilizing  $\text{Cu}^{\text{II}}$  instead.<sup>5</sup> While in non-disproportionating solvents, such as acetonitrile,  $\text{Cu}^{\text{I}}$  complex was found to remain stable at 25°C with the same ligand combination.<sup>5,20,25</sup> Mixtures of DMSO and acetonitrile were investigated to compare the effects of disproportionating versus non-disproportionating solvents on SET-LRP.<sup>25</sup> A polymerization rate in acetonitrile showed non-linear behavior. Deviation from the linearity of the  $\ln([M]_0/[M])$  versus time plot seen in Figure 2-4a indicated that the concentration of active species decreased over time and the polymerization was not truly living.<sup>25</sup> Chain-end functionality was well maintained throughout polymerization of methyl acrylate in DMSO, but was significantly lost in acetonitrile. The examination of binary mixtures of DMSO with acetonitrile (70/30, 50/50, 30/70 v/v) showed a decrease in chain-end functionality with conversion and with increasing fraction of acetonitrile (Figure 2-4b).<sup>25</sup>



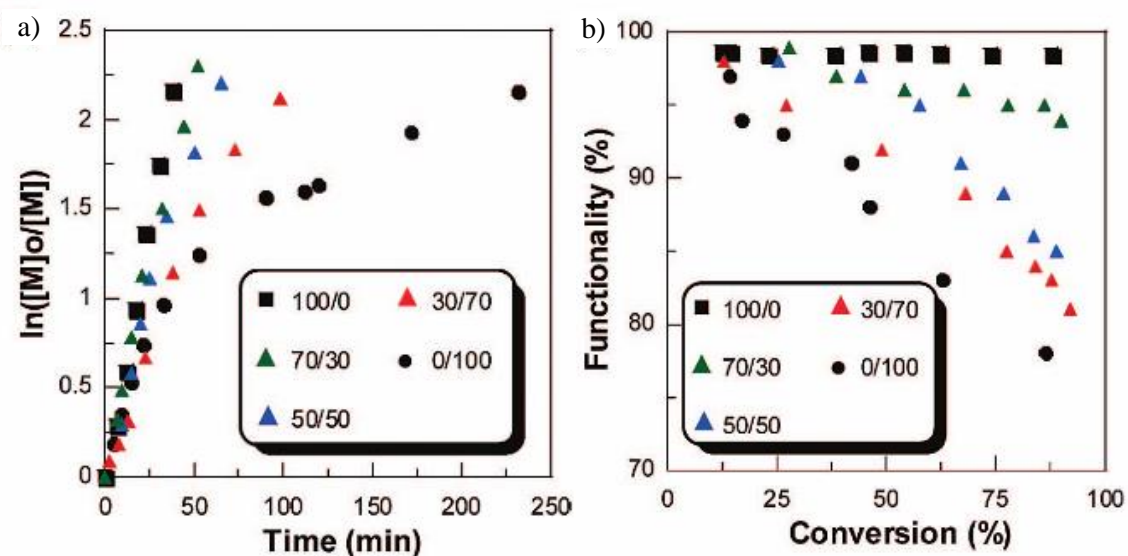


Figure 2-4. PMA polymerization in mixtures of DMSO (■) and acetonitrile (●)<sup>25</sup>

Polymerization was faster with higher amounts of DMSO (Figure 2-4a), where increasing concentration of acetonitrile transitioned kinetics from a living to a non-living polymerization.<sup>25</sup>

Toluene, similarly to acetonitrile, is considered to be a poor solvent for SET-LRP.<sup>24</sup> The polymerization rate observed in toluene was not found to be first order. It was noted to be very slow (66% conversion in 17 hours in toluene versus 100% in 45 min in DMSO) with considerable loss of chain-end functionality (80% in toluene, 98% in DMSO).<sup>24</sup> A downwards curvature of the  $\ln([M]_0/[M])$  versus time plot at 40% conversion represented a decrease in the living radical concentration and increase in the concentration of the  $\text{Cu}^{\text{II}}\text{X}/\text{Me}_6\text{-TREN}$  species formed by an irreversible termination.<sup>24</sup> In toluene, chain-end functionality decreased to 82% at 66% conversion, whereas, it remained constant at 98% for the polymerization in DMSO, indicating an absence of the irreversible bimolecular termination. Hence, disproportionation of  $\text{Cu}^{\text{I}}$  in toluene is very slow, and is likely to be facilitated mostly by the  $\text{Me}_6\text{-TREN}$ .<sup>24</sup>

Next, to expand the list of solvents capable of providing living polymerization conditions, the effect of a wide range of binary solvent mixtures was explored for SET-LRP of the hydrophobic polymer, PMA.<sup>22,23</sup> It was demonstrated that addition of 5-10% of water to DMSO,

DMF, Dimethylacetamide (DMAC), N-Methyl-2-pyrrolidone (NMP), ethylene carbonate (EC), methanol, ethanol, methoxyethanol, and even acetone resulted in a linear increase in the apparent rate constant of propagation,  $k_{app}$ , improved control over molecular weight and decreased dispersity with conversion.<sup>23</sup> Then, a full range of volume fractions of DMSO/acetone, DMSO/methanol, DMSO/EC, DMF/EC, DMAC/EC and ethyl-acetate/methanol was investigated, the results of which are summarized in Table 2-2.

**Table 2-2. SET-LRP of MA in binary mixtures of organic solvents at 25°C<sup>22</sup>,  $[M]_0/[I]/[L]=222/1/0.1$**

No.	Solvent	$k_p^{1app}$ (min <sup>-1</sup> )	$k_p^{2app}$ (min <sup>-1</sup> )	Time (min)	Conv (%)	$M_n$ (GPC)	$M_w/M_n$
1	Acetone	0.0166	0.0041	230	83.0	18,605	1.23
2	DMAC	0.0200	N/A	100	85.7	17,672	1.39
3	DMAC/10% EC	0.0281	0.0175	80	82.9	16,897	1.22
4	DMAC/30% EC	0.0450	0.0313	56	87.5	18,085	1.28
5	DMAC/50% EC	0.0655	0.0405	46	89.6	19,462	1.20
6	DMAC/70% EC	0.0713	0.0454	44	90.8	19,020	1.18
7	DMAC/80% EC	0.0702	N/A	38	86.5	17,785	1.20
8	DMAC/90% EC	0.0686	N/A	36	85.0	17,527	1.21
9	DMF	0.0338	N/A	63	88.0	18,920	1.21
10	DMF/10% EC	0.0410	0.0322	50	82.3	17,619	1.22
11	DMF/30% EC	0.0603	0.0302	50	88.8	18,385	1.21
12	DMF/50% EC	0.0686	0.0457	44	90.6	18,452	1.24
13	DMF/70% EC	0.0607	N/A	44	89.3	18,382	1.26
14	DMF/90% EC	0.0517	N/A	44	86.2	18,073	1.24
15	DMSO/5% acetone	0.0756	NA	25	81.3	18,784	1.21
16	DMSO/10% acetone	0.0724	NA	28	83.6	18,686	1.22
17	DMSO/20% acetone	0.0626	NA	30	83.8	19,054	1.20
18	DMSO/40% acetone	0.0471	NA	36	80.5	18,038	1.21
19	DMSO/60% acetone	0.0304	NA	60	83.4	18,116	1.29
20	DMSO/80% acetone	0.0223	NA	70	78.0	17,331	1.21
21	DMSO/10% EC	0.0767	NA	30	86.0	17,911	1.21
22	DMSO/20% EC	0.0810	N/A	30	89.3	19,045	1.21
23	DMSO/30% EC	0.0763	N/A	32	84.4	17,836	1.24
24	DMSO/40% EC	0.0735	N/A	33	85.2	18,155	1.26
25	DMSO/60% EC	0.0682	N/A	35	83.4	19,026	1.22
26	DMSO/80% EC	0.0666	N/A	36	86.0	19,310	1.22
27	DMSO/10% MeOH	0.0710	N/A	30	81.2	18,700	1.24
28	DMSO/25% MeOH	0.0750	N/A	40	88.1	20,000	1.28
29	DMSO/50% MeOH	0.0820	N/A	40	90.0	19,200	1.20
30	DMSO/75% MeOH	0.0840	N/A	40	89.1	18,200	1.17
31	DMSO/90% MeOH	0.0680	N/A	40	87.1	19,000	1.16
32	DMSO	0.0719	NA	32	88.2	19,310	1.19
33	EC	0.0493	N/A	44	84.7	19,578	1.22
34	Ethyl acetate	0.0140	N/A	120	72.6	15,700	1.31
35	Ethyl acetate/10% MeOH	0.0310	NA	50	69.5	20,000	1.13
36	Ethyl acetate/25% MeOH	0.0480	N/A	45	76.9	19,000	1.15
37	Ethyl acetate/50% MeOH	0.0590	N/A	30	77.0	17,700	1.13
38	Ethyl acetate/75% MeOH	0.0680	N/A	45	86.7	19,700	1.17
39	Ethyl acetate/90% MeOH	0.0640	N/A	40	83.7	18,900	1.31
40	MeOH	0.0360	N/A	70	91.0	20,342	1.14

It was found that unlike addition of water to organic solvents, binary mixtures of organic solvents did not exhibit linear or monotonic effect on the rate constant.<sup>22,23</sup> These findings suggested that multiple solvent parameters are responsible for affecting SET-LRP kinetics.<sup>22, 23</sup> It was noted that even 20% v/v of DMSO in acetone was enough to support first-order kinetics. Nearly a linear decrease of the rate constant was observed with increasing the fraction of acetone ( $K_{dis}$  0.03) in DMSO ( $K_{dis}$  1.5-4.4).<sup>22</sup>

The effect of solvent polarity on the rate constant ( $k_{app}$ ) was investigated with DMSO and ethylene carbonate mixtures.<sup>22</sup> Dimroth-Reichardt parameter ( $E_T^N$ ), ionizing power, displayed in Table 2-3 was used as a comparative measure of solvent polarity in Jiang *et al.* study.<sup>22</sup> Since EC ( $E_T^N=0.552$ ) is more polar than DMSO ( $E_T^N=0.444$ ), the authors expected  $k_{app}$  to increase with polarity. Increasing the fraction of EC in DMSO to 20% increased  $k_{app}$ , and then unexpectedly  $k_{app}$  decreased with further increase of the EC fraction in DMSO to pure EC.  $K_{dis}$  of EC is not available, but initial UV-VIS measurement indicated that EC is less effective in disproportionating  $Cu^I$  than DMSO.<sup>22</sup> This finding suggested that a combination of both properties, solvent polarity and  $K_{dis}$ , was responsible for influencing the control over polymerization to some extent.<sup>22</sup>

**Table 2-3. Normalized Dimroth-Reichardt solvent parameters,  $E_T^N$ , of select solvents<sup>22</sup>**

Solvent	$E_T^N$
Acetone	0.355
DMAC	0.377
DMF	0.386
DMSO	0.444
EtOH	0.654
EC	0.552
PC	0.472
H <sub>2</sub> O	1.000
MeCN	0.460
MeOH	0.762
Phenol	0.701
Toluene	0.099

In a similar analysis of the DMF/EC mixtures (DMF has higher  $K_{dis}$  than DMSO, but lower polarity),  $k_{app}$  increased up to 50% volume of EC in DMF.<sup>22</sup> This increase was attributed to the polarity improvement of the mixture provided by EC. Then,  $k_{app}$  continuously decreased from 50% volume to pure EC as a result of a decreased disproportionation of  $Cu^I$ . The evaluation of the DMAC/EC mixtures showed analogous results to DMF/EC, but with  $k_{app}$  peaking at 70% volume of EC instead of 50%. This shift was attributed to the lower polarity of DMAC compared to DMF, where  $K_{dis}$  is similar for both solvents. The behavior observed in methanol/DMSO mixtures was more difficult to explain. Polarity and  $K_{dis}$  of methanol are higher than that of DMSO, but  $k_{app}$  decreased from 75% to pure methanol. Therefore, there must be another factor, other than polarity and disproportionation constant, contributing to the SET-LRP rate, and it was suggested that H-bonding of methanol may have contributed to this dynamic.<sup>22</sup>

Of the solvents investigated, the best control over SET-LRP was found to be provided by DMSO and DMF, but these are high boiling solvents, and may not be desirable for a given case. Acetone and water was the first low boiling point organic solvent system for SET-LRP of a hydrophilic polymer that was investigated.<sup>23</sup> As there is a need of such, mixtures of ethyl acetate and methanol were examined by Nguyen *et al.*<sup>23</sup> Ethyl acetate is inexpensive, but has a similar effect on SET-LRP to toluene and acetonitrile, and is immiscible with water. The addition of methanol to ethyl acetate was expected to improve the polymerization kinetics. From 0% to 75% of methanol in ethyl acetate, a linear increase in the  $k_{app}$  was observed, then  $k_{app}$  decreased from this point on to pure methanol. It was also observed that increasing a fraction of a more polar solvent in the mixture resulted in a narrower dispersity of final polymers.<sup>22,23</sup> Based on these studies it was concluded:

*“Solvent polarity affects the stabilization of the dipolar transition states and intermediates involved with SET activation (heterolytic bond dissociation). The  $K_{dis}$  determines the ability to produce more reactive “nascent”  $Cu^0$  and the needed levels of  $Cu^{II}$  in the early stages of the reaction to prevent irreversible*

*termination of chains. Ability to stabilize “nascent” Cu<sup>0</sup> and prevent their agglomeration to less reactive species must also be considered.”<sup>22</sup>*

As previously mentioned, SET-LRP performed in solvents that are not thought to support the disproportionation of Cu<sup>I</sup> resulted in chain-end functionalities ranging from 50% to 80%, which is an indication of a large extent of irreversible termination.<sup>26</sup> However, it was found that dispersity is narrow even in some of the non-disproportionating solvents.<sup>27</sup> A narrow dispersity in those solvents is generally explained by a low rate of initiation rather than of propagation, where generated polymers are expected to have lower dispersity.<sup>28</sup> Hence, omitting a chain-end functionality analysis can be misleading in the evaluation of the control and livingness of a polymerization.

Chain-end functionality, the fraction of polymer chains effectively capped with a halogen atom, is one of the key features of polymers synthesized via CLRP, which can subsequently be used for chain extension, block co-polymerization, and grafting applications.<sup>28</sup> Determination of the chain-end functionality of bromine capped PMA was performed using various techniques: <sup>1</sup>H NMR, MALDI-TOF and chain extension. It was found that using <sup>1</sup>H NMR as a method of assessing the chain-end functionality of PMA is a relatively simple and accurate technique, and is comparable to other methods within 1-3%.<sup>28,29</sup> An important finding worth noting is that chain-end fidelity is affected by the timing of the polymerization reactions. Once a polymerization reaches full or limited conversion, bimolecular termination will increase with prolonged time; therefore, stopping the reaction at an appropriate conversion is required to maintain desired dispersity and chain-end functionality.<sup>28,30</sup> Moreover, polymers with a lower degree of polymerization spend less time being “active”, which minimizes the possibility of termination and other side reactions, thereby, preserving chain-end fidelity.<sup>30</sup>

Further studies were performed to understand which solvent properties beyond polarity and a disproportionation constant could affect SET-LRP kinetics and the characteristics of the

final polymer. These key properties were found to be the ability of solvents to stabilize “nascent”  $\text{Cu}^0$  nanoparticles generated from disproportionation and the solubility of  $\text{Cu}^{\text{II}}$ .<sup>31,32</sup> The ability of solvents to stabilize “nascent”  $\text{Cu}^0$  particles is suggested to primarily control the rates of nucleation and activation, and to determine the amounts of  $\text{Cu}^0$  deposited on the wire surface and of the “free nascent”  $\text{Cu}^0$  nanoparticles.<sup>31</sup> These nanoparticles are considered to be generated from the disproportionation and to be responsible for activation of the dormant species.  $\text{Cu}^0$  nanoparticles were found to be stable in DMSO, which may explain why SET-LRP in DMSO tends to proceed faster than in a more polar methanol with a higher disproportionation constant.<sup>31</sup>

Percec *et al.* thoroughly analyzed the disproportionation of  $\text{Cu}^{\text{I}}$  species in polar and non-polar solvents, to demonstrate the dependence of SET-LRP kinetics on the nature of solvent system. They discovered the importance of the solubility of the  $\text{Cu}^{\text{II}}\text{X}/\text{Ligand}$  complex in the solvent and even in the monomer. It was found that  $\text{Cu}^{\text{I}}\text{Br}/\text{Me}_6\text{-TREN}$  also disproportionated in less polar solvents and monomers, but the solubility of  $\text{Cu}^{\text{II}}$  was negligible as its precipitation was observed in the non-polar media, such as dioxane, anisole, ethyl acetate, hexane, toluene, styrene, acrylates and methacrylates.<sup>32</sup> The low solubility of  $\text{Cu}^{\text{II}}$  may have been the cause of poor control over polymerization reaction observed in a non-polar media, resulting in “surface disproportionation” of  $\text{Cu}^{\text{I}}$  and a bimolecular termination. These findings were used to explain the progressive loss of chain-end functionality (displayed in Figure 2-4b), and limited conversion in non-polar solvents. Improving the solubility of  $\text{Cu}^{\text{II}}$  in non-polar solvents with binary mixtures was shown to improve control and chain-end retention.<sup>32</sup>

### **2.3.2 Solvent effect on SARA-ATRP**

A different approach to evaluating the effects of solvent selection on the copper-mediated CLRP was taken in the studies supporting the SARA-ATRP mechanistic assumptions, where  $\text{Cu}^0$  is considered to be a reducing agent and a supplemental activator, the  $\text{Cu}^{\text{I}}$  complex is the main

activator and the Cu<sup>II</sup> complex is the deactivator. All CLRP system components (solvent, catalyst, ligand, initiator) are typically characterized by the value of the  $K_{\text{ATRP}}$  equilibrium constant, determined from a kinetic plot of  $\ln([M]_0/[M])$  versus time. A low  $K_{\text{ATRP}}$  ( $K_{\text{ATRP}} = \frac{k_{\text{act}}}{k_{\text{deact}}}$ ) value is required to minimize termination and maintain low radical concentration, as more rapid polymerizations seemingly lead to more termination, which is a diffusion controlled process.<sup>17, 19</sup> The Cu<sup>II</sup> complexes are cationic and are more stable in polar solvents, while Cu<sup>I</sup> is considered to be a neutral complex, of low polar character. It is therefore expected that the polarity of the solvent will vary the ratio of Cu<sup>I</sup> to Cu<sup>II</sup> and consequently  $k_{\text{act}}/k_{\text{deact}}$ .<sup>17</sup> Disproportionation of Cu<sup>I</sup> is neglected as it has been shown that only 10% of Cu<sup>I</sup> complex disproportionates in DMSO, and even less in the presence of a low-polarity monomers, such as methyl acrylate.<sup>8,33</sup>

A comprehensive evaluation by Braunecker *et al.* of the solvent effects on the  $K_{\text{ATRP}}$  equilibrium constants was performed for Cu<sup>I</sup> catalyzed ATRP.<sup>19</sup> The group verified and predicted the effects using a thermodynamic scheme: electron transfer - reduction/oxidation of the metal complex and halogen atom, and the affinity of the catalyst in the particular oxidation state for the halide anions. Solvent and ligand systems were specifically chosen to decrease the possibility of the Cu<sup>I</sup> disproportionation, preventing formation and accumulation of Cu<sup>0</sup> and Cu<sup>II</sup>.<sup>19</sup> The effects were quantitatively analyzed using Kamlet-Taft parameters and linear solvation energy, and  $K_{\text{ATRP}}$  was predicted for 17 solvents including water. These are displayed in Figure 2-5 and it can be seen that  $K_{\text{ATRP}}$  is higher in polar solvents like DMSO and lower in acetone and toluene.<sup>19</sup>

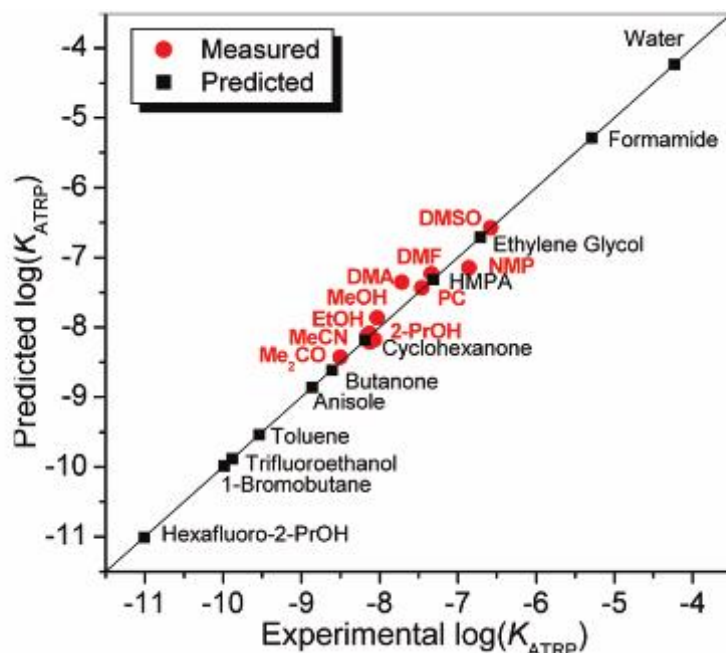


Figure 2-5. Measured and Predicted (represented by the line)  $\text{Log}(K_{\text{ATRP}})$  values.<sup>19</sup>

Horn and Matyjaszewski also studied the effect of various solvent characteristics on the activation rate constant ( $k_{\text{act}}$ ) and deactivation rate constant ( $k_{\text{deact}}$ ) for CuBr catalyzed CLRP. Parameters such as dielectric constant, dipolarity/polarizability  $\pi^*$  (a measure of nonspecific solute–solvent interactions), solvation and stabilization of copper species were evaluated and 14 different solvents were analyzed using the Kamlet–Taft approach, as shown in Figure 2-6.<sup>34</sup>

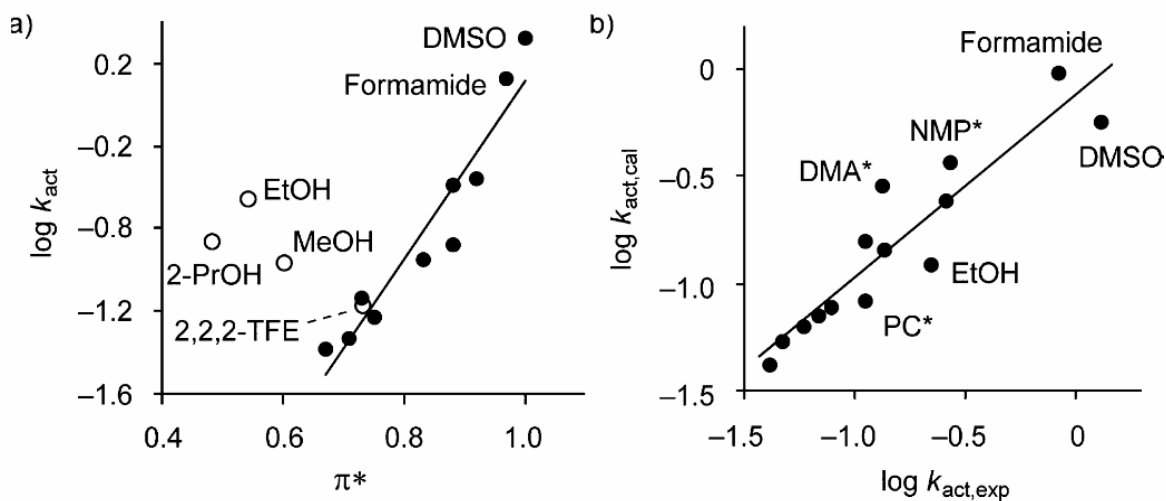


Figure 2-6. a)  $\log k_{\text{act}}$  vs.  $\pi^*$  b)  $\log k_{\text{act}}$  calculated vs. experimental<sup>34</sup>



Dielectric constant and Dimroth's and Reichardt's values of solvents were not correlated to the  $k_{act}$ , but dipolarity/polarizability  $\pi^*$  were demonstrated to have the largest impact on the activation rate. This would suggest that nonspecific "solvent polarity" mostly determines the magnitude of  $k_{act}$ . Thus, an activation step is faster with an increased polarity of solvent, resulting in a higher value of  $K_{ATRP}$ .<sup>34</sup> Interestingly, activation in alcohols was much faster than expected and could not be correlated with polarizability, and was excluded from the linear regression presented in Figure 2-6a. Furthermore, activation rate showed a high dependency on  $\text{Cu}^{\text{I}}$  and  $\text{Cu}^{\text{II}}$  solvation. The difference between the two copper complexes, where  $\text{Cu}^{\text{II}}\text{Br}_2/\text{L}$  is more dipolar than  $\text{Cu}^{\text{I}}\text{Br}/\text{L}$ , makes the activation and the deactivation rate constants solvent-dependent.<sup>34</sup> Polarity change as a function of increasing volume fraction (from 20% to 80%) of monomer (MA, MMA, and methyl propionate) to solvent (DMSO and acetonitrile) was investigated, as polymerizations actually occur in mixtures of monomer and solvents. The effect was similar for all monomers tested; a linear decrease in  $\log k_{act}$  with decrease in polarity.<sup>34</sup>

A number of informative studies were performed in different solvents to demonstrate that  $\text{Cu}^{\text{I}}$  disproportionation, guided by a disproportionation constant of the solvent, is not a control process for SARA mechanism, but rather  $\text{Cu}^{\text{I}}$  species react with alkyl halide to form  $\text{Cu}^{\text{II}}$  and a radical. Copper mediated polymerization of methyl methacrylate (MMA) was performed in a non-disproportionating and non-polar media, toluene by Hornby *et al.*<sup>35</sup> The authors of the study reported that without disproportionation of  $\text{Cu}^{\text{I}}$ , a well-defined PMMA was formed, with dispersities ranging from 1.3 to 1.45 at monomer conversion below 80%. However, these results were achieved with  $\text{CuBr}_2$  added, prior to which polymerization was not well-controlled. The fraction of living chains was determined to be 90% by chain extension, as chain-end functionality cannot be determined for PMMA using NMR.<sup>35</sup> Similarly, Magenau *et al.* performed polymerization of MMA in anisole, a non-polar solvent, using a copper wire, with added  $\text{Cu}^{\text{II}}$  and excess ligand, where the key role of  $\text{Cu}^0$  was argued to be a reducing agent of  $\text{Cu}^{\text{II}}$ , forming an

activator,  $\text{Cu}^{\text{I}}$ . Increasing surface area of  $\text{Cu}^{\text{0}}$  decreased conversion, which was assumed to be a result of an accumulated deactivator,  $\text{CuBr}_2$ . The dispersities of the polymer ranged from 1.12 to 1.39, with livingness of 94%.<sup>36</sup>

More recently, comproportionation of  $\text{Cu}^{\text{0}}$  and  $\text{Cu}^{\text{II}}$  is another parameter of copper-mediated polymerization that is claimed to reduce the deactivator,  $\text{Cu}^{\text{II}}$ , to an activator,  $\text{Cu}^{\text{I}}$ . A study examining the extent of comproportionation versus disproportionation reactions was performed by Harrison *et al.*, evaluating the rates of activation by  $\text{Cu}^{\text{0}}$  ( $k_{a0}$ ) and comproportionation of  $\text{Cu}^{\text{0}}$  and  $\text{Cu}^{\text{II}}$  ( $k_{comp}$ ) in the copper wire-mediated CLRP.<sup>37</sup> The analysis was performed in polar and non-polar solvents, including DMSO, acetonitrile, toluene, ethanol, DMF, ethyl acetate and ethanol/water mixture (1:1). It was concluded that solvent polarity and the ability to stabilize  $\text{Cu}^{\text{I}}$  and  $\text{Cu}^{\text{II}}$  complexes played an important role in establishing these rates. Rates of activation were highest in the most polar solvents (DMSO, ethanol/water, DMF).<sup>37</sup> Acetonitrile is known to stabilize  $\text{Cu}^{\text{I}}$  species and therefore should favor comproportionation, and it was demonstrated that comproportionation was in fact dominant in acetonitrile, ethanol, and DMF. DMSO is however characterized by high activation rate with low comproportionation relative to the rate of supplemental activation by  $\text{Cu}^{\text{0}}$ .<sup>37</sup>

Peng *et al.* evaluated the activation rate by  $\text{Cu}^{\text{0}}$  and  $\text{Cu}^{\text{I}}$  in the copper wire mediated polymerization of methyl acrylate in DMSO, acetonitrile and their mixtures, with  $\text{Me}_6\text{-TREN}$  as a ligand. They demonstrated that disproportionation was negligible in DMSO mixture with MA, that comproportionation dominated over disproportionation and that the main activator was  $\text{Cu}^{\text{I}}$  not  $\text{Cu}^{\text{0}}$ .<sup>38</sup> In solvents favoring comproportionation, an upwards curvature of conversion versus time plot was observed, indicating rate acceleration by autocatalysis, caused by a rapid increase in radical concentration, resulting in termination and lost control. The strongest auto acceleration was in acetonitrile, indicating that disproportionation played no role in the initial rate determining reaction (reaction of copper metal with initiator), but the effect was self-limiting.<sup>37</sup>

Chain-end functionality is an important measure of the livingness of polymerizations, as previously mentioned. Since  $\text{Cu}^{\text{II}}$  complex is required for copper-mediated CLRP and is formed by termination, the halogen conservation principle permits for some chain-end loss. However, loss of chain-end functionality in nonpolar solvents, such as acetonitrile, was found to be excessive (also seen in Figure 2-4). Wang *et al.* attempted to determine if there are other reactions responsible for the loss of chain-end functionality during polymerization of MA in acetonitrile.<sup>39</sup> They found that other than termination reactions, chain breaking reactions, such as disproportionation and irreversible chain transfer to monomer, catalyst, and solvent, cause a more significant loss of chain-end functionality. The rate of termination in acetonitrile was noted to increase with increased degree of polymerization and conversion. Terminated chain-ends were found to contain predominately saturated and unsaturated end groups, which are typically expected in the presence of disproportionation and chain transfer reactions.<sup>39</sup>

It was found that  $\text{Cu}^{\text{I}}$  catalyzed these chain-end loss reactions. This catalytic radical termination (CRT) is believed to contribute more significantly to chain-end loss than conventional termination between two radicals.<sup>39</sup>  $\text{Cu}^{\text{I}}$  induced termination is assumed to proceed as follows:  $\text{Cu}^{\text{I}}$  reacts with a radical and forms an intermediate that reacts with another radical, regenerating  $\text{Cu}^{\text{I}}$  species and forming dead chains. To improve livingness, polymerization conditions need to be chosen that suppress the loss of chain-end functionality.<sup>39</sup>

## 2.4 Conclusion

The only consensus on both sides of the debated copper wire mediated CLRP mechanism is that a combination of solvent properties influences the extent of livingness and control over the polymerization. These properties include solvent polarity and ability to solubilize and stabilize  $\text{Cu}^{\text{I}}$  and  $\text{Cu}^{\text{II}}$  species. The groups agreeing with SARA-ATRP mechanism conclude that the effectiveness of DMSO lies in high  $K_{\text{ATRP}}$  and maintaining appropriate ratio of  $\text{Cu}^{\text{I}}$  to  $\text{Cu}^{\text{II}}$ , not in

the ability to disproportionate  $\text{Cu}^{\text{I}}$  complex. These characteristics of DMSO are responsible for good control and minimizing the  $\text{Cu}^{\text{I}}$  catalyzed radical loss, and therefore maintaining good chain-end functionality and polymerization rates.<sup>16</sup> Non-specific solvent polarity and solvation of  $\text{Cu}^{\text{I}}$  and  $\text{Cu}^{\text{II}}$  were shown to have the largest impact on the activation rate, and therefore  $K_{\text{ATRP}}$ , which increases with polarity.<sup>34</sup> The reason for poor control in less polar solvents (acetonitrile and toluene) is assumed to be the stability of  $\text{Cu}^{\text{I}}$  that leads to loss of radicals by  $\text{Cu}^{\text{I}}$  catalyzed process. Comproportionation, forming  $\text{Cu}^{\text{I}}$ , was found to be faster in acetonitrile than in DMSO, which explains a progressive loss of chain-end functionality in acetonitrile.<sup>16,40</sup>

The groups assuming SET-LRP mechanism suggest that effectiveness of DMSO as a solvent for copper mediated CLRP lies in the high disproportionation constant, polarity, ability to stabilize “nascent”  $\text{Cu}^0$ , and ability to solvate and stabilize  $\text{Cu}^{\text{II}}$ .<sup>22</sup> It was observed that non-polar and non-disproportionating solvents, such as acetonitrile, stabilize  $\text{Cu}^{\text{I}}$  instead, which resulted in non-first order polymerizations and loss of chain-end functionality.<sup>25</sup> Some binary mixtures of solvents were shown to improve polymerization kinetics and final polymer characteristics by tuning solvent properties. For example, altering polarity or a disproportionation constant with a secondary solvent will improve polymerization rate and chain-end retention, but the effect is limited. Currently, there is no straight forward method for predicting the effects of tuning solvent properties on copper mediated CLRP.

## Chapter 3.

# Development of Greener Solvent Systems for Copper Wire Mediated Controlled/Living Radical Polymerization of Methyl Acrylate

### Abstract

In an effort to develop greener solvent systems for copper wire mediated controlled living radical polymerization, synthesis of poly(methyl acrylate) was conducted at 30°C in DMSO, PEG and PPG, and binary mixtures of PEG-DMSO, PEG-Ethanol, PPG-DMSO and PPG-Ethanol with total volume of solvent to monomer at 33% and 50%. Secondary solvent fractions were examined at 10% and 25% of total solvent volume. Two effective green solvent systems were established, 33% 75-25 PEG-Ethanol and 33% 75-25 PPG-Ethanol, that provide good control over polymerization and livingness characteristics. The polymers produced in these solvent systems retained high chain-end functionality (>90%) and narrow dispersity (~1.1).

### 3.1 Introduction

Growing environmental awareness is the driving force behind recent efforts to decrease pollution from chemical processes, including production of commodity polymers. All aspects of the process must be evaluated to find and implement alternative routes, in order to accommodate newly emerging environmental policy restrictions on manufacturing and disposal of reactants and solvents. The use of greener solvents is one of the effective process improvement strategies, and a key principle of green chemistry and engineering.<sup>41</sup> However, changing a reaction medium can result in increased or decreased reaction rates, changes in product quality and yields. Even a slight difference could result in millions of dollars in benefits or costs, which would deter “greening” of a production process.<sup>41</sup>

Typical organic solvents are toxic and volatile, with over 20 million tons of volatile organic compounds being discharged into the atmosphere annually.<sup>42</sup> Alternative solvents, such as water, ionic liquids, fluorinated solvents, supercritical fluids and some polymers may be greener for a particular process, as well as safer and more environmentally friendly.<sup>41,42</sup> There is no perfectly green solvent, as each selection is case specific, and requires weighing costs and benefits. A few of the parameters that can be taken into a consideration when selecting a solvent for a specific process is cost of manufacturing, energy requirements, environmental risks, flammability, recyclability, viscosity, heat absorption if required, purification, toxicity, etc.<sup>43</sup> This study is focused only on the effects of the examined solvent systems on the polymerization kinetics and final polymer characteristics. The effects of replacing a solvent in copper wire mediated Controlled Living Radical Polymerization (CLRP) may manifest themselves in a different polymerization rate, dispersity, limited monomer conversion, and loss of chain-end functionality. The solvent is responsible for facilitating activity, solubility and stability of copper species ( $\text{Cu}^0$ ,  $\text{Cu}^{\text{I}}$  and  $\text{Cu}^{\text{II}}$ ) and therefore directly affects livingness and control over the polymerization.

Copper wire mediated CLRP of methyl acrylate (MA) has been thoroughly studied, and exhibits good control and livingness in DMSO.<sup>28</sup> Consequently, greener solvents investigated in this study, low molecular weight polyethylene glycol (PEG200) and polypropylene glycol (PPG400) were selected based on their similarities to DMSO (aprotic, polar and basic) using a Kamlet-Taft diagram. Figure 3-1 and Figure 3-2 illustrate two Kamlet-Taft diagrams for common organic aprotic solvents and of some greener solvents, identified by basicity, polarity and polarizability.<sup>9</sup>

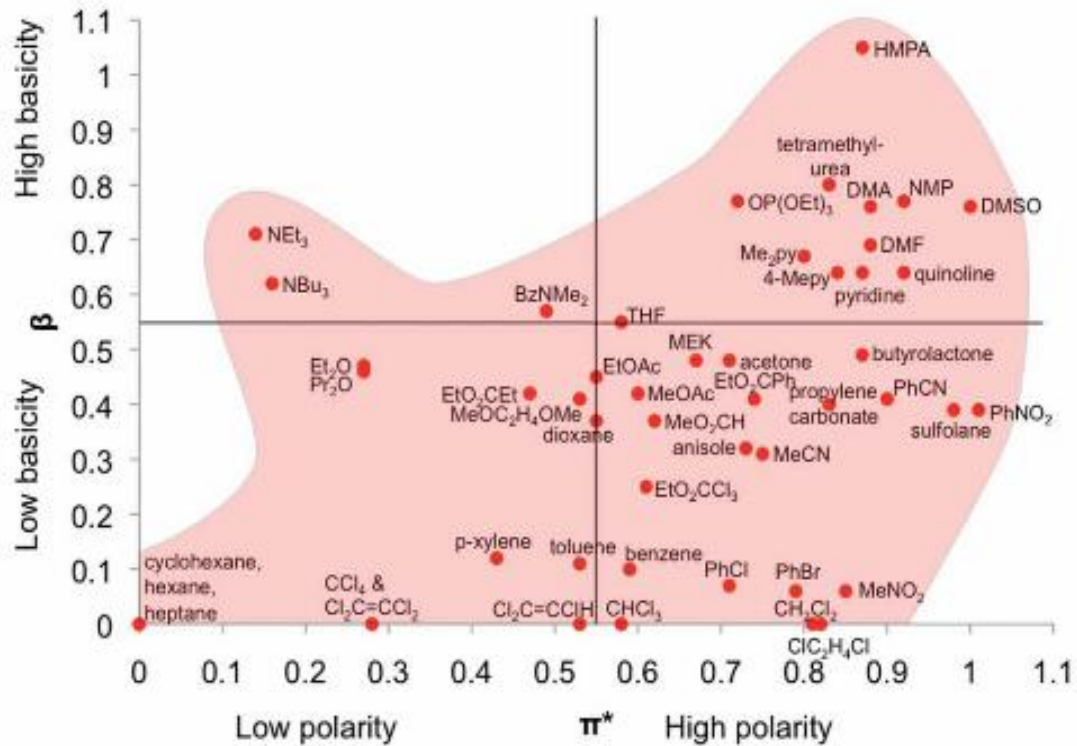


Figure 3-1. Kamlet-Taft plot for common organic aprotic solvents<sup>9</sup>

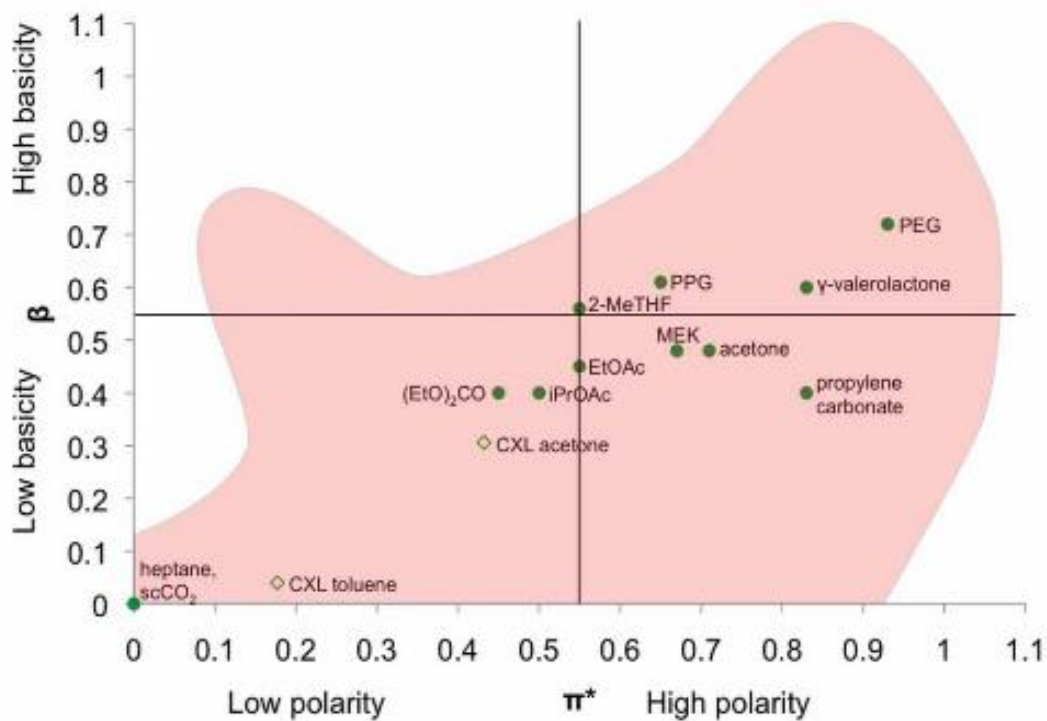


Figure 3-2. Kamlet-Taft plot of select greener solvents<sup>9</sup>

PEG is regarded as “a protic solvent with aprotic sites for binding constituted by the ethylene oxide units”.<sup>44</sup> Low molecular weight ( $M_n < 600$  g/mol) PEG is a polar, viscous, colorless liquid. It is considered to be a greener solvent, because it is easily degradable, relatively environmentally benign, and a non-volatile solvent with well-known low toxicity levels (approved by US FDA for internal consumption) and low flammability.<sup>45</sup> PEG can also be easily separated from the precipitation media by direct distillation, which may be utilized depending on the process, size and cost efficiency.<sup>44,46</sup> Perrier *et al.* reported the first study of PEG400 being used as a medium for Cu<sup>I</sup> powder mediated radical polymerization of methyl methacrylate and styrene. It was found that polymerization remained living for both monomers, and that the rate of polymerization of MMA was faster in PEG than in a typically used solvent, toluene.<sup>46</sup>

An additional reported benefit is that an amount of the residual copper catalyst was reduced in a precipitated polymer after a polymerization in PEG. This was attributed to the complexation of PEG with copper.<sup>46</sup> The ability of PEG to coordinate metal cation has been previously studied, establishing that PEG can serve as a phase transfer catalyst (PTC), as polyethylene oxide chains can form complexes with cations.<sup>44</sup> Therefore, during a phase transfer process, PEG may transfer copper to an aqueous precipitation media, leaving the polymer nearly catalyst free. The higher polarity of PEG (compared to toluene) and competing copper complexation may have also contributed to faster polymerization rates of MMA. Polypropylene glycol (PPG) has similar properties to PEG, but with lower toxicity and less reactive secondary hydroxyl groups.<sup>47</sup> Detailed studies on PEG or PPG as solvent systems of copper wire mediated CLRP of MA have not been found in the literature.

Methyl acrylate was chosen as a model monomer as it has been studied well, its polymerization is typically fast (under 2 hours), and chain-end functionality can be accurately determined using Nuclear Magnetic Resonance (NMR) within 3%.<sup>28,29</sup> Polymerization reactions were performed at 30°C, with a few exceptions of 50°C to demonstrate an effect of temperature



on the polymerization rate. Initial experiments in pure PEG and PPG showed that increase in viscosity with conversion of monomer detrimentally affects dispersity and results in a limited conversion. To reduce this viscosity effect on the final polymer dispersity and chain-end functionality retention the following were examined: a) increased volume fraction of solvent (from 33% to 50% v/v), and b) binary mixtures of PEG-DMSO, PEG-Ethanol, PPG-DMSO and PPG-Ethanol. For all experiments the following parameters were assessed: a) normalized conversion plot, ( $\ln([M]_0/[M])$  versus time) where the slope of the line is the apparent rate of polymerization,  $k_{app}$ , and the linearity indicates a living behavior and a constant concentration of active species throughout polymerization; b) dispersity ( $\mathcal{D}$ ,  $M_w/M_n$ ), narrowing with conversion; c) chain-end functionality ( $f\%$ ), fraction of chains effectively capped with a halogen atom; and d) linear increase of molecular weight ( $M_n$ ) with conversion.

## 3.2 Experimental

### 3.2.1 Materials

Ethyl 2-bromoisobutyrate (EBiB) (98%, Aldrich), tris[2-(dimethylamino)ethyl]amine (Me<sub>6</sub>-TREN) (97%, Aldrich), dimethyl sulfoxide (DMS) (99.5%, Aldrich), tetrahydrofuran (THF) (Fisher, HPLC grade), ethanol (Anhydrous, Commercial Alcohols), polyethylene glycol (PEG) ( $M_n$  200, Aldrich), and polypropylene glycol (PPG) ( $M_n$  400, Aldrich) were used as received. Methyl acrylate (MA, 99%) was purchased from Sigma Aldrich and passed through a column of basic aluminum oxide (Al<sub>2</sub>O<sub>3</sub>, Aldrich) prior to use in order to remove a radical inhibitor. Copper wire (1mm diameter, Aldrich), was immersed in hydrochloric acid (HCl, Fisher) for 10 minutes and washed with methanol prior to use.

### 3.2.2 Characterization

Gel permeation chromatography (GPC) of PMA was performed on a Waters 2695 GPC separation module with a 410 differential refractometer as a detector and five Waters Styragel columns in series at a temperature of 40°C. Distilled THF (Fisher, HPLC grade) was used as an eluent with a flow rate of 0.3 mL/min. The weight average ( $M_w$ ) and number-average ( $M_n$ ) molecular weights were determined with polystyrene standards and corrected using Mark-Houwink parameters ( $K=0.000611$  mL/g,  $\alpha=0.799$ ).<sup>48</sup> Monomer conversion and chain-end functionality were measured using 400MHz  $^1\text{H}$  NMR Bruker Avance instrument. Spectra were recorded at 23°C in chloroform-d ( $\text{CDCl}_3$ ) with tetramethylsilane (TMS) as an internal standard. For monomer conversion analysis the number of scans was set to 64 and for chain-end functionality analysis of PMA, the number of scans was set at 160 with 8s delay ( $D_1$ ).<sup>28</sup>

### 3.2.3 Typical polymerization procedure

Prior to the reaction, copper wire (4 pieces of 1cm long, 1mm diameter) was submerged in HCl for 10 minutes and washed with methanol. In the 100 mL three neck round bottom flask, solvent (DMSO, 5 mL) was combined with copper wire, ligand  $\text{Me}_6\text{-TREN}$  (99  $\mu\text{L}$ , 0.37 mmol) and initiator EBiB (0.272 mL, 1.85 mmol). The flask was placed in the oil bath at 30°C and purged with nitrogen. Methyl acrylate (10 mL, 111.2 mmol), was passed through a basic alumina column to remove an inhibitor and injected into the reaction flask. A reaction mixture was continuously stirred with a magnetic stirrer. All polymerization reactions were stopped when a magnetic stirrer began to skip rotations due to an increased viscosity. Samples were taken periodically throughout the polymerization and dissolved in cold  $\text{CDCl}_3$ . First, conversion was measured by  $^1\text{H}$  NMR. Then, samples were passed through a small aluminum oxide column to remove residual copper, and analyzed with GPC to determine  $M_n$ ,  $M_w$  and  $M_w/M_n$  ( $\bar{D}$ ). The final polymerization mixture was precipitated in deionized cold water, dissolved in THF and

precipitated (washing procedure was repeated three times). The final polymer was dried under vacuum, and analyzed with  $^1\text{H}$  NMR to determine chain-end functionality.

### 3.3 Results and Discussion

The copper wire mediated CLRP of MA initiated by EBiB was carried out in DMSO, PEG, PPG, and mixtures of PEG-Ethanol, PEG-DMSO, PPG-Ethanol, and PPG-DMSO in order to determine an effective green solvent system. For all reactions, the volume of monomer (10 mL) was kept constant, while the volume of solvent was evaluated at 33% v/v (5 mL) and 50% v/v (10 mL) to reduce the effect of increasing viscosity with conversion of monomer. Solvent systems with PEG and PPG were optimized for low molecular weight PMA (4K), with  $[\text{M}_0]:[\text{I}]:[\text{L}]$  ratio at [50]:[1]:[0.2], and select solvent systems were evaluated for 5K PMA [60]:[1]:[0.2], 10K PMA [120]:[1]:[0.2] and 25K PMA [290]:[1]:[0.2]. Unless stated otherwise, reproducibility studies were performed for all experiments. For most samples a photograph of the polymerization mixture was taken before final polymer precipitation to capture the color, which may provide some qualitative inference of the difference in  $\text{Cu}^{\text{I}}/\text{Cu}^{\text{II}}$  ratio between solvent systems (increase in the intensity of blue would suggest higher  $\text{Cu}^{\text{II}}$  presence).

For each experiment, conversion of methyl acrylate was measured using NMR. An example of obtained spectra is displayed in Figure 3-3, where alkene peaks (5.4 – 6.2 ppm) of methyl acrylate decrease with conversion and methyl ester (-O-CH<sub>3</sub>) signal at 3.5 ppm is shifted upfield as polymerization proceeds. The change in the area under the alkene peaks relative to the constant area of the methyl ester peak corresponds to the change in concentration of monomer.

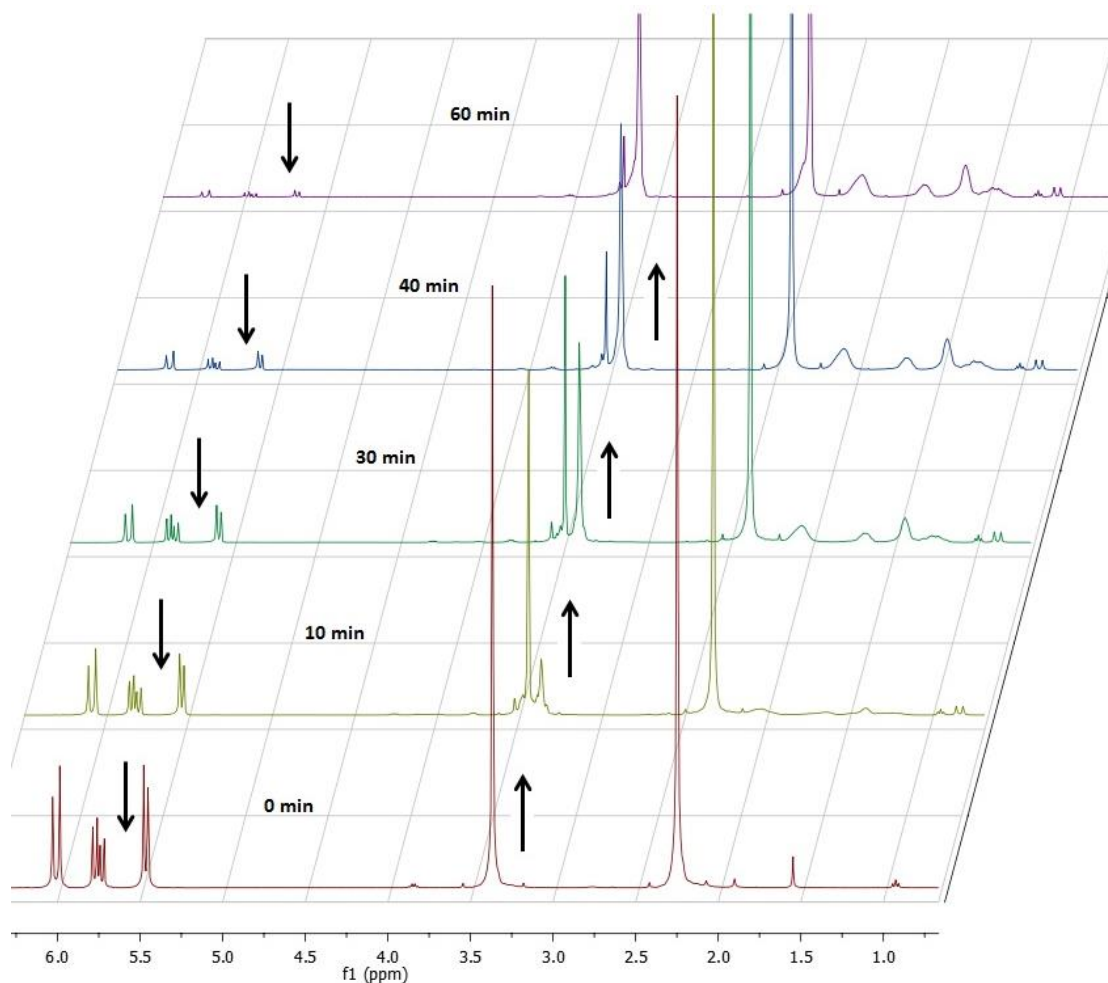


**Figure 3-3. 400Hz  $^1\text{H}$  NMR spectra ( $\text{CDCl}_3$ ) of PMA from polymerization catalyzed with copper wire/ $\text{Me}_6\text{-TREN}$  and initiated with EBiB used for monomer conversion measurement**

The chain-end functionality ( $\%f$ ), fraction of chains capped with bromine, of synthesized PMA was measured using NMR to establish the effect of the solvent systems on the livingness of polymerization. An example of  $^1\text{H}$  NMR spectrum is displayed in Figure 3-4, with signals assigned as follows: protons of the main chain  $\text{CH}_2$  and  $\text{CH}$  at 1.30 – 2.70 ppm, methyl ester group ( $-\text{O}-\text{CH}_3$ ) at 3.6 ppm, proton in the alpha position of the brominated chain-end  $\text{H}_h$  at 4.2 ppm, and initiator protons  $\text{H}_b$  ( $\text{CH}_2$ ) at 4.0 ppm,  $\text{H}_c$  ( $\text{CH}_3$ ) at 1.2 ppm, and  $\text{H}_a$  ( $2\text{CH}_3$ ) at 1.14 ppm.<sup>49</sup> Chain-end functionality was estimated using the integrals of peaks  $\text{H}_b$ ,  $\text{H}_c$  and  $\text{H}_a$  (initiator protons) and  $\text{H}_h$  (proton in the vicinity of bromine) (eqs. 1, 2, 3). At least two of the following equations were used to verify  $\%f$ .

$$\%f = \frac{H_h}{H_b/2} \times 100 \quad (1)$$

$$\%f = \frac{H_h}{H_c/3} \times 100 \quad (2)$$

$$\%f = \frac{H_h}{H_a/6} \times 100 \quad (3)$$

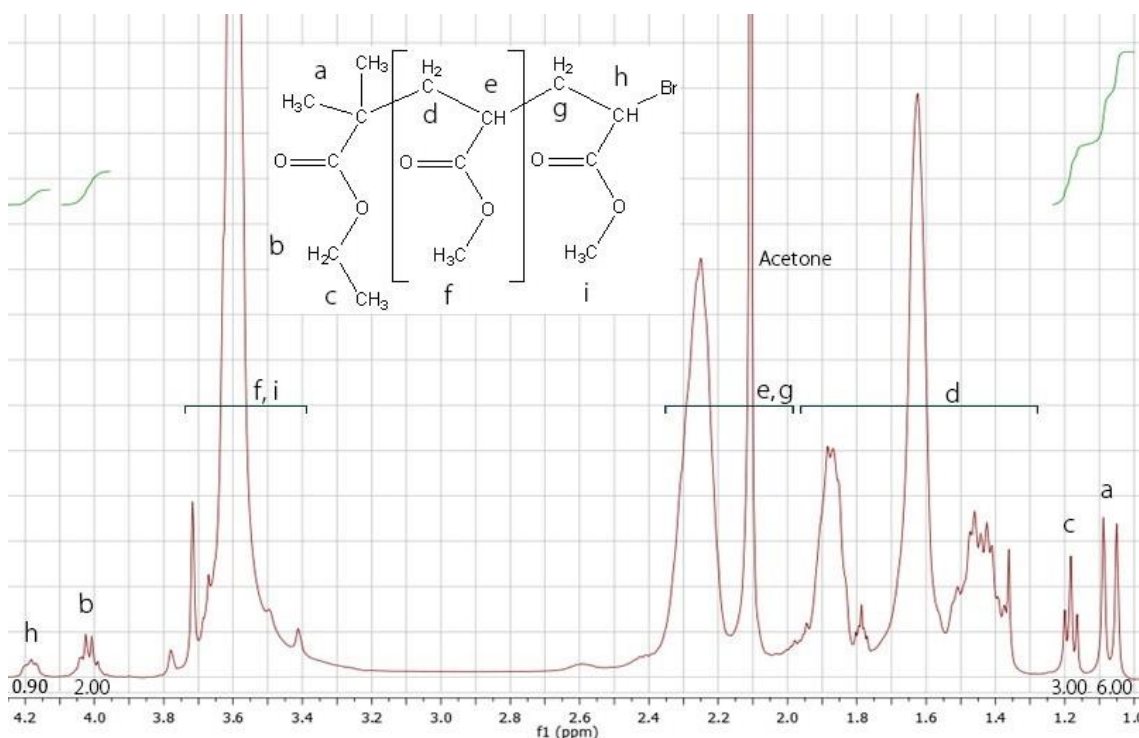


**Figure 3-4. 400Hz  $^1\text{H}$  NMR spectrum ( $\text{CDCl}_3$ ) of PMA from polymerization catalyzed with copper wire/ $\text{Me}_6\text{-TREN}$  and initiated with  $\text{EBiB}$ .**

### 3.3.1 Polymerization of MA in DMSO

The copper wire mediated polymerization of MA in DMSO was rapid (entry 84 and 85 in Table 3-1), with conversion reaching 80% in less than 50 minutes. The decline in polymerization rate observed in the normalized conversion plot ( $\ln([M]_0/[M])$  versus time) in Figure 3-6, once conversion reached 85%, indicates a decreasing number of radicals and presence of termination reactions, resulting in the loss of chain-end functionality (%f: 80% entry 84, 75% entry 85). An apparent rate of polymerization is represented by in two parameters ( $k_{app1}$  and  $k_{app2}$ ) in Table 3-1. The  $k_{app1}$  and  $k_{app2}$  values were estimated for qualitative analysis only, using the line of best fit, before and after the observed slope change in the normalized conversion plot respectively. The

color of the diluted mixture seen in Figure 3-5 had a greater hint of blue, indicating a shift of  $\text{Cu}^{\text{I}}/\text{Cu}^{\text{II}}$  ratio with increased fraction of solvent and, thus, decreased concentration of active species.

**Table 3-1. Polymerization of MA [50]:[1]:[0.2] in DMSO, 33%v/v (84) and 50%v/v (85), at 30°C**

Entry	v/v%	Time [min]	Conv.	%f	$M_w$	$M_n$	$\bar{D}$	$k_{app1}$ [ $\text{min}^{-1}$ ]	$k_{app2}$ [ $\text{min}^{-1}$ ]
84	33%	122	97%	82%	4,969	4,696	1.06	0.069	0.021
85	50%	180	99%	70%	5,241	4,965	1.06	0.054	0.017

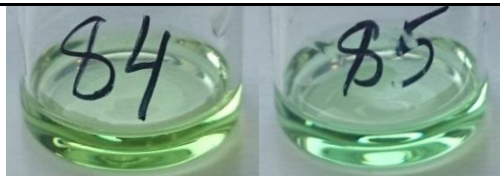


**Figure 3-5. Polymerization mixtures of MA [50]:[1]:[0.2] in DMSO 33%v/v (84) and 50%v/v (85) at 30°C**

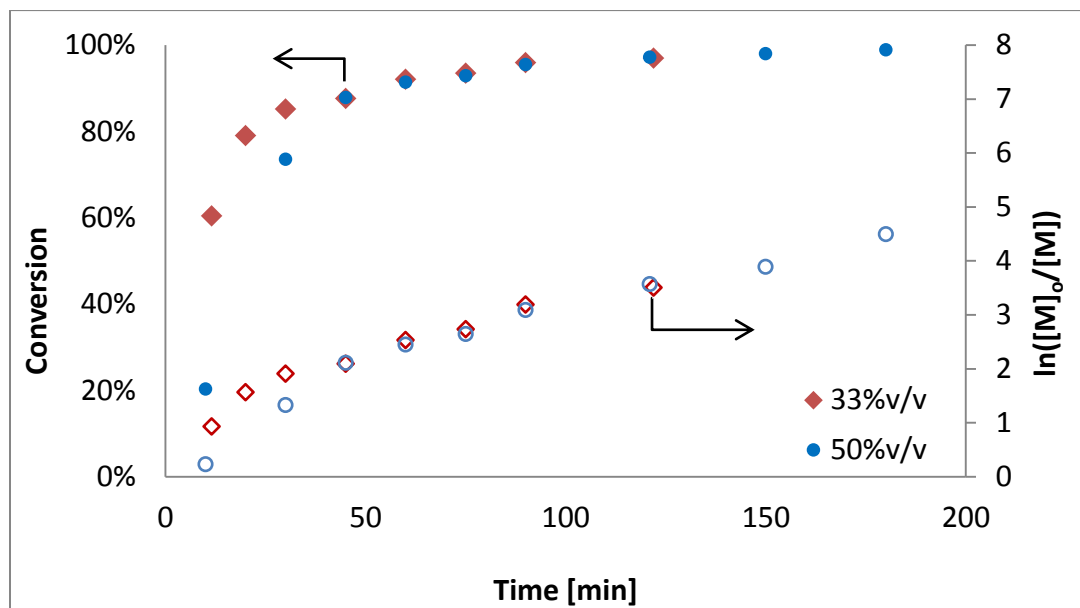


**Figure 3-6. Conversion and normalized conversion vs. time for MA [50]:[1]:[0.2] polymerized in DMSO, 33%v/v (84) and 50%v/v (85), at 30°C**

For both cases, 33%v/v and 50%v/v of DMSO, monomer conversion was high (97% and 99%), and molecular weight increased linearly with narrow dispersity (1.06, Figure 3-7). Increasing solvent volume from 33% to 50% decreased the rate of polymerization slightly from  $0.069 \text{ min}^{-1}$  to  $0.054 \text{ min}^{-1}$ . Dispersity broadening may have occurred as conversion approached

99% in the 50% v/v system; however, it cannot be stated with certainty, as the difference in values is low and may be due to an experimental error.

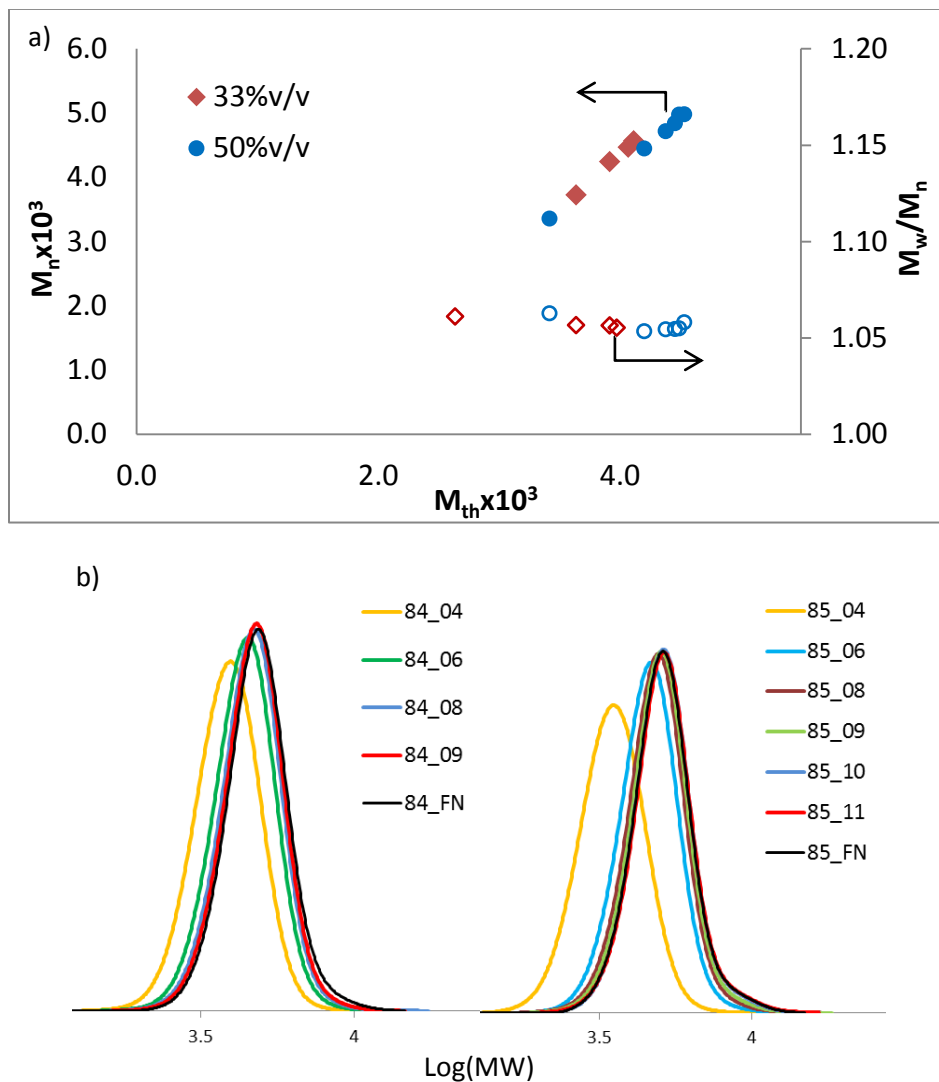


**Figure 3-7. Evolution of a) number-average molecular weight ( $M_n$ , filled symbols) and dispersity ( $M_w/M_n$ , open symbols) vs. theoretical molecular weight ( $M_{th}$ ), and b) Molecular weight distribution of PMA [50]:[1]:[0.2] synthesized in DMSO, 33%v/v (84) and 50%v/v (85), at 30°C**

In the diluted reaction mixture, with 50% v/v DMSO, polymerization proceeded for 180 minutes, rather than 120 minutes as in 33% v/v DMSO, before reaction needed to be stopped due to increased viscosity (the magnetic stirrer starts to skip rotations). The more dilute conditions and the extended reaction time increased conversion from 97% to 99%. However, chain-end functionality was lower in the 50% v/v solvent system (70% versus 82%), where possible causes

were 1) an extended reaction time, which led to increased termination, and/or 2) a decreased concentration of participating species due to the increased solvent fraction. Activation and deactivation of radicals is a diffusion-controlled process and as viscosity of a solution increases, diffusion of participating species is decreased.

Deviation from the results reported by Percec *et al.*, where nearly perfect chain-end retention was achieved, might be attributed to a 5°C temperature difference (30°C vs. 25°C with  $k_{app}$  of 0.020 min<sup>-1</sup>), and use of a different reaction volume (15-20 mL vs. 3 mL)<sup>28</sup> although these seem unlikely to have such a large effect. An increase in temperature would be expected to increase rate of polymerization, which may result in loss of some control and increased termination. This effect of temperature change on polymerization rate was evaluated for the 33% v/v DMSO system at 50°C with results summarized in Table 3-2.

**Table 3-2. Effect of increased temperature on polymerization of MA [50]:[1]:[0.2] in DMSO, 33%v/v, at 30°C (84) and 50°C (47)**

Entry	v/v%	Time [min]	Conv.	%f	M <sub>w</sub>	M <sub>n</sub>	Đ	$k_{app1}$ [min <sup>-1</sup> ]	$k_{app2}$ [min <sup>-1</sup> ]
84 – 30°C	33%	122	97%	82%	4,969	4,696	1.06	0.069	0.021
47 – 50°C	33%	60	95%	81%	5,037	4,768	1.06	0.106	0.032

Figure 3-8 shows an increase in polymerization rate with increased temperature, evident in the first 30 minutes, where the loss of radicals (represented by decreased slope in the normalized conversion plot) occurred at 78% instead of 85% at 30°C. These results would suggest that the initial increase in polymerization rate in DMSO at 30° (0.069 min<sup>-1</sup> vs. reported with  $k_{app}$  of 0.020 min<sup>-1</sup> at 25°C)<sup>28</sup> may have led to the loss of chain-end functionality noted in Table 3-1.



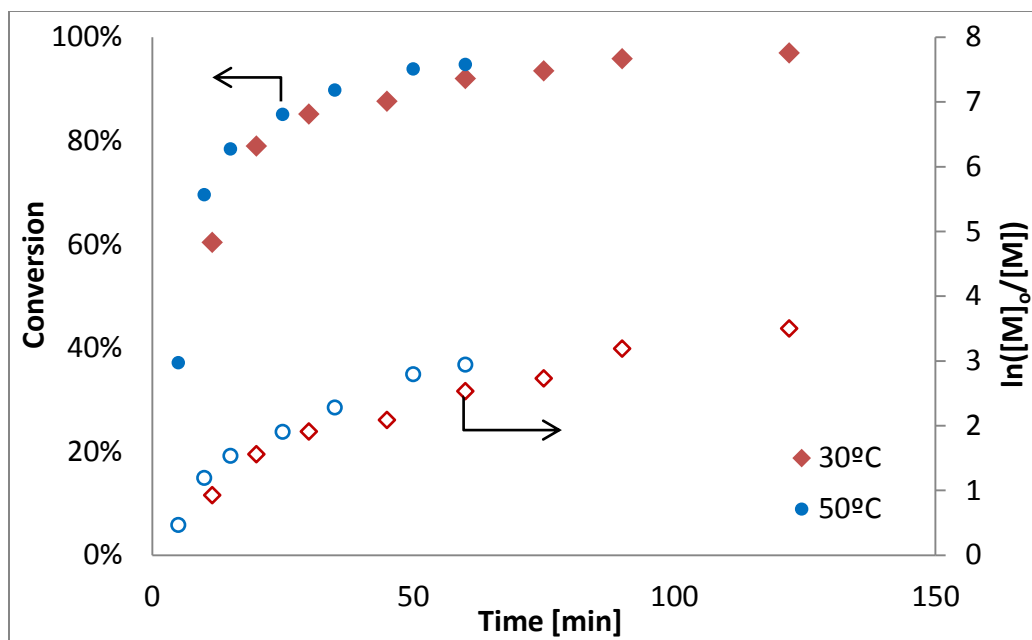


Figure 3-8. Conversion and normalized conversion vs. time for MA [50]:[1]:[0.2] polymerized in DMSO, 33%v/v, at 30°C (84) and 50°C (47)

Therefore, loss of chain-end functionality is a cumulative result of change in rate, concentration of active species, rate of activation versus deactivation, and extended reaction time.

### 3.3.2 Polymerization of MA in PEG and its binary mixtures

Under the same reaction conditions, MA was polymerized in PEG, entry 96 and 75 in Table 3-3, with good control (Figure 3-10), high conversion and well-preserved chain-end functionality. Compared to the polymerization kinetics in DMSO, the effect on the rate of polymerization with increased fraction of PEG was smaller, where the apparent rate ( $k_{app1}$ ) decreased slightly from 0.033 to 0.031  $\text{min}^{-1}$ . A decrease in radical concentration was not evident from the normalized conversion plot in Figure 3-10. The color of the polymerization mixtures (Figure 3-9) had a higher blue intensity than in DMSO, which were not transparent.

Table 3-3. Polymerization of MA [50]:[1]:[0.2] in PEG, 33%v/v (96) and 50%v/v (75), at 30°C

Entry	v/v%	Time [min]	Conv.	%f	$M_w$	$M_n$	$\bar{D}$	$k_{app1}$ [ $\text{min}^{-1}$ ]	$k_{app2}$ [ $\text{min}^{-1}$ ]
96	33%	105	94%	92%	4,883	4,274	1.14	0.033	-
75	50%	142	95%	92%	6,677	4,648	1.44	0.031	-

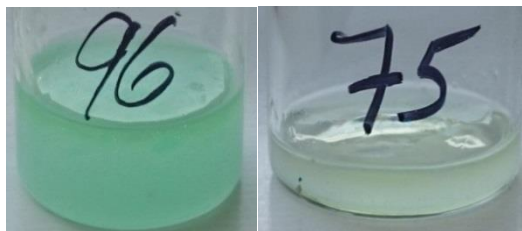


Figure 3-9. Polymerization mixtures of MA [50]:[1]:[0.2] in PEG 33%v/v (96) and 50%v/v (75) at 30°C

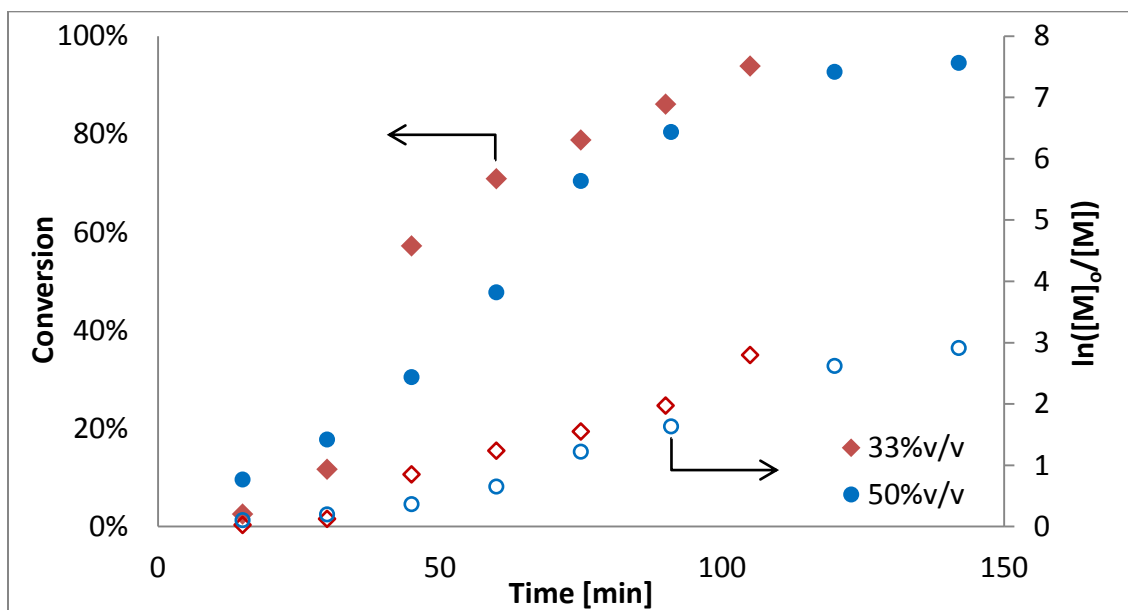
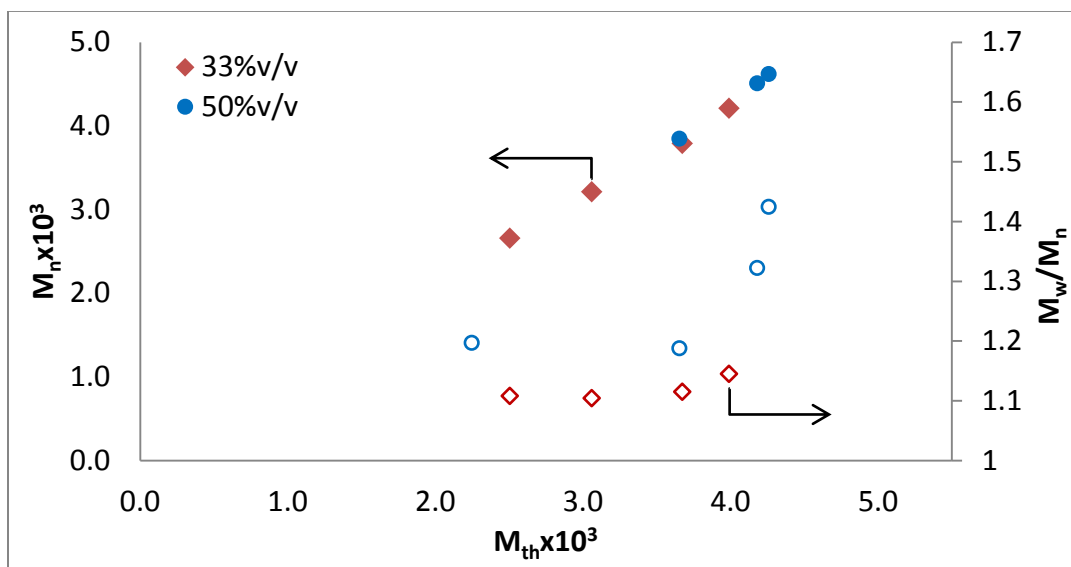


Figure 3-10. Conversion and normalized conversion vs. time for MA [50]:[1]:[0.2] polymerized in PEG, 33%v/v (96) and 50%v/v (75), at 30°C

A transition from a clear to opaque mixture may be associated with the observed increase in viscosity as polymerization proceeded. This observation correlated with broadening of dispersity after the conversion reached 80% (Figure 3-11 and Figure 3-12), possibly an indication of an inhibited diffusion process. The increase in dispersity (from 1.19 at 80% to 1.44 at 95% conversion) was more pronounced in the 50%v/v system, where the concentration of radicals was lower due to the increased volume of solvent. Slight upwards curvature (also seen in Harrison *et al.*<sup>37</sup>) in the conversion and the normalized conversion versus time plot (Figure 3-10) may indicate inefficient deactivation by  $\text{Cu}^{\text{II}}$  or faster activation, which may have been another contributing factor for the broadened dispersity. Since chain-end functionality was well preserved, the broader dispersity may not have been caused by bimolecular termination, but was

due to the increased viscosity, decreased diffusion of active species (radicals and monomer) and inhibited reversible termination.



**Figure 3-11. Evolution of number-average molecular weight ( $M_n$ , filled symbols) and dispersity ( $M_w/M_n$ , open symbols) vs. theoretical molecular weight ( $M_{th}$ ) of PMA [50]:[1]:[0.2] synthesized in PEG, 33%v/v (96) and 50%v/v (75), at 30°C**

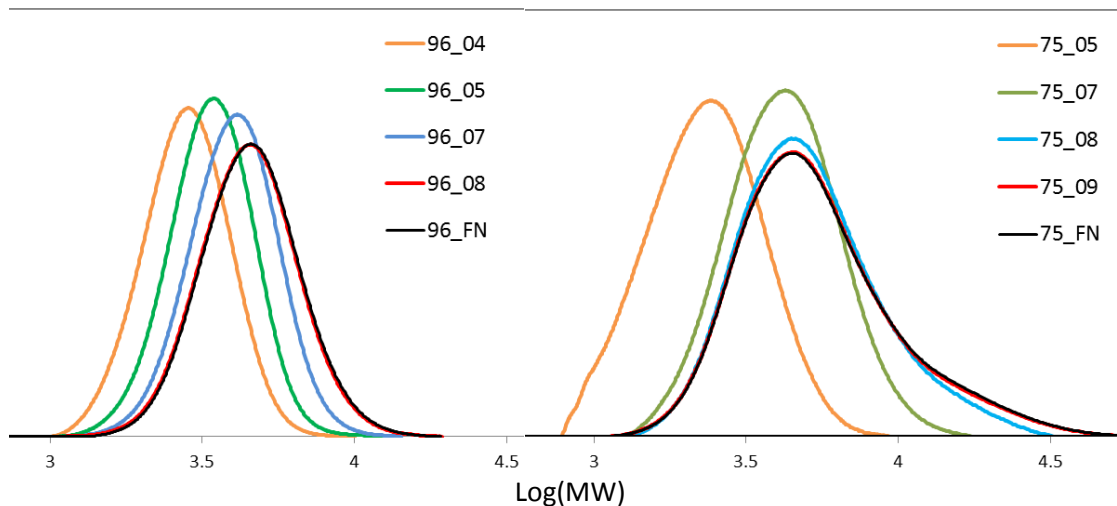


**Figure 3-12. Molecular weight distribution of PMA [50]:[1]:[0.2] synthesized in PEG, 33%v/v (96) and 50%v/v (75), at 30°C**

Another reason for broadening of dispersity with conversion may be inferred from the observed color of the reaction mixture (Figure 3-9), which had a higher blue intensity than the mixture in DMSO, indicating increased concentration of  $Cu^{II}$  species. This may suggest that  $Cu^{II}$  species are more stable in PEG, slowing down reversible termination, which is more pronounced

with a decreased amount of monomer as it also plays a role in stabilizing copper species.<sup>34</sup> Nevertheless, polymerizations in PEG showed good control and high chain-end retention (>90%). Furthermore, removal of copper was noticeably easier as reported by Perrier *et al.*, where PMA synthesized in PEG needed to be precipitated twice versus three times for PMA synthesized in DMSO to obtain a clear polymer.<sup>46</sup> To utilize these advantageous characteristics, overcome the viscosity effect and shift the balance between Cu<sup>I</sup> and Cu<sup>II</sup> species, binary mixtures of PEG with DMSO and ethanol were evaluated.

### 3.3.2.1 Polymerization of MA in PEG-DMSO mixtures

Results of polymerization of MA in binary mixtures of PEG and DMSO with secondary solvent fractions at 10% and 25% of the total solvent volume are summarized in Table 3-4.

**Table 3-4. Polymerization of MA [50]:[1]:[0.2] in binary PEG-DMSO mixtures, 33%v/v (70, 88) and 50%v/v (71, 89), at 30°C**

#	PEG-DMSO	v/v%	Time [min]	Conv.	%f	M <sub>w</sub>	M <sub>n</sub>	Đ	$k_{app1}$ [min <sup>-1</sup> ]	$k_{app2}$ [min <sup>-1</sup> ]
70	90-10	33%	75	91%	87%	4,707	4,264	1.10	0.027	-
88	75-25	33%	105	92%	90%	4,216	3,919	1.08	0.031	-
71	90-10	50%	125	95%	81%	5,118	4,568	1.12	0.023	-
89	75-25	50%	181	97%	83%	4,800	4,317	1.11	0.021	-

As demonstrated in Figure 3-13, the four solvent systems exhibited linear polymerization rates. The final dispersity was slightly broader in 50%v/v solvent systems (Table 3-4), but the values were still reasonably low for all cases. Higher conversion was reached in 50%v/v solvent systems as expected, but chain-end functionality was not as well preserved (<85%) as in pure PEG (>90%). The decreased fraction of chains effectively capped with bromine may be attributed to the diluted conditions and to the increased presence of DMSO as a secondary solvent, as higher chain-end loss was observed in pure DMSO (Table 3-1).

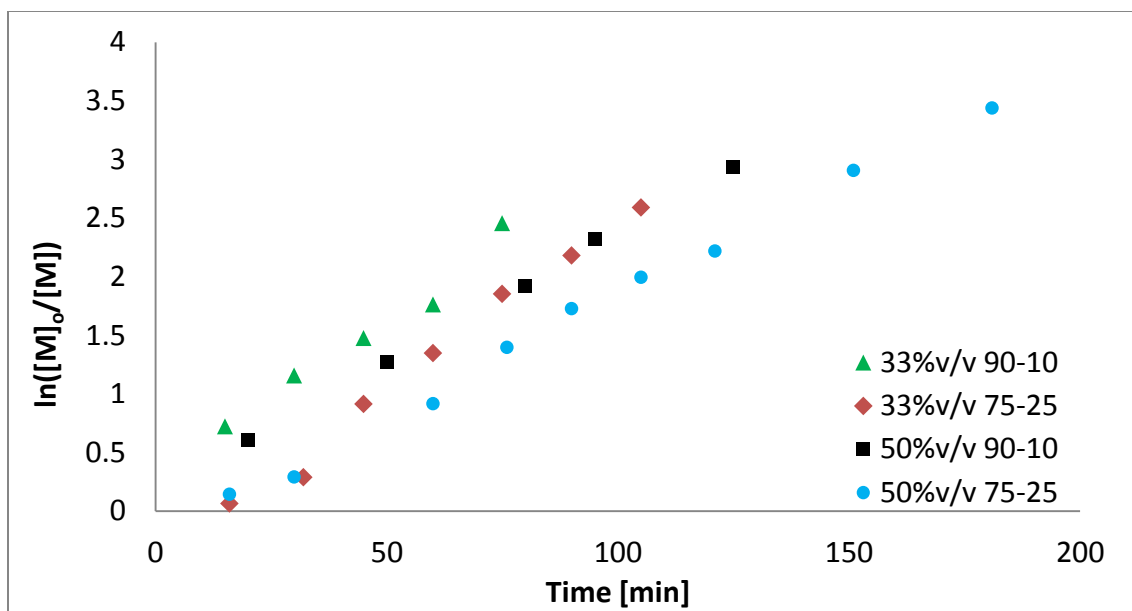


Figure 3-13. Normalized conversion vs. time for MA [50]:[1]:[0.2] polymerized in binary mixtures of PEG-DMSO, 33%v/v (70, 88) and 50%v/v (71, 89), at 30°C

As shown in Figure 3-14, even at 10% fraction of DMSO in both the 33% v/v and 50% v/v systems, control over dispersity was improved. However, broadening was still observed after 80% conversion. With 25% of DMSO in PEG, the dispersity continued to decrease with conversion.

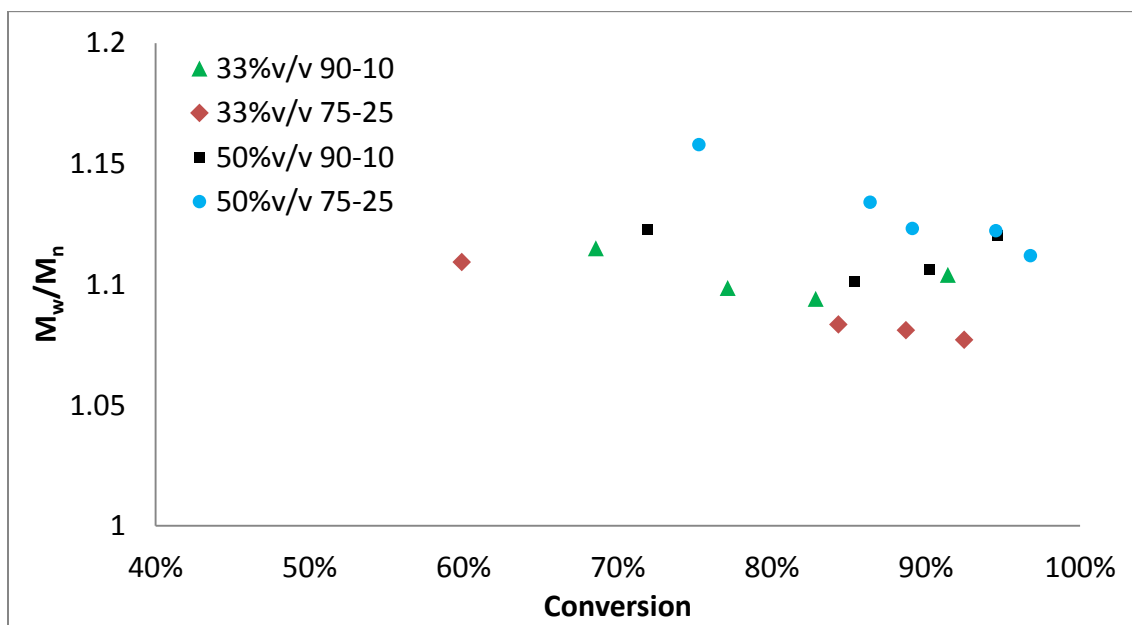
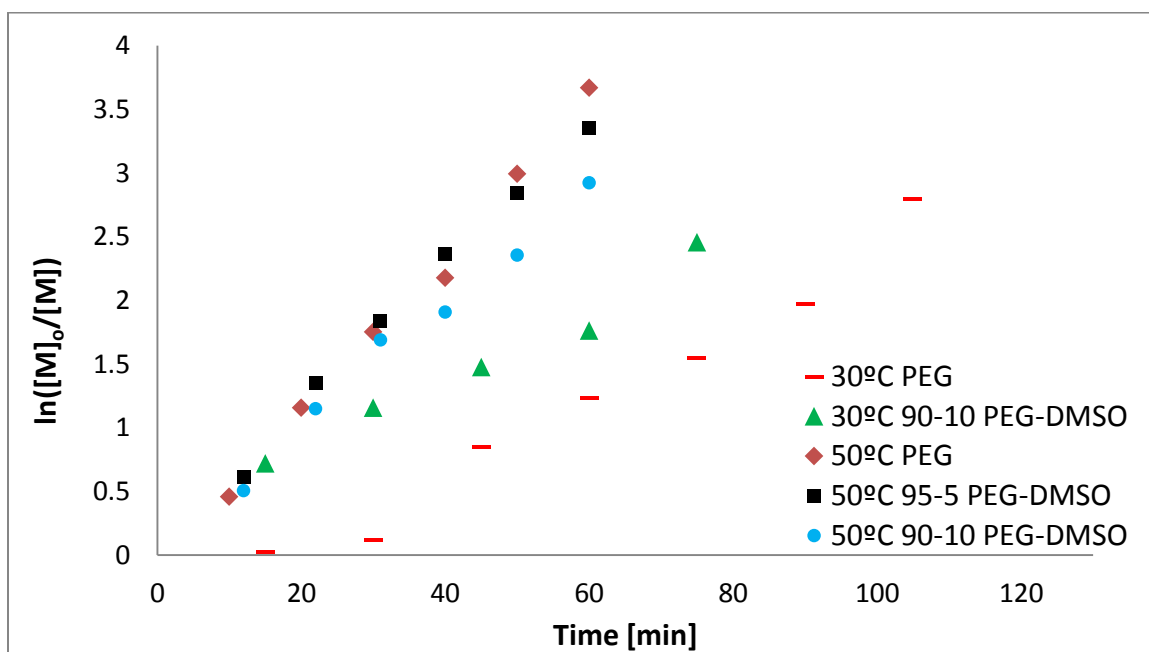


Figure 3-14 Dispersity ( $M_w/M_n$ ) vs. conversion for PMA [50]:[1]:[0.2] synthesized in binary mixtures of PEG-DMSO, 33%v/v (70, 88) and 50%v/v (71, 89), at 30°C

The effect of temperature increase from 30°C to 50°C was evaluated for PEG-DMSO mixtures (Table 3-5 and Figure 3-15).

**Table 3-5. Effect of temperature increase on polymerization of MA in PEG based solvent systems**

# - Temperature	PEG-DMSO	v/v%	Time [min]	Conv.	%f	$M_w$	$M_n$	$\bar{D}$	$k_{app1}$ [min <sup>-1</sup> ]	$k_{app2}$ [min <sup>-1</sup> ]
96 – 30°C	100-0	33%	105	94%	92%	4,883	4,274	1.14	0.033	-
70 – 30°C	90-10	33%	75	91%	87%	4,707	4,264	1.10	0.027	-
41 – 50°C	100-0	33%	60	97%	77%	6,068	5,566	1.09	0.061	-
45 – 50°C	95-5	33%	60	96%	87%	4,996	4,660	1.07	0.057	-
46 – 50°C	90-10	33%	60	95%	87%	5,047	4,705	1.07	0.048	-



**Figure 3-15. Normalized conversion vs. time for MA polymerized in PEG based solvent systems, 33%v/v, at 30°C (96, 70) and 50°C (41, 45, 46)**

The rate of polymerization increased with temperature as expected, and broadening of dispersity with conversion was eliminated. High conversions were achieved, with some loss of chain-end functionality observed in pure PEG. Increased temperature increased conversion as well, perhaps due to a decrease in viscosity effect. Based on these observations it can be concluded that if necessary, temperature increase could be used to improve the rate of polymerization, conversion and dispersity.

### 3.3.2.2 Polymerization of MA in PEG-Ethanol mixtures

Polymerizations in PEG-Ethanol solvent systems (Table 3-6 and Figure 3-17) displayed different characteristics compared to mixtures of PEG with DMSO, with the initial rate of polymerization higher in solvents containing ethanol. The dispersity continued to narrow with conversion for all systems, which may suggest that ethanol is a better diluting solvent for PEG, likely due to the lower density of ethanol. Increasing the fraction of ethanol content from 10% to 25% slightly decreased the dispersity and increased the rate of polymerization. Chain-end functionality was better preserved in 50% PEG-Ethanol, than 50% PEG-DMSO mixtures, and the conversion was slightly lower for 33% v/v systems.

**Table 3-6. Polymerization of MA [50]:[1]:[0.2] in binary PEG-Ethanol mixtures, 33% v/v (81, 86) and 50% v/v (83, 87), at 30°C**

#	PEG-Eth	v/v%	Time [min]	Conv.	%f	M <sub>w</sub>	M <sub>n</sub>	Đ	k <sub>app1</sub> [min <sup>-1</sup> ]	k <sub>app2</sub> [min <sup>-1</sup> ]
81	90-10	33%	80	87%	90%	4,571	4,186	1.09	0.037	-
86	75-25	33%	122	89%	87%	4,565	4,292	1.06	0.046	0.010
83	90-10	50%	153	95%	87%	5,110	4,577	1.12	0.029	-
87	75-25	50%	180	92%	87%	4,089	3,803	1.08	0.033	0.012



**Figure 3-16. Polymerization mixtures of MA in PEG-Ethanol 33% v/v (81, 86) and 50% v/v (83, 87)**

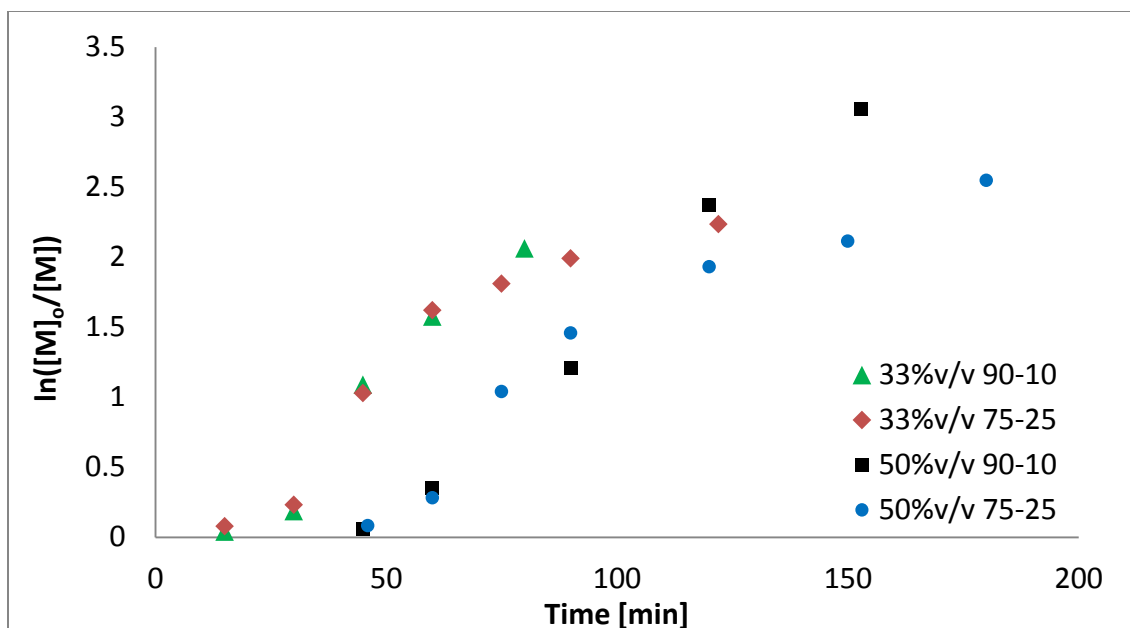


Figure 3-17. Normalized conversion vs. time for MA [50]:[1]:[0.2] polymerized in binary mixtures of PEG-Ethanol, 33%v/v (81, 86) and 50%v/v (83, 87), at 30°C

It would appear that the viscosity effect was minimized for the 50%v/v 90-10 PEG-Ethanol solvent system, allowing for conversions of 95%, acceptably narrow dispersity and chain-end functionality at 87%. The color of the final polymerization mixture (83, Figure 3-16) had a higher blue intensity, suggesting that  $\text{Cu}^{\text{I}}$  to  $\text{Cu}^{\text{II}}$  ratio may be similar to pure PEG.

### 3.3.2.3 5K, 10K and 25K PMA synthesized in 50% 90-10 PEG-Ethanol system

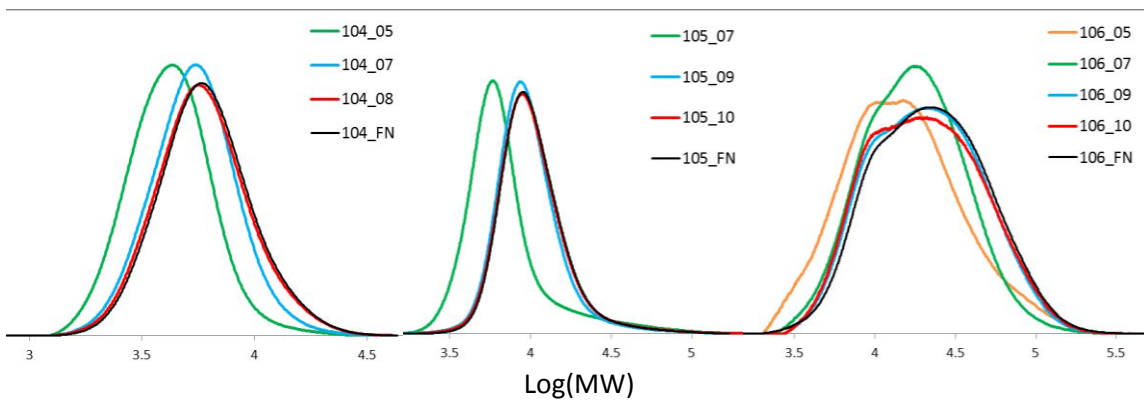
Based on the observations noted above, the 50%v/v 90-10 PEG-Ethanol mixture showed potential as an effective green solvent system for the synthesis of low molecular weight PMA. As such, it was investigated in further detail for PMA of 5K, 10K and 25K molecular weights, with results summarized in Table 3-7.

Table 3-7. Synthesis of 5K (104), 10K (105) and 25K (106) PMA in 50% 90-10 PEG-Ethanol mixtures, at 30°C

#	PEG-Eth	v/v%	Time [min]	Conv.	%f	$M_w$	$M_n$	$\mathcal{D}$	$k_{app1}$ [min <sup>-1</sup> ]	$k_{app2}$ [min <sup>-1</sup> ]
104 - 5k	90-10	50%	139	93%	91%	6,822	5,462	1.25	0.022	-
105 - 10k	90-10	50%	196	84%	89%	11,911	9,412	1.27	0.007	-
106 - 25k	90-10	50%	245	76%	91%	30,329	16,236	1.87	0.006	-



Polymerizations showed poor control over dispersity, especially for 25K PMA, although the rate of polymerization exhibited linear characteristics in normalized conversion plots (Figure 3-20) and good preservation of the chain-end functionality. This suggests that most chains were initiated with the initiator, but propagated at a different rate before conversion reached 20%, which may be attributed to slow activation. This effect was more evident with 25K PMA, where the concentration of radicals was very low, and therefore the activation rate was lower. The initially acquired broad dispersity carried throughout the rest of polymerization. Furthermore, phase separated domains were observed in the polymerization mixture as seen in Figure 3-19.



**Figure 3-18. Molecular weight distribution of 5K (104), 10K (105) and 25K (106) PMA synthesized in 50% 90-10 PEG-Ethanol, at 30°C**

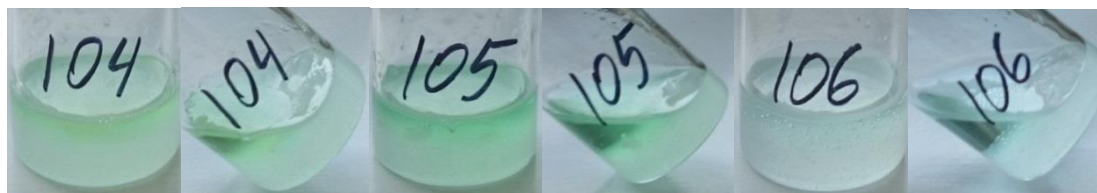


**Figure 3-19. Polymerization mixtures of MA in 50% 90-10 PEG-Ethanol at 30°C; 5K(104), 10K(105) and 25K(106)**

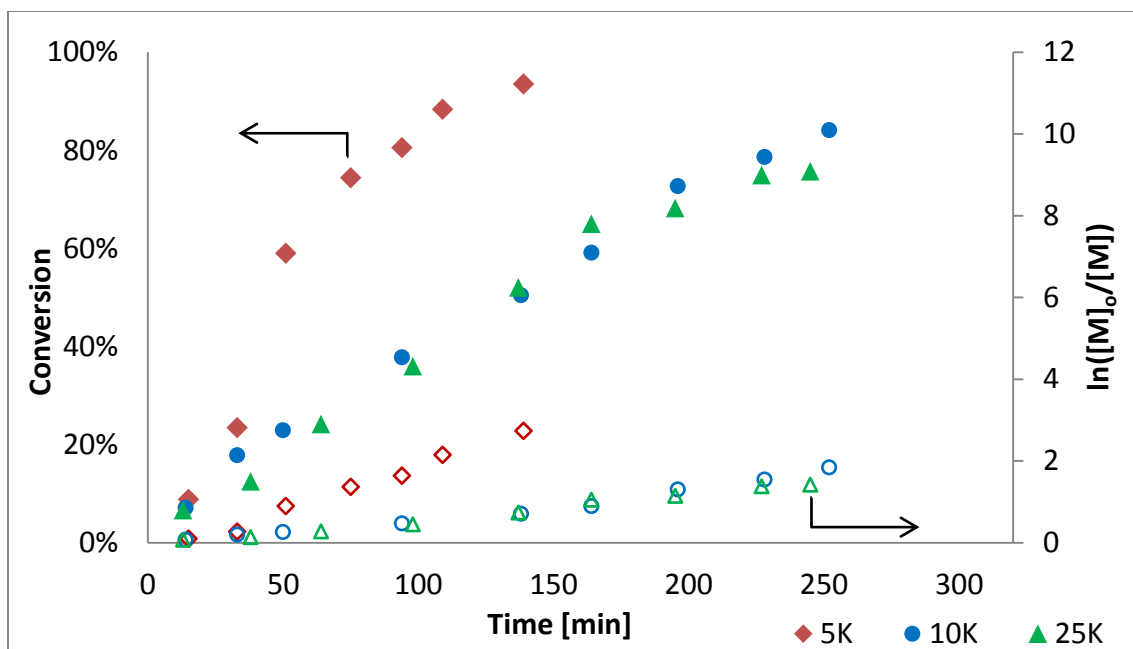


Figure 3-20. Conversion and normalized conversion vs. time for 5K (104), 10K(105) and 25K(106) PMA synthesized in 50% 90-10 PEG-Ethanol at 30°C

It was also noted that obtained dispersities varied significantly for 4K (entry 83) and 5K (entry 104) PMA. However, reproducibility studies were not performed, since the 50% 90-10 PEG-Ethanol mixture failed as a greener solvent system for copper wire mediated LRP of PMA. Next, a 33% 75-25 PEG-Ethanol mixture was evaluated as the next option based on entry 86 in Table 3-6, which overcame the viscosity effect, provided a narrow dispersity (1.06) and acceptable chain-end functionality (87%).

#### 3.3.2.4 5K, 10K and 25K PMA synthesized in 33% 75-25 PEG-Ethanol system

Synthesis of 5K, 10K and 25K PMA was performed in 33% 75-25 PEG-Ethanol at 30°C with results summarized in Table 3-8. Synthesis of 25K PMA was also performed in pure PEG for comparison (entry 113), which showed limited conversion (under 70%), possibly due to high viscosity, and broadening of the dispersity with conversion. The polymerization mixtures in 33% 75-25 PEG-Ethanol were uniform for all cases, without visible phase separation throughout the entire reaction time (Figure 3-21). The dispersity remained narrow (Figure 3-23) with conversion

(<1.1) and polymerizations were well-controlled (Figure 3-22). Chain-end functionality was preserved well, (~90%), which was higher than that of polymerization in pure DMSO.

**Table 3-8. Synthesis of 5K (109), 10K (110) and 25K (111) PMA in 33% 75-25 PEG-Ethanol mixtures, and 25K in pure PEG at 30°C**

# - Target MW	PEG-Eth	v/v%	Time [min]	Conv.	%f	$M_w$	$M_n$	$\bar{D}$	$k_{app1}$ [min <sup>-1</sup> ]	$k_{app2}$ [min <sup>-1</sup> ]
109 – 5K	75-25	33%	164	88%	91%	5,643	5,281	1.07	0.029	0.005
110 – 10K	75-25	33%	120	76%	90%	8,693	8,260	1.05	0.026	0.007
111 – 25K	75-25	33%	107	83%	86%	24,151	21,940	1.10	0.016	-
113 - 25K	100-0	33%	53	68%	94%	16,492	13,745	1.20	0.020	-

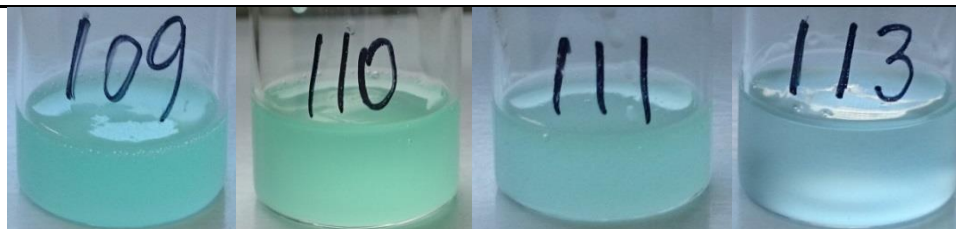


**Figure 3-21. Polymerization mixtures of MA in 33% 75-25 PEG-Ethanol, 5K(109), 10K(110) and 25K(111)**

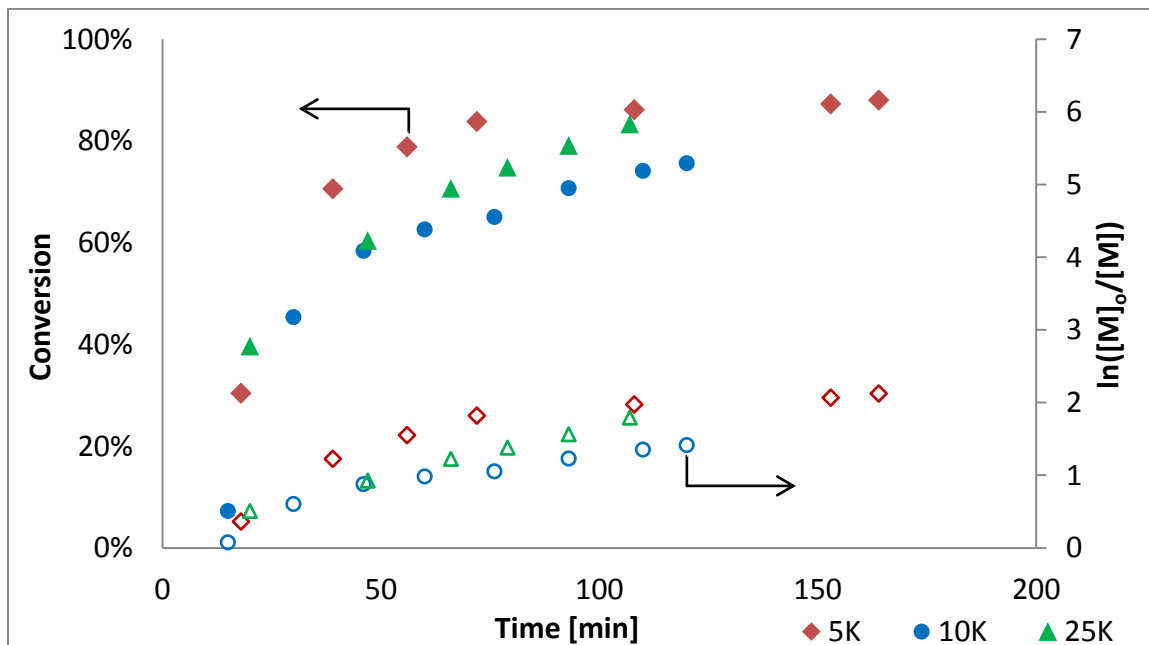


**Figure 3-22. Conversion and normalized conversion vs. time for 5K(109), 10K(110) and 25K(111) PMA synthesized in 33% 75-25 PEG-Ethanol at 30°C**

The evaluation showed that the 33% 75-25 PEG-Ethanol system can be considered an effective green solvent system that provides good control over polymerization, and results in PMA with narrow dispersity and well-preserved chain-end functionality. Since polymerizations

were stopped as viscosity increased, conversions were below 90%. However, further investigation should be performed to determine an optimal reaction time and temperature to maximize monomer conversion without significant change in the chain-end functionality and dispersity.

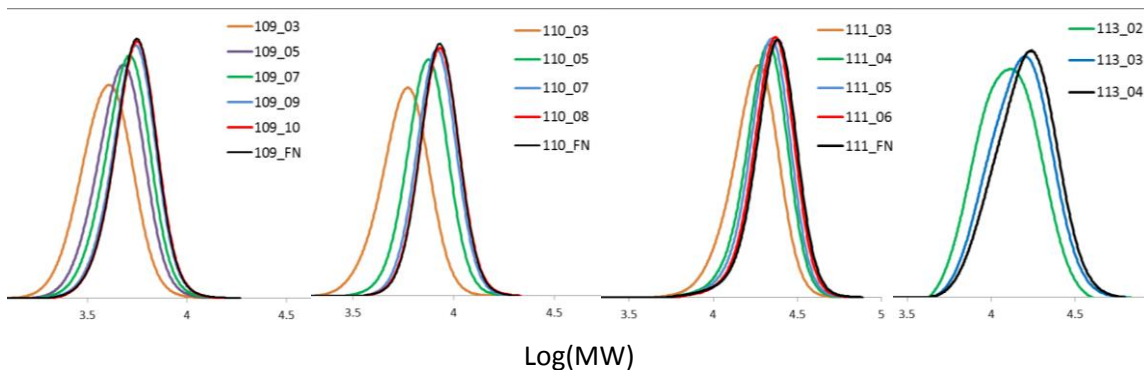


**Figure 3-23. Molecular weight distribution of 5K (109), 10K (110) and 25K (111) PMA synthesized in 33% 75-25 PEG-Ethanol, at 30°C**

### 3.3.3 Polymerization of MA in PPG and its binary mixtures

An analogous investigation was performed for the synthesis of 4K PMA in PPG and its binary mixtures with DMSO and ethanol. Polymerizations of MA in pure PPG resulted in a broad dispersity (Table 3-9), 1.42 in 33%v/v and 1.85 in 50%v/v. As seen in Figure 3-25, a high molecular weight polymer (~11K in 33%v/v and 19K in 50%v/v) formed at the start of the reaction, with monomer conversion below 5%. These long polymer chains exhibited dead chain behavior, as their growth was not apparent in the GPC data. Following this initial period, a controlled polymerization started, with chains growing slowly over 900 minutes. Chain-end functionality was over 80% for both systems, but the high dispersity suggests that initiation was very slow, and conditions in pure PPG were not favorable for the necessary ratio between the  $\text{Cu}^{\text{I}}$  and  $\text{Cu}^{\text{II}}$  species. Based on the color of the final mixtures, seen in Figure 3-25, it appears that  $\text{Cu}^{\text{I}}$  species were more stable in PPG, which may have decreased the activation rate of dormant chains.

**Table 3-9. Polymerization of MA [50]:[1]:[0.2] in PPG, 33%v/v (92) and 50%v/v (93) at 30°C**

#	v/v%	Time [min]	Conv.	%f	$M_w$	$M_n$	$\bar{D}$	$k_{app1}[\text{min}^{-1}]$	$k_{app2}[\text{min}^{-1}]$
92	33%	990	89%	85%	5,664	3,979	1.42	0.006	0.002
93	50%	990	93%	88%	9,131	4,938	1.85	0.003	-



**Figure 3-24. Polymerization mixtures of MA [50]:[1]:[0.2] in PPG, 33%v/v (92) and 50%v/v (93), at 30°C**

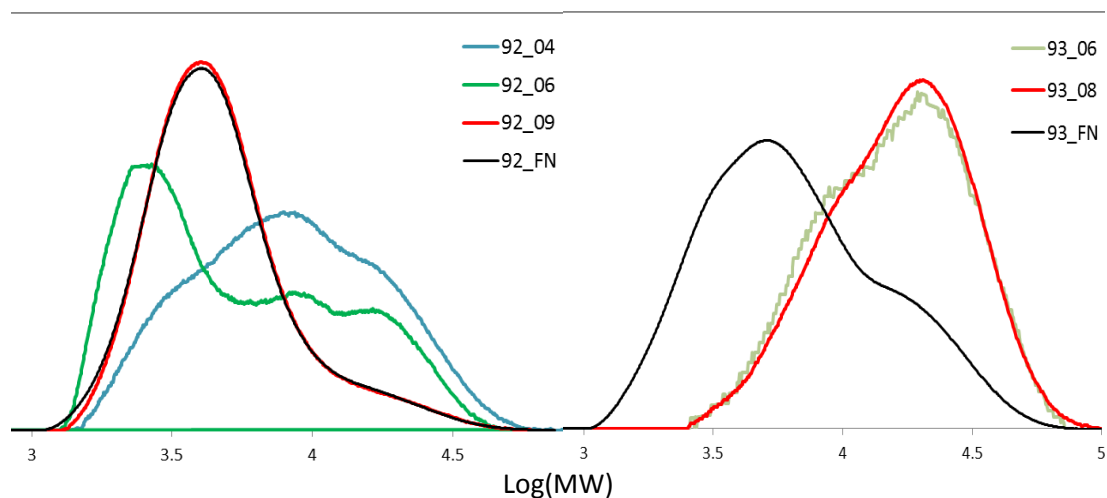


**Figure 3-25. Molecular weight distribution of PMA [50]:[1]:[0.2] synthesized in PPG, 33%v/v (92) and 50%v/v (93), at 30°C**

A control reaction was performed without the initiator, to determine if there were any impurities in the system that might have initiated the polymerization, but no polymer was formed without the initiator. This observation confirms that initiation was very slow in pure PPG, which resulted in a poorly controlled polymerization in the first hour until all radicals were activated.

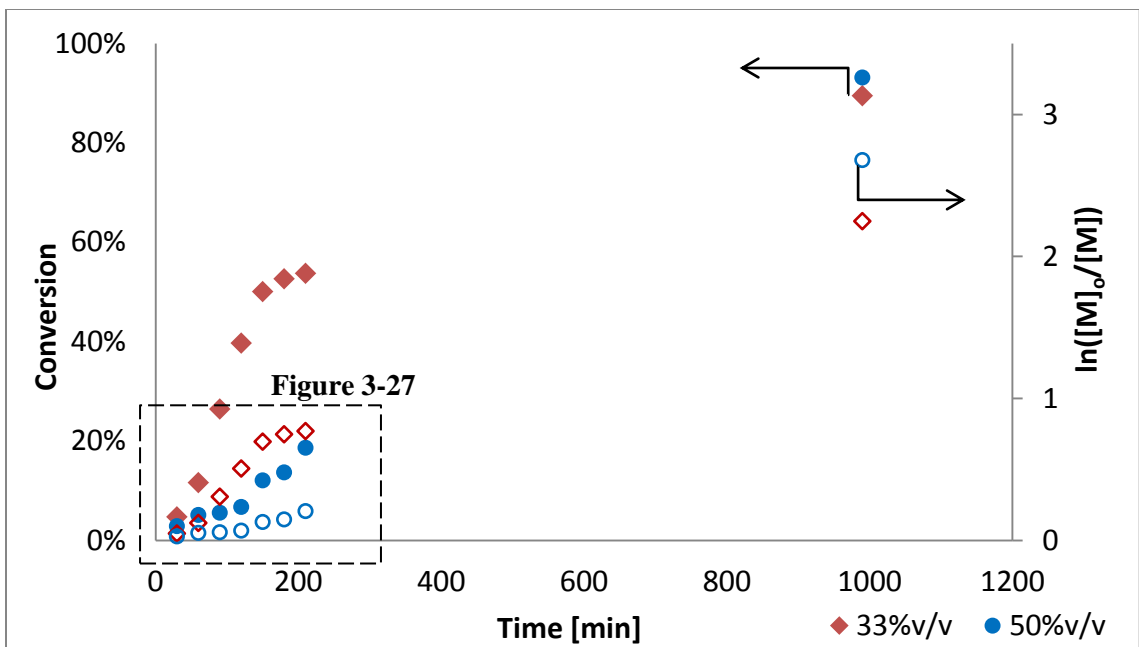


Figure 3-26. Conversion and normalized conversion vs. time for MA [50]:[1]:[0.2] polymerized in PPG, 33%v/v (92) and 50%v/v (93), at 30°C

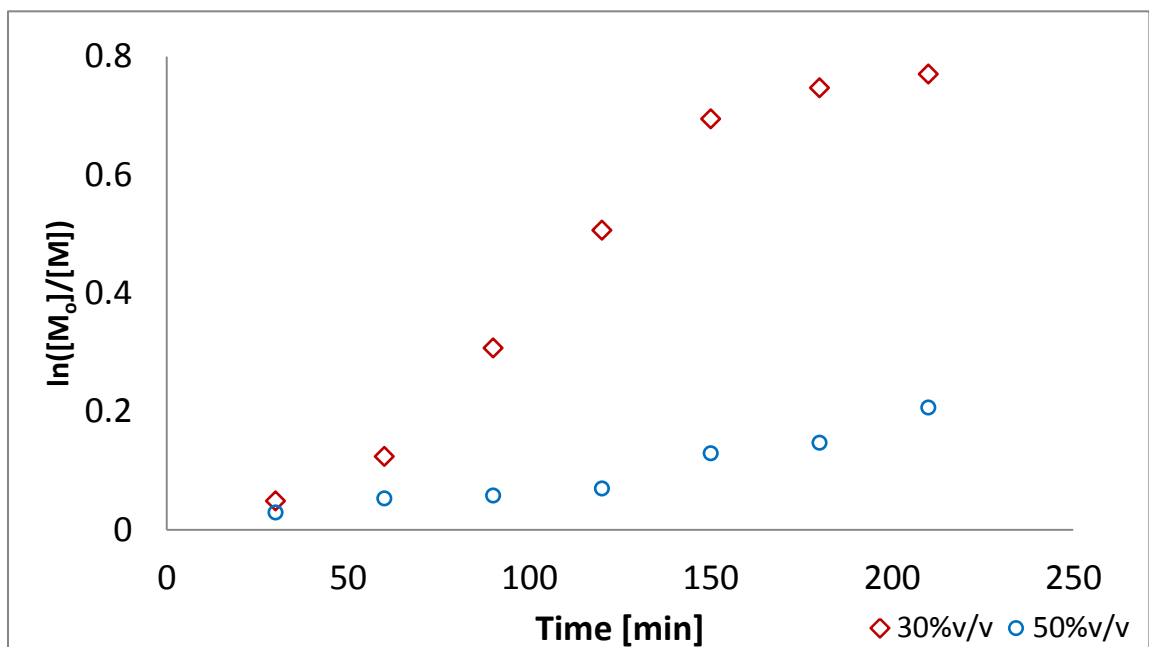


Figure 3-27. Expanded view of Figure 3-26, normalized conversion vs. time MA [50]:[1]:[0.2] polymerized in PPG, 33%v/v (92) and 50%v/v (93), at 30°C

The linear characteristics of the normalized conversion plot in Figure 3-26 and Figure 3-27 indicate that controlled polymerization occurred. The evidence for the initial formation of the

high molecular weight polymer was not expected to be seen in these plots as it appeared with monomer conversion under 5%.

### 3.3.3.1 Polymerization of MA in PPG-DMSO mixtures

Binary mixtures of PPG with DMSO were examined to determine if the addition of a secondary solvent known to provide good control over copper mediated LRP could improve polymerization in PPG. The results of adding 10% and 25% of DMSO to PPG are summarized in the Table 3-10. The addition of small amounts of DMSO (at least 10% of the total solvent volume) provided exceptional control over polymerization and dispersity, possibly by establishing necessary conditions for stabilization and solubility of the active copper species. This was also evident from the photograph of the final polymerization mixtures (Figure 3-28). The addition of 5% DMSO did not improve polymerization conditions and was comparable to pure PPG.

**Table 3-10. Polymerization of MA in binary PPG-DMSO mixtures, 33%v/v (94) and 50%v/v (95, 112, 103), at 30°C**

#	PPG-DMSO	v/v%	Time [min]	Conv.	%f	M <sub>w</sub>	M <sub>n</sub>	Đ	$k_{app1}$ [min <sup>-1</sup> ]	$k_{app2}$ [min <sup>-1</sup> ]
94	75-25	33%	238	88%	90%	4,038	3,808	1.06	0.014	0.006
95	75-25	50%	210	93%	88%	4,413	4,161	1.06	0.012	-
112	90-10	50%	365	77%	94%	4,419	4,036	1.09	0.006	-
103	95-5	50%	185	73%	94%	-	-	-	0.008	-

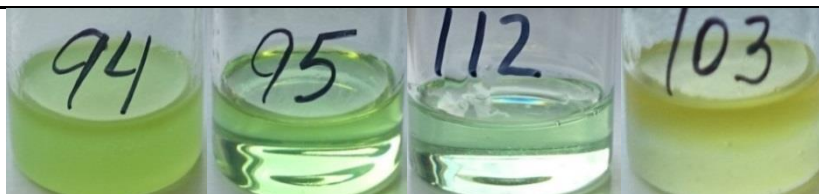


**Figure 3-28. Polymerization mixtures of MA in PPG-DMSO systems: 33%v/v 75-25 (94), 50%v/v 75-25 (95), 50%v/v 90-10 (112), and 50%v/v 95-5 (103)**

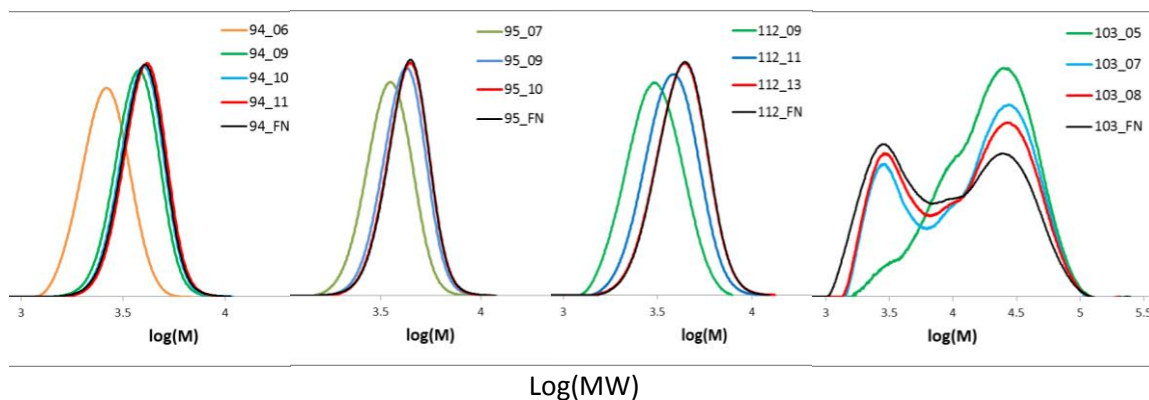


**Figure 3-29. Molecular weight distribution of PMA synthesized in PPG-DMSO systems: 33%v/v 75-25 (94), 50%v/v 75-25 (95), 50%v/v 90-10 (112), and 50%v/v 95-5 (103)**

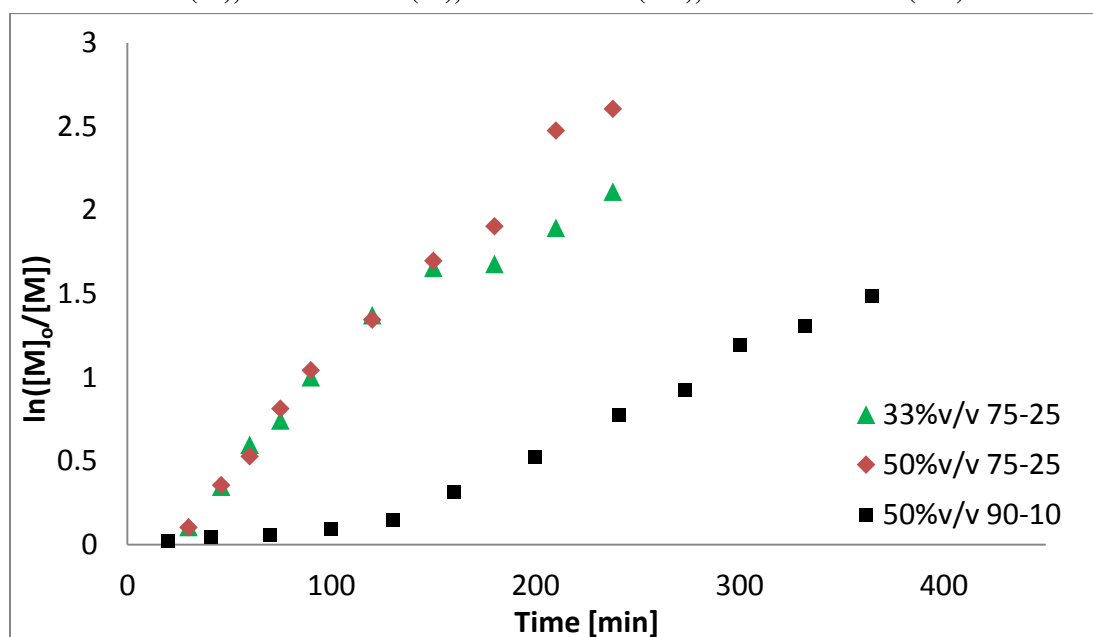


**Figure 3-30. Normalized conversion vs. time for MA polymerized at 30°C in PPG-DMSO systems: 33%v/v 75-25 (94), 50%v/v 75-25 (95), and 50%v/v 90-10 (112)**

The polymerization rate increased with increased fraction of DMSO added, however initiation remained slow with 10% of DMSO. Chain-end functionality was well-preserved for all cases. Control and livingness of polymerization in 33% 75-25 PPG-DMSO showed similar results and quality of polymer to that of the 33% 75-25 PEG-Ethanol system. Therefore, the 33% 75-25 PPG-Ethanol mixture was evaluated next as another potentially green MA polymerization media.



### 3.3.3.2 Polymerization of MA in 33% 75-25 PPG-Ethanol mixtures

Polymerizations of 4K and 10K PMA were performed at 30°C in a 33% 75-25 PPG-Ethanol mixture with results summarized in Table 3-11. An induction period was observed, which was longer with lower concentration of radicals (entry 99 – 10K). The dispersity decreased with conversion (Figure 3-32), and the polymerization mixture remained uniform throughout (Figure 3-31). Conversion was limited to 87% for 4K, and to 78% for 10K, where further investigation is required to determine the effect of extended reaction time and increased conversion, which may result in broader dispersity and decreased chain-end functionality.

**Table 3-11. Synthesis of 4K (97) and 10K (99) PMA in 33% 75-25 PPG-Ethanol mixtures, at 30°C**

# - Target MW	PPG-Ethanol	v/v%	Time [min]	Conv.	%f	M <sub>w</sub>	M <sub>n</sub>	Đ	k <sub>app1</sub> [min <sup>-1</sup> ]	k <sub>app2</sub> [min <sup>-1</sup> ]
97 – 4K	75-25	33%	255	87%	92%	4,083	3,667	1.11	0.012	0.003
99 – 10K	75-25	33%	460	78%	96%	6,154	5,518	1.12	0.008	-



**Figure 3-31. Polymerization mixtures of 4K (97) and 10K (99) PMA in 33%v/v 75-25PPG-Ethanol**

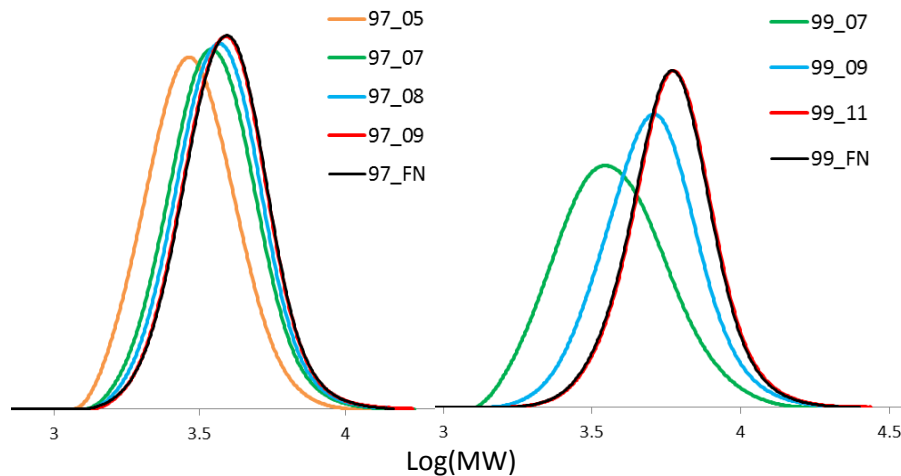


**Figure 3-32. Molecular weight distribution of 4K (97) and 10K (99) PMA synthesized in 33%v/v 75-25 PPG-Ethanol at 30°C**

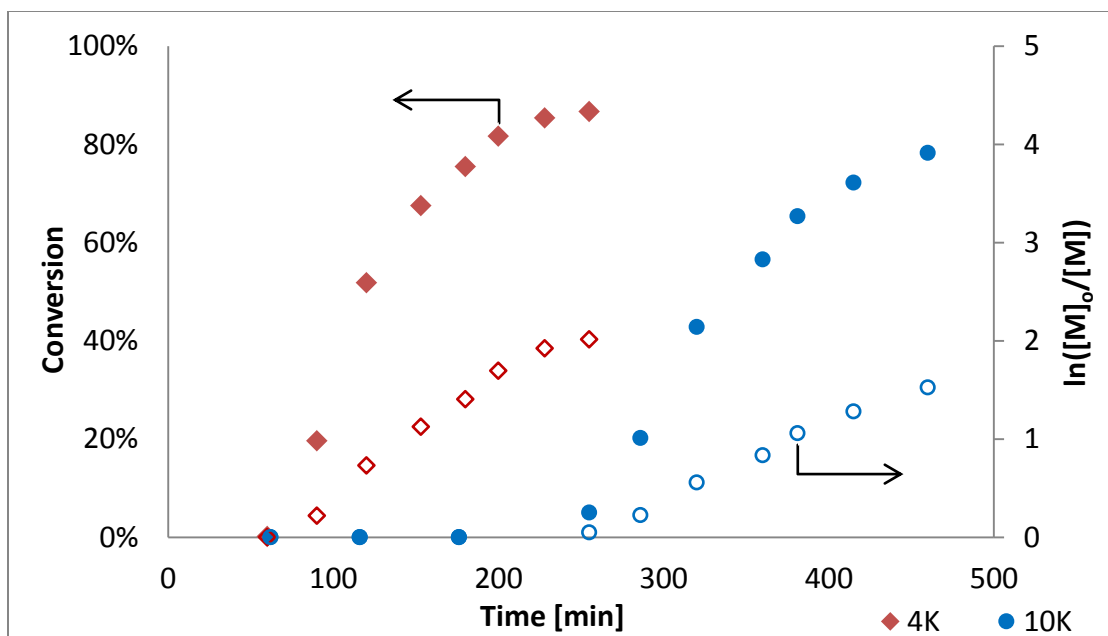


Figure 3-33. Conversion and normalized conversion vs. time for 4K (97) and 10K (99) PMA synthesized in 33%v/v 75-25 PPG-Ethanol at 30°C

Based on these observations and results, 33% 75-25 PPG-Ethanol can be considered a reasonably good green solvent system for the polymerization of low molecular weight PMA with narrow dispersity and well-preserved chain-end functionality. Chain-end retention was higher in solvent systems with PPG than with PEG (96% vs. 89% for 10K PMA, entry 105 in Table 3-7 vs. entry 99 in Table 3-11), but reaction time was significantly longer (460 min vs. 196 min) with an induction period of 250 minutes (Figure 3-33). An increase in temperature can be used to improve the rate of polymerization, but an effect on dispersity and chain-end retention needs to be investigated further.

### 3.4 Conclusion & Recommendations

In this study, two greener solvent systems for copper wire mediated CLRP of MA were successfully developed. These novel solvent systems consist of 75% PEG or PPG and 25% ethanol, where total volume of solvent to monomer is 33%. Synthesis of 5K, 10K and 25K PMA was performed in the PEG-Ethanol mixture with good control, narrow dispersity (<1.1) and well-preserved chain-end functionality (91%, 90% and 86% respectively). If higher chain-end

functionality is desired for subsequent utilization, polymerizations can be stopped under 80% of monomer conversion to avoid any further chain terminating reactions.

Polymerization of MA (4K and 10K) in the PPG-Ethanol mixture was significantly slower (255 and 460 minutes respectively), with slow initiation and an induction period (50 and 250 minutes). Rates of polymerizations in PPG-Ethanol solvent were three times lower than in PEG-Ethanol. Nevertheless, control over the polymerization and characteristics of PMA were comparable to those of PMA synthesized in PEG-Ethanol. Retained chain-end functionality was over 90%, and dispersity remained narrow (~1.1).

Increase in temperature was demonstrated to increase rate of polymerization, conversion, and dispersity, with some loss of chain-end functionality, in the evaluation of the PEG-DMSO mixtures at 30°C and 50°C. Therefore, it is reasonable to assume that increasing temperature in the established PEG-Ethanol and PPG-Ethanol systems will reduce viscosity, improve the kinetics, conversion and dispersity if required, with possible decrease in chain-end retention.

During the development of these greener systems, an increase in the total solvent volume from 33% to 50% of DMSO, PEG and PPG, and binary mixtures of PEG-DMSO, PEG-Ethanol, PPG-DMSO and PPG-Ethanol were examined in detailed. The following solvent effects were observed. Dispersity increased with monomer conversion exceeding 80% in mixtures based on PEG or PPG with lower fraction or in the absence of a diluting solvent (Ethanol or DMSO). A decrease in the rate of polymerization, seen in the slope change of the normalized conversion versus time plot was often correlated with the broadening of dispersity. In some of these cases, chain-end functionality remained high (>90%), suggesting increase in dispersity may have been caused by increased viscosity with conversion, which lead to inhibited diffusion and inefficient reversible termination. Increasing the overall solvent fraction from 33% to 50% resulted in even broader dispersity and lower chain-end functionality, which may have been a result of a

decreased concentration of participating species and an extended reaction time due to diluted conditions, leading to increased termination.

An interesting effect was a result of a slow initiation in PPG, where high molecular weight polymer formed in the first hour of polymerization with conversion of monomer under 5%. Then, controlled polymerization dominated the reaction. This behavior resulted in a double peak molecular weight distribution and a broad dispersity. The addition of at least 10% of DMSO to PPG improved the activation step and resulted in an exceptional control, good livingness and narrow dispersity. It was also observed, as previously reported in the literature by Perrier *et al.*, that the removal of copper was faster during precipitation in systems with PEG and PPG mixtures when comparing to pure DMSO.<sup>46</sup> The recyclability potential of these solvents was not evaluated in this study, but should be considered for large scale reactions.

## Chapter 4.

# **‘Grafting-*to*’ Cellulose using Thio-Bromo Click Reaction by Utilizing Bromine Chain-End Functionality of PMA Synthesized via Copper Wire Mediated Controlled Living Radical Polymerization**

### **Abstract**

The purpose of this study was to utilize a bromine chain-end functionality of polymer grafts for grafting *to* cellulose and its derivatives. Bromine terminated low molecular weight poly(methyl acrylate) grafts were synthesized via copper wire-mediated controlled living radical polymerization with ethyl 2-bromoisobutyrate (EBiB) as the initiator. Microcrystalline cellulose and cellulose acetate were functionalized with ethylene sulfide to obtain thiol functionality. The grafting step was performed by attaching a well-defined poly(methyl acrylate) chains *to* thiol sites on the cellulose backbone using thio-bromo click reaction. Resulting materials were analyzed gravimetrically and with gel permeation chromatography and nuclear magnetic resonance spectroscopy to determine molecular weights, molecular structures and grafting efficiency.

### **4.1 Introduction**

Cellulose is the most abundant renewable polymer in the world, which makes it an attractive alternative to petroleum-based feedstocks for polymers. Facing numerous environmental challenges, it is becoming increasingly important to utilize such an abundant resource. This natural polymer is biocompatible, biodegradable, inexpensive, and has good mechanical and unique optical properties, but it is poorly soluble, hygroscopic and difficult to process.<sup>50</sup> Hence, it requires modification prior to use. Cellulose and its derivatives have been used for over 150 years in fibers, films, coatings, and as additives to food, pharmaceuticals and building materials.<sup>50</sup> Developing new uses for cellulose by exploiting emerging techniques and

technologies can help meet a growing demand for environmentally friendly and biocompatible products.

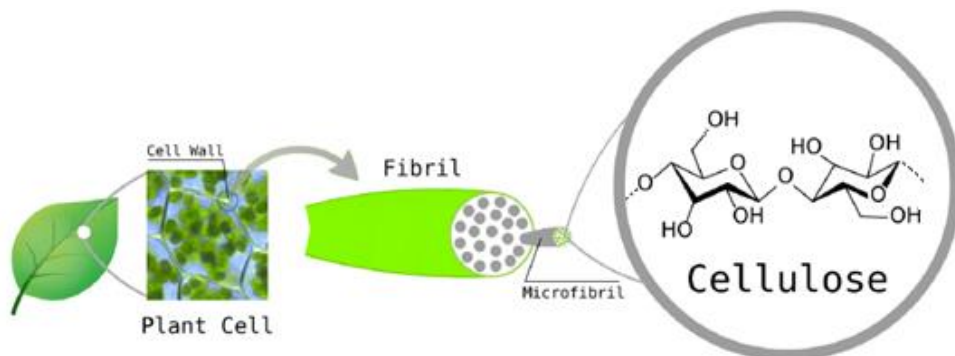


**Figure 4-1. Cellulose Structure**

Cellulose is a long chain polymer, with three hydroxyl group per anhydroglucose unit (AGU) as shown in Figure 4-1. Hydroxyl groups on the backbone are typically replaced with functional groups to form a product or cellulose derivative, such as a widely used material, cellulose acetate (Figure 4-2).

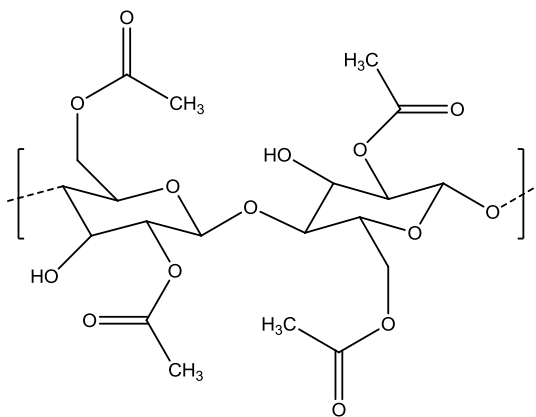


**Figure 4-2. Cellulose Acetate**

One of the evolving methods of modifying cellulose is graft copolymerization, where synthetic polymer grafts replace hydroxyl groups on the cellulose backbone to alter properties such as elasticity, sorption, temperature responsiveness, thermal and microbial resistance, flexibility and resistance to abrasion.<sup>51</sup> The two main approaches of cellulose modification noted in the literature are the grafting *from* and grafting *to* techniques, as displayed in Figure 4-3. In the

grafting *from* method, cellulose is converted into a macroinitiator *from* which polymerization of synthetic grafts is performed. Whereas, in the grafting *to* approach grafts are synthesized separately, cellulose is functionalized by converting hydroxyl groups into accepting sites, and grafts are then attached *to* the accepting sites on the cellulose backbone or surface.

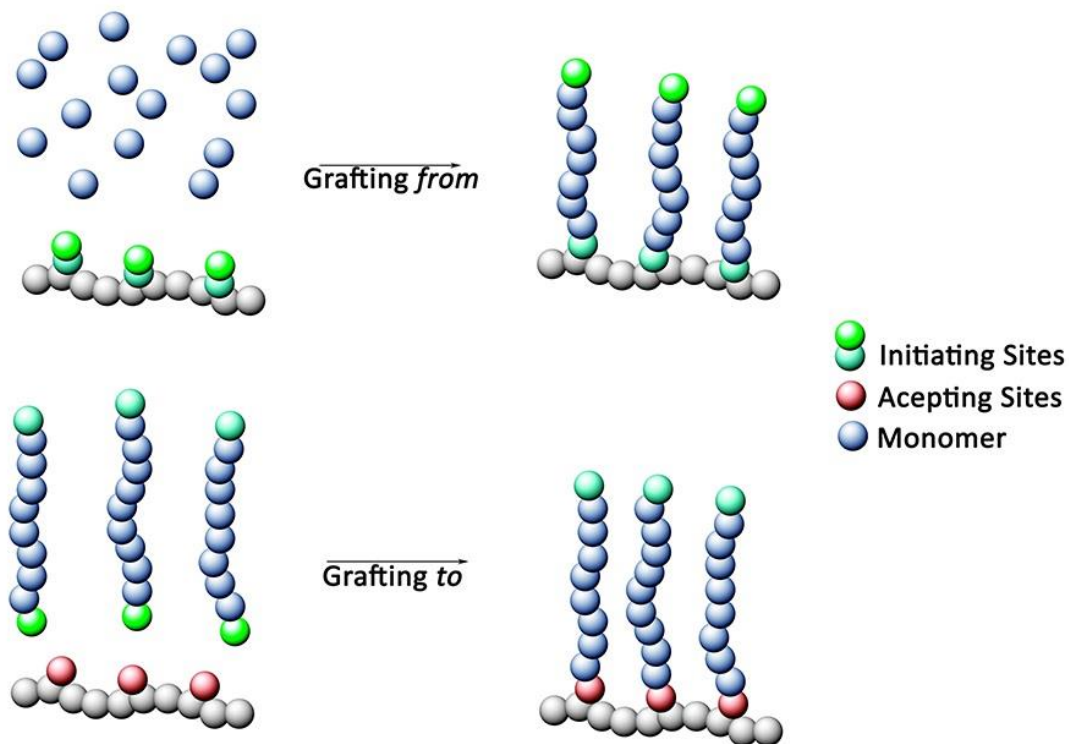


**Figure 4-3. Grafting *from* and Grafting *to* scheme**

In the last decade, the grafting *from* approach has been thoroughly studied, with grafts polymerized from initiating sites on the cellulose backbone using controlled living radical polymerization.<sup>51,52</sup> However, rates of initiation and polymerization are often slow, and characterization of grafted chains is difficult.<sup>53-56</sup> One of the advantages of the grafting *from* mechanism is that grafts can be synthesized in-situ and lead to higher grafting efficiency as smaller monomer molecules will diffuse to reactive sites more readily. In the grafting *to* method, previously attached polymer chains may result in steric hindrance and block access to the accepting sites for other chains.<sup>10,51,52,57-60</sup> One of the key disadvantages of the grafting *from*

technique is characterization of grafts, as polymer chains need to be cleaved from the cellulose for analysis, which makes tuning of properties of the final materials challenging. The use of a sacrificial initiator to form a free polymer in the same reaction media as grafting has been shown to have similar molecular weight and dispersity as the grafts.<sup>10,53,58,61</sup>

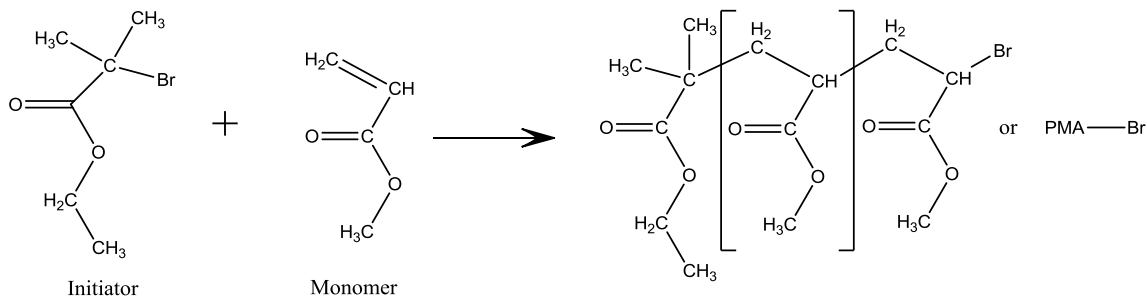
In the grafting-*to* technique, polymer grafts with an appropriate end group can be synthesized using facile and well-established controlled polymerization techniques. Grafts can be characterized prior to attachment to the substrate, allowing for easier tuning of the final material properties by targeting specific molecular weight and dispersity of grafts. Although the grafting density is expected to be lower than in the grafting *from* approach<sup>10</sup>, this aspect is of a lesser concern since higher cellulose content is generally desired. Numerous efficient conjugation reactions for grafting *to* method have been studied, which include thiol-ene,<sup>62-65</sup> hetero Diels-Alder,<sup>66,67</sup> and azide-alkyne cycloaddition.<sup>10,68-70</sup> Often, an additional step is required to impart necessary chain-end functionality to the polymer grafts for grafting *to* an accepting site on the cellulose backbone. The goal of this study is to evaluate thio-bromo click reaction as a grafting mechanism *to* cellulose and exploit the existing bromine chain-end functionality of low molecular weight poly(methyl acrylate) prepared by copper wire mediated controlled living radical polymerization (CLRP). In case of successful grafting, this method could be expanded to other polymers to create new cellulose-based copolymers. The correlation between the properties of these new copolymers and characteristics (dispersity and molecular weight) of polymer grafts could also be established.

The grafting *to* procedure performed in this study is outlined in Figure 4-4, consisted of three steps. First, poly(methyl acrylate) grafts with bromine chain-end functionality were synthesized with copper wire mediated CLRP. The molecular weights of the polymer grafts evaluated to demonstrate the effect of steric hindrance were ~2,500 g/mol and ~5,500 g/mol, which was expected to increase with the molecular weight of grafts, thereby decreasing the

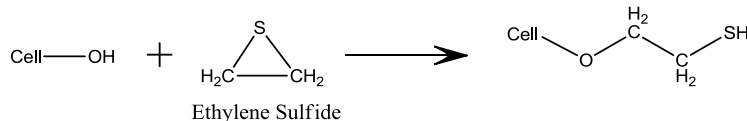


achievable grafting density.<sup>10,71</sup> Second, cellulose was functionalized with thiol groups via ring opening reaction with ethylene sulfide.<sup>72-74</sup> Third, grafting was performed with a facile thio-bromo click reaction.<sup>11,29,75,76</sup>

**Step 1. Polymer grafts synthesis**



**Step 2. Cellulose functionalization**



**Step 3. Grafting of polymer grafts to cellulose**

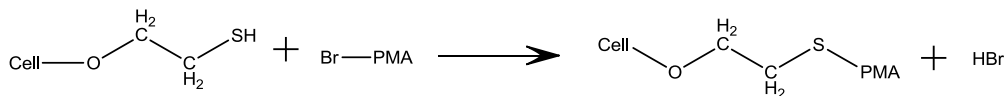


**Figure 4-4. Grafting to scheme**

One-pot and two-pot reactions were investigated. In the one-pot system, cellulose functionalization and grafting steps were performed subsequently in the same reaction vessel. One-pot reactions were performed to minimize the possibility of losing thiol groups by oxidation during purification. In two-pot system, thiol functionalized cellulose was first purified, and then used for grafting, as functionalization reaction conditions may not have been effective for the subsequent grafting. Cellulose substrates investigated in parallel in this study included Avicel © microcrystalline cellulose (MCC) and cellulose acetate, as cellulose acetate is soluble in many organic solvents and can be characterized with NMR and GPC.

## 4.2 Experimental

### 4.2.1 Materials

Ethyl 2-bromoisobutyrate (EBiB) (98%, Aldrich), tris[2-(dimethylamino)ethyl]amine (Me<sub>6</sub>-TREN) (97%, Aldrich), dimethyl sulfoxide (DMSO) (99.5%, Fischer), triethylamine (Et<sub>3</sub>N) (99%, Aldrich), Avicel © PH-101 microcrystalline cellulose (MCC) (~50µL, Aldrich), cellulose acetate (M<sub>n</sub> ~30,000g/mol, DS ~2.5, Aldrich), boron trifluoride diethyl etherate (BF<sub>3</sub>.Et<sub>2</sub>O, Aldrich) and ethylene sulfide (98%, Aldrich), dimethylformamide (DMF) (99.8%, Fischer), tetrahydrofuran (Reagent grade, Fischer), acetonitrile (CH<sub>3</sub>CN) (HPLC Grade, Fischer), pyridine (99.9%, Fischer) were used as received. 1,4-dioxane (99%, Fischer) was dried with magnesium sulfate prior to use. Methyl acrylate (MA, 99%) was purchased from Sigma Aldrich and passed through a column of basic aluminum oxide (Al<sub>2</sub>O<sub>3</sub>, Sigma Aldrich) prior to use in order to remove a radical inhibitor. Copper wire (1mm diameter, Sigma) was submerged in hydrochloric acid (HCl, Fisher) for 10 minutes and washed with methanol prior to use. All reactions were performed under N<sub>2</sub> atmosphere.

### 4.2.2 Characterization

Grafting yield was analyzed gravimetrically, by comparing weights of cellulose substrate and polymer after unattached grafts were removed from the cellulose acetate by soxhlet extraction with methanol for three days, and from microcrystalline cellulose by filtration with THF. Gel permeation chromatography (GPC) was performed on a Waters 2695 GPC separation module with a 410 differential refractometer as a detector and five Waters Styragel columns in series at temperature of 40°C. Distilled THF (Fisher, HPLC grade) was used as an eluent with a flow rate of 0.3 mL/min. Weight average (M<sub>w</sub>) and number-average (M<sub>n</sub>) molecular weights were determined with polystyrene standards and corrected using Mark-Houwink parameters (K=0.000611 mL/g, α=0.799).<sup>48</sup>

Monomer conversion and PMA chain-end functionality were measured using 400MHz  $^1\text{H}$  NMR Bruker Avance instrument. For monomer conversion analysis the number of scans was set to 64, spectra were recorded at 23°C in chloroform-d ( $\text{CDCl}_3$ ) with tetramethylsilane (TMS) as an internal standard. For chain-end functionality analysis of PMA grafts, the number of scans was set at 160 with an 8s delay ( $D_1$ )<sup>28</sup>, spectra were recorded at 23°C in acetone- $d_6$  with tetramethylsilane (TMS) as an internal standard. Cellulose acetate and PMA grafts were also analyzed with HSCQ NMR to determine if there were any changes to the molecular structure following the grafting procedure. HSQC spectra were recorded with 10 scans in acetone- $d_6$ .  $^1\text{H}$  NMR spectra of cellulose acetate before and after the grafting procedure was recorded with 160 scans at 23°C in acetone- $d_6$  with tetramethylsilane (TMS) as an internal standard.

#### 4.2.1 Procedure

The grafting *to* procedure consisted of three steps: 1) synthesis of poly(methyl acrylate) grafts with bromine chain-end functionality using copper wire mediated CLRP; 2) functionalization of cellulose substrate with ethylene sulfide to obtain thiol groups (accepting sites); and 3) grafting of PMA to the cellulose substrate using a thio-bromo click reaction. In the one-pot reaction systems step two and step three were performed in the same vessel. In the two-pot reaction, functionalized cellulose substrate was precipitated and washed prior to grafting.

##### 4.2.1.1 Synthesis of PMA grafts with bromine chain-end functionality

For each polymerization reaction, copper wire (6cm long, 1mm diameter) was immersed in HCl for 10 minutes and washed with methanol. The target molecular weights of PMA grafts were 2,500 g/mol and 5,500 g/mol, where the  $[\text{M}_0]:[\text{I}]:[\text{L}]$  ratios were [25]:[1]:[0.1] and [60]:[1]:[0.2], respectively. In a 250 mL three neck round bottom flask, solvent (DMSO, 25 mL) was combined with copper wire wrapped around a magnetic mixer, ligand  $\text{Me}_6\text{-TREN}$  (0.59 mL, 2.22 mmol or 0.49 ml, 1.85 mmol) and initiator EBiB (3.26 mL, 22.2 mmol or 1.36 mL, 9.26

mmol). The reaction vessel was then placed in an oil bath at 30°C and purged with nitrogen. Methyl acrylate (50 mL, 555.8 mmol) was passed through a basic alumina column to remove an inhibitor and injected into the reaction flask. Samples were taken periodically and dissolved in cold CDCl<sub>3</sub>. First, conversion was measured by <sup>1</sup>H NMR. Then, samples were passed through a small aluminum oxide column to remove residual copper, and analyzed with GPC to determine M<sub>n</sub>, M<sub>w</sub> and M<sub>w</sub>/M<sub>n</sub> (Đ). The final polymerization mixture was precipitated in cold deionized water, dissolved in THF and precipitated (repeated three times). The final polymer was dried under vacuum, and analyzed with <sup>1</sup>H NMR to determine chain-end functionality.

#### ***4.2.1.2 Example of one-pot ‘Grafting to’ procedure***

In a 100 mL three neck round bottom flask, 0.5 g (~0.56 mmol of reactive sites) of cellulose acetate was dissolved in 16 mL of dioxane or 0.5 g (~9.26 mmol of reactive sites) of microcrystalline cellulose was suspended in 20 mL of dioxane at 60°C under nitrogen. 45 μL (0.7 mmol) of ethylene sulfide (varied for different experiments to determine if grafting density could be controlled) and 100 μL of BF<sub>3</sub>·Et<sub>2</sub>O were added to the solution. The reaction was left overnight. The reaction temperature was then reduced to 50°C, and 0.3 mL (2.15 mmol) of Et<sub>3</sub>N and 3g of PMA (0.85 mmol of bromine chain-ends) dissolved in 10 mL of dioxane were added to the reaction media. The reaction was again left overnight. The solution was precipitated in cold deionized water, and washed with THF. Unattached polymer was removed from the cellulose acetate using soxhlet extraction with methanol for three days, and from microcrystalline cellulose by filtration with THF. Products were evaluated gravimetrically, to determine if grafting had occurred and if the weight of the used cellulose substrate has increased due to the attached polymer chains. The recovered cellulose acetate and unattached polymer were analyzed by GPC and NMR to determine if any changes had occurred in the molecular structure.

#### ***4.2.1.3 Example of the procedure of the 'Grafting to' via a two-pot process***

In a 100 mL three neck round bottom flask, 0.5 g (~0.56 mmol of reactive sites) of cellulose acetate (CA) was dissolved in 16 mL of dioxane or 0.5 g (~9.26 mmol of reactive sites) of microcrystalline cellulose (MCC) was suspended in 20 mL of dioxane at 60°C under nitrogen. 0.3 mL (5.0 mmol) of ethylene sulfide (varied for different experiments to determine if grafting density can be controlled) and 100  $\mu$ L of  $\text{BF}_3 \cdot \text{Et}_2\text{O}$  were added to the solution. The reaction was left overnight. The solution was precipitated in cold acetonitrile and washed several times.

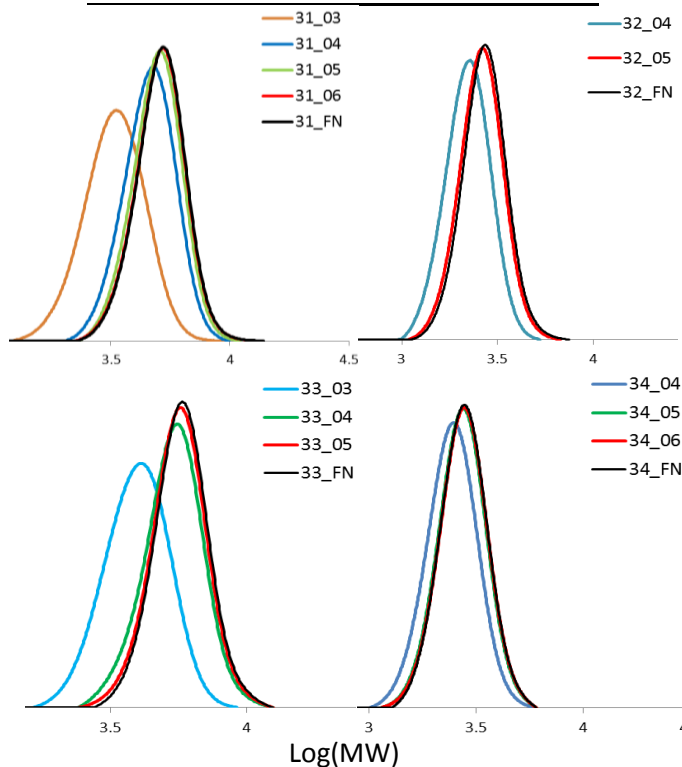
The product was mixed with 16 mL (CA) or 20 mL (MCC) of acetonitrile at 50°C. 0.3 mL (2.15 mmol) of  $\text{Et}_3\text{N}$  and 4.7 g of PMA (1.48 mmol of bromine chain-end functionality) dissolved in 10 mL of acetonitrile were added to the reaction medium and the reaction left overnight. The solution was precipitated in cold deionized water, and washed with THF. Unattached polymer was removed from cellulose acetate using soxhlet extraction with methanol for three days, and from microcrystalline cellulose by filtration with THF. To determine if grafting had occurred, the products were evaluated gravimetrically, establishing whether the weight of the cellulose substrate had increased due to the attached polymer chains. The recovered cellulose acetate and unattached polymer were analyzed by GPC and NMR to determine if any changes had occurred in the molecular structure.

### **4.3 Results and Discussion**

PMA grafts with bromine chain-end functionality were prepared in batches of ~50 g and separated into 3-5 g portions to be used for the grafting experiments. Molecular weight characteristics and chain-end functionality (%) of the obtained grafts are summarized in Table 4-1, with the molecular weight distribution of PMA during synthesis and of the final product shown in Figure 4-5.

**Table 4-1. PMA grafts characteristics**

Batch #	%f	M <sub>w</sub>	M <sub>n</sub>	Đ
31	87%	5,100	4,781	1.07
32	88%	2,709	2,516	1.08
33	78%	5,940	5,540	1.07
34	82%	2,934	2,713	1.08

**Figure 4-5. Molecular weight distribution of PMA grafts during synthesis and of the final polymer**

The chain-end functionality of the PMA grafts was estimated using <sup>1</sup>H NMR spectrum, an example of which is displayed in Figure 4-6. Signals were assigned as follows: protons of the main chain CH<sub>2</sub> and CH at 1.30 – 2.70 ppm, methyl ester group (-O-CH<sub>3</sub>) at 3.6 ppm, proton in the alpha position of the brominated chain-end H<sub>h</sub> at 4.2 ppm, and initiator protons H<sub>b</sub> (CH<sub>2</sub>) at 4.0 ppm, H<sub>c</sub> (CH<sub>3</sub>) at 1.2 ppm, and H<sub>a</sub> (2CH<sub>3</sub>) at 1.14 ppm.<sup>49</sup> The integrals under the peaks H<sub>b</sub>, H<sub>c</sub> and H<sub>a</sub> (initiator protons) and H<sub>h</sub> (proton in the vicinity of bromine) (eqs. 1, 2, 3) were used for estimation of %f. At least two of the following equations were used for verification:

$$\%f = \frac{H_h}{H_b/2} \times 100 \quad (1)$$

$$\%f = \frac{H_h}{H_c/3} \times 100 \quad (2)$$

$$\%f = \frac{H_h}{H_a/6} \times 100 \quad (3)$$

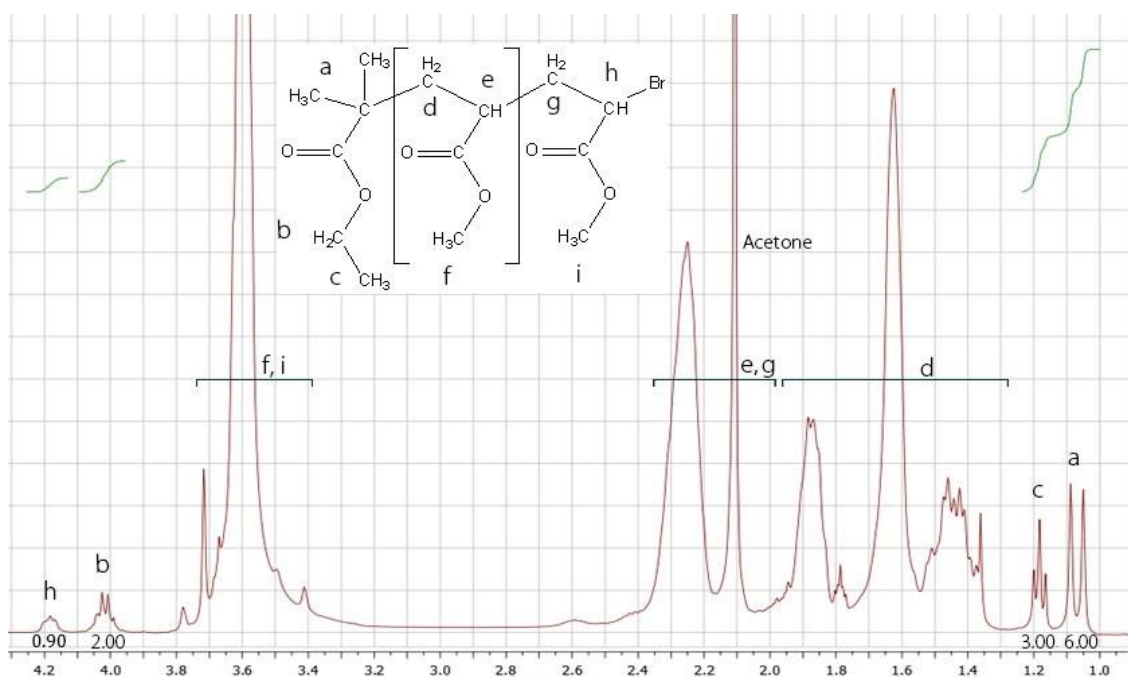


**Figure 4-6. Chain-end functionality determination using 400Hz  $^1\text{H}$  NMR of PMA grafts synthesized via CLRP catalyzed by wire copper wire/ $\text{Me}_6\text{-TREN}$  and initiated with EBiB**

Functionalization reactions of cellulose acetate (CA) were performed with different amounts of ethylene sulfide (ES) (entry 100-1, 100-2 and 131-1 in Table 4-2). The resulting cellulose acetate was analyzed by GPC and NMR. GPC analysis of cellulose acetate was abandoned as the variance between different samples in even one batch of pure CA was within several thousands. Therefore, a small change in molecular weight of samples after functionalization would not be conclusive evidence of new functionality. Examples of  $^1\text{H}$  and HSQC HMR spectra of cellulose acetate before functionalization are displayed in Figure 4-7 and Figure 4-8.  $^1\text{H}$  peak assignments are seen in Figure 4-7: AGU unit from 5.25 to 3.0 ppm, methyl groups ( $-\text{CH}_3$ ) at 2.25-1.75 ppm, water at 2.85 ppm, and acetone at 2.05 ppm.  $^{13}\text{C}$  peak assignments are shown in Figure 4-8: C1 at 100 ppm, C2 at 71 ppm, C3 at 72 ppm, C4 at 76 ppm, C5 at 76 ppm, and C6 at 62 ppm, methyl groups ( $-\text{CH}_3$ ) at 20 ppm and acetone at 29 ppm.<sup>77</sup>

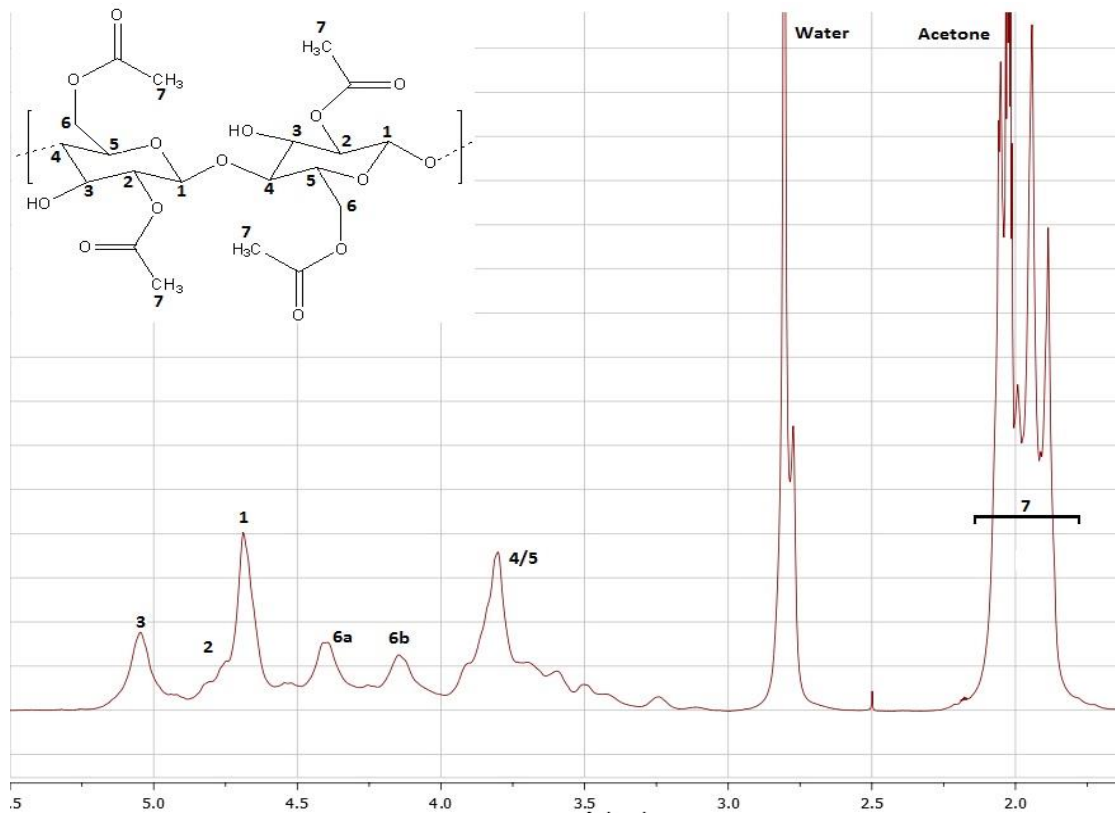


Figure 4-7. An examples of  $^1\text{H}$  NMR of unmodified Cellulose Acetate in  $\text{acetone-d}_6$

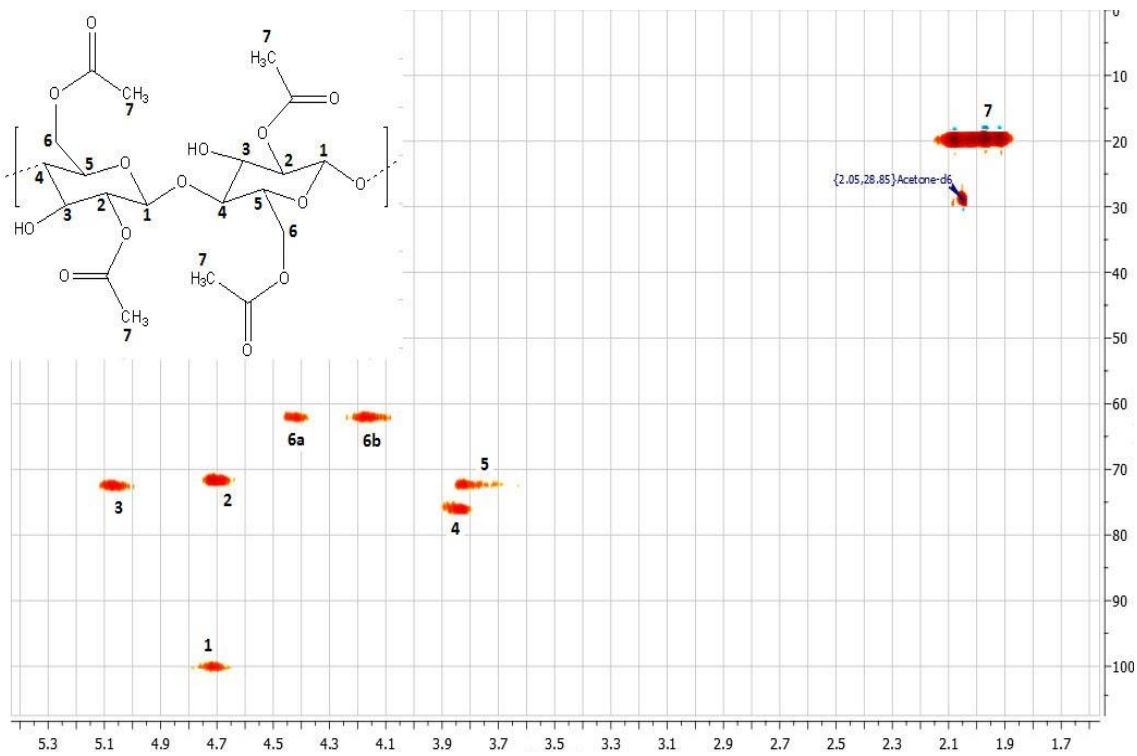


Figure 4-8. An example of HSQC NMR of unmodified Cellulose Acetate in  $\text{acetone-d}_6$



$^1\text{H}$  and HSQC NMR spectra, after the functionalization was conducted, showed no observable changes or new peaks when compared to the spectra of the unfunctionalized cellulose acetate. A deuterium oxide ( $\text{D}_2\text{O}$ ) ‘shake’ experiment<sup>78</sup> was performed, as  $-\text{SH}$  may have been overlapping with other peaks. Spectra before and after the ‘shake’ procedure were compared; thiol signal (expected to be around  $\delta$ : 1.90 - 2.15 ppm in  $^1\text{H}$ -NMR) should have disappeared and a new HOD peak should have appeared at  $\sim 4.7$  ppm. However, the results were inconclusive due to the presence of a number of overlapping signals. This would suggest that any thiol peak present may have been very small and/or possibly overlapping with the cellulose acetate signals, or thiols may have oxidized during a purification step. In case of successful functionalization it was also expected that two carbons from methylene units of ethylene sulfide ( $-\text{O}-\text{CH}_2-\text{CH}_2-\text{SH}$ ) would appear in the HSQC spectra at  $\delta$ : $\{-\text{C}-\text{SH}, 2.73, 24\}$  and  $\delta$ : $\{-\text{O}-\text{C}-, 3.60, 70\}$  ppm, where  $\delta$ : $\{\text{unit}, ^1\text{H}, ^{13}\text{C}\}$ , but these signals were not visible either. Based on the NMR analysis it is possible that 1) ethylene sulfide did not attach to cellulose acetate or 2) the intensity of the signals was not high enough to appear in  $^1\text{H}$  and HSQC NMR spectra.

Next, in order to evaluate the thio-bromo grafting procedure, the grafting reaction was performed with EBiB (entry 111-1 in Table 4-2), where bromine groups are not attached to the polymer chains and are more readily accessible. If attached, EBiB signals in  $^1\text{H}$  and HSQC NMR are expected around  $\delta$ :  $\{-\text{O}-\text{CH}_2-\text{CH}_3, 1.3, 14.7\}$ ,  $\{2\times\text{CH}_3, 1.4, 30\}$ , and  $\{-\text{O}-\text{CH}_2-\text{CH}_3, 4.20, 62.5\}$  ppm). The spectra obtained are displayed in Figure 4-9 and Figure 4-10. Several new peaks appeared in the expected regions, suggesting that grafting had occurred. Based on the integration under *a* and *c* signals relative to C3 hydrogen of CA, the estimated degree of substitution (DS) was 0.026 (1 unit of EBiB per 39 AGU units).

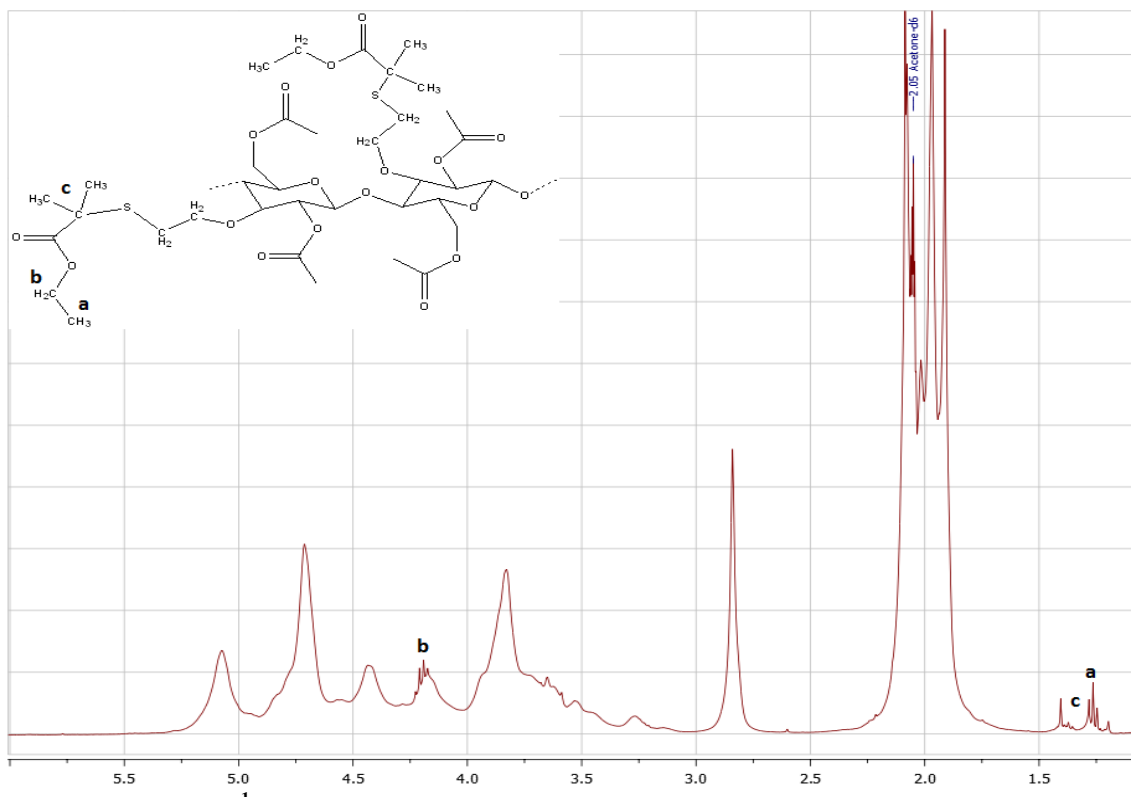


Figure 4-9.  $^1\text{H}$  NMR of Cellulose Acetate grafted with EBiB (111-1) in acetone- $d_6$

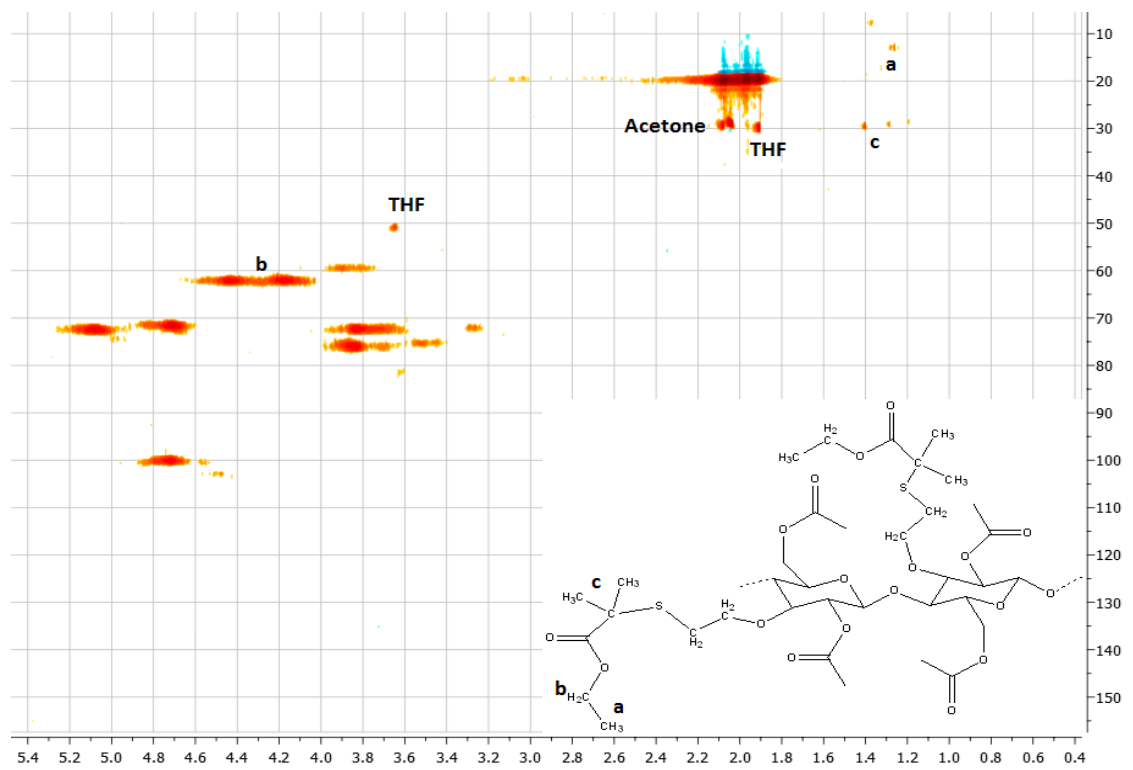


Figure 4-10. HSQC NMR of Cellulose Acetate grafted with EBiB (111-1) in acetone- $d_6$

It is possible that cellulose acetate was functionalized with thiol groups with similarly low DS, which would explain the low intensity or low visibility of methylene signals of the ethylene sulfide. Functionalization could not be determined by NMR due to the numerous overlapping peaks. The low DS also suggested that excess ethylene sulfide should be used for the functionalization step.

**Table 4-2. List of experimental conditions of the grafting to cellulose acetate experiments**

#	ES	Solvent	BF <sub>3</sub> ·Et <sub>2</sub> O	Grafts
100-1	22 μL	Dioxane	0.1 mL	-
100-2	45 μL	Dioxane	0.1 mL	-
131-1	22 μL	Dioxane	-	-
111-1	22 μL	Dioxane	-	EBiB, 1mL
101-1	45 μL	Dioxane	0.1 mL	PMA#33
102-1	45 μL	Dioxane	-	PMA#34
102-2	0.5 mL	DMF	-	PMA#34 (Cu removed)
102-3 (2 pot)	0.3 mL	1.Dioxane 2. Acetonitrile	0.1 mL	PMA#34 (Cu removed)

Further grafting experiments were performed with PMA. It was assumed that an attachment of long polymer chains would cause a substantial increase in the weight of cellulose acetate and grafting could be confirmed gravimetrically as well as by NMR. In the entries of 101 and 102 series in Table 4-2 cellulose acetate functionalization procedures were performed with and without BF<sub>3</sub>·Et<sub>2</sub>O catalyst as outlined by Penn *et al.* and Chaudhuri *et al.*, respectively.<sup>72-74</sup> Residual copper catalyst was removed from the PMA by passing it through a basic alumina column, to eliminate any possible interference of copper with the grafting step. Furthermore, the use of excess of ethylene sulfide (ES) in the functionalization step was evaluated. However, it was anticipated its use might that it result in autopolymerization to give poly(ethylene sulfide) (PES)<sup>79,80</sup> or the functionalization of cellulose substrate with longer units of PES. Results of these experiments obtained by gravimetric analysis are outlined in Table 4-3. The column denoted 'Used' indicates the initial amount of cellulose acetate and PMA used for the grafting procedure.

The polymer yield and cellulose acetate were weighed after a three-day soxhlet separation procedure with methanol. Expected values were calculated based on the assumption that DS of grafted chains was 0.2 (1 polymer chain per 5 AGU units).

**Table 4-3. Gravimetric analysis of cellulose acetate and PMA following the grafting *to* procedure**

#	Sample	Used [g]	Obtained [g]	Expected* [g]
101-1	CA	0.5	0.43	2.68
	PMA#33	4	3.41	1.81
102-1	CA	0.5	0.43	1.56
	PMA#34	3	2.3	1.93
102-2	CA	0.5	0.39	1.56
	PMA#34	4	3.22	2.93
102-3	CA	0.5	0.41	1.56
	PMA#34	4.7	4.3	3.63

\*Expected values are calculated based on the assumption of DS = 0.2

Following all of the attempted grafting *to* procedures with cellulose acetate, gravimetric analysis showed that no grafting has occurred. All of the used PMA was removed from cellulose acetate by soxhlet with methanol. It should be noted that some of the sample was lost during purification and collection. The cellulose acetate and PMA obtained were analyzed by NMR and GPC. Analysis of cellulose acetate did not show any changes in the molecular structure. Whereas, the analysis of PMA showed some loss of the chain-end functionality (%f) and broadening of the dispersity (Table 4-4 and Figure 4-11).

**Table 4-4. Results of GPC and NMR analysis of PMA following the grafting procedure *to* CA**

#	$M_w$	$M_n$	$\mathcal{D}$	%f
33 FN	5,940	5,540	1.07	78%
101-1	5,680	5,246	1.08	56%
34 FN	2,934	2,713	1.08	82%
102-1	2,912	2,679	1.09	51%
102-2	3,246	2,896	1.12	53%
102-3	2,852	2,612	1.09	54%

Loss of chain-end functionality may have been caused by the soxhlet extraction procedure with methanol. Broadening of the dispersity could have been a result of bimolecular termination. The most apparent evidence of bimolecular termination was observed in sample 102-2, where a shoulder of 6,500 g/mol (double of the original molecular weight) was seen in the molecular weight distribution graph in Figure 4-11. This may have been caused by the excess ethylene sulfide in the system.

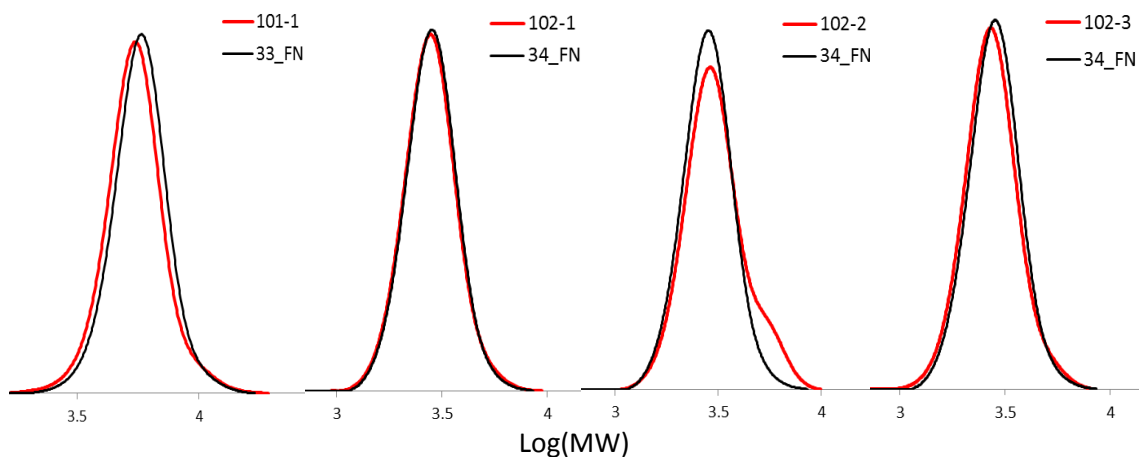


**Figure 4-11. Molecular weight distribution of PMA following the grafting procedure to CA**

PMA grafts were analyzed with  $^1\text{H}$  and HSQC NMR and compared to spectra of PMA prior to the grafting procedure. The HSQC spectrum of pure PMA is displayed in Figure 4-12. Carbon signals were assigned as follows: main chain methylene (*d*) at 34 ppm, main chain methine (*e*) at 41 ppm, methyl ester group (*f*)  $-\text{O}-\text{CH}_3$  at 51 ppm, methylene (*g*) at 42 ppm, methine (*h*) in the alpha position next to bromine at 43 ppm, and initiator carbons (*b*,  $\text{CH}_2$ ) at 60 ppm, (*c*,  $\text{CH}_3$ ) at 14 ppm, and (*a*,  $2\text{CH}_3$ ) at 24 ppm.

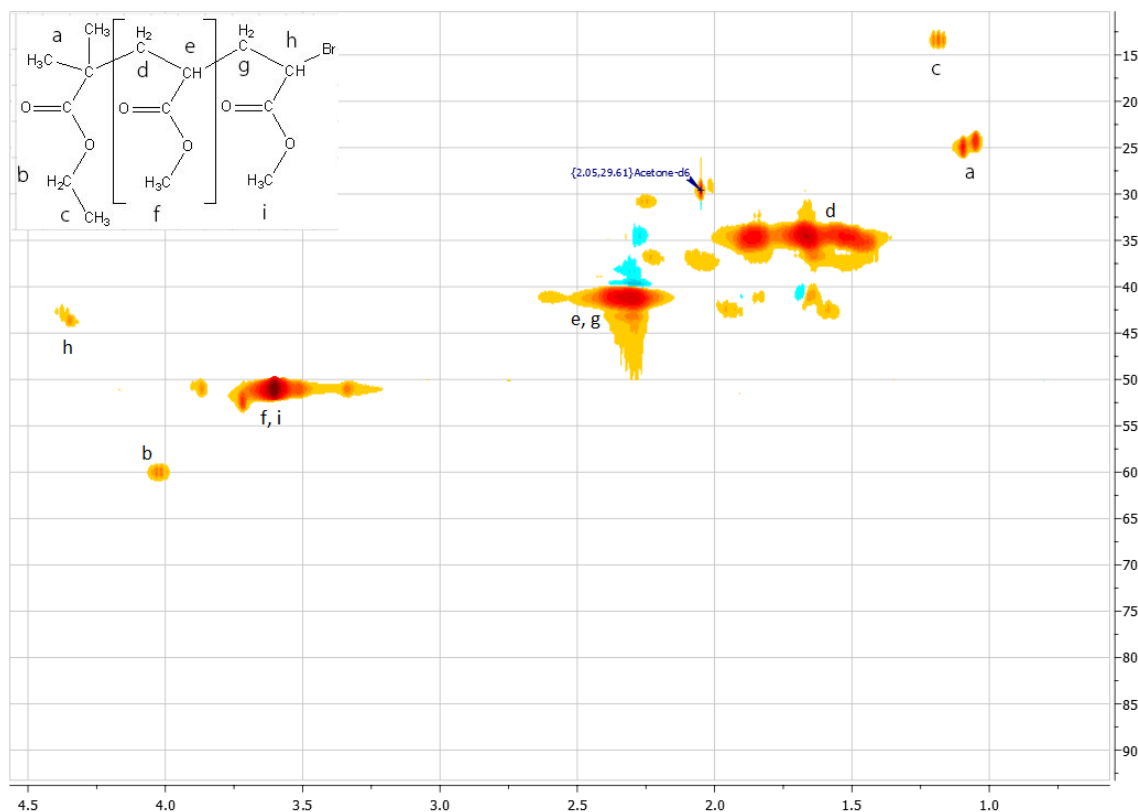


**Figure 4-12. HSQC NMR of PMA grafts in acetone- $d_6$  synthesized via CLRP catalyzed by wire copper wire/ $Me_6$ -TREN and initiated with EBiB**

The NMR spectrum of the 102-3 sample (Figure 4-13) suggests that there may have been another phenomenon occurring in the two-pot reaction system, as the double molecular weight shoulder was absent in the molecular weight distribution graph in Figure 4-11. Instead of bimolecular termination, as observed in 102-2, an attachment of ethylene sulfide to PMA may have occurred in the 102-3 experiment. As can be seen in Figure 4-13 and Figure 4-14, new signals appeared at {3.18, 45}, {2.85, 32} and {2.78, 28} ppm when compared to pure PMA in Figure 4-6 and Figure 4-12. If a thio-bromo click reaction had occurred between a bromine chain-end of PMA and a thiol of ethylene sulfide, the following signals were expected appear: methine next to the sulfide at {3.15, 45} ppm, methylene signals at {2.75, 32} and {2.85, 36} ppm, and terminal  $CH_3$ {2.14, 14.7}.

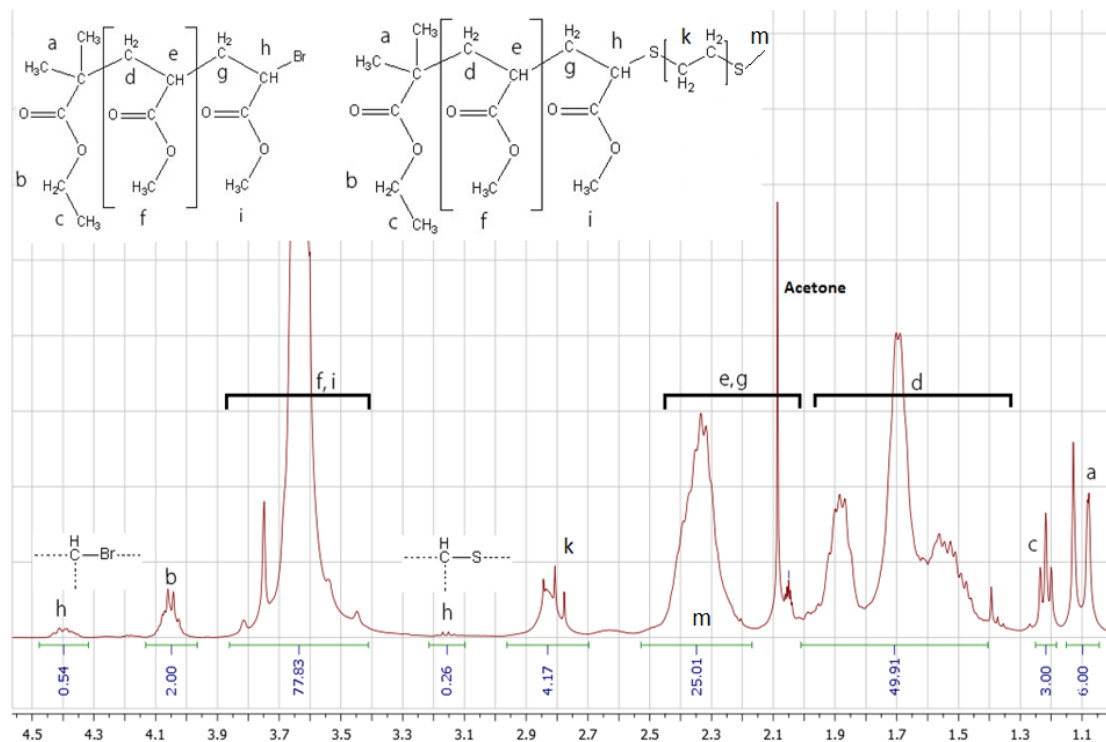


Figure 4-13.  $^1\text{H-NMR}$  of 102-3 PMA analysis following the grafting to cellulose acetate procedure

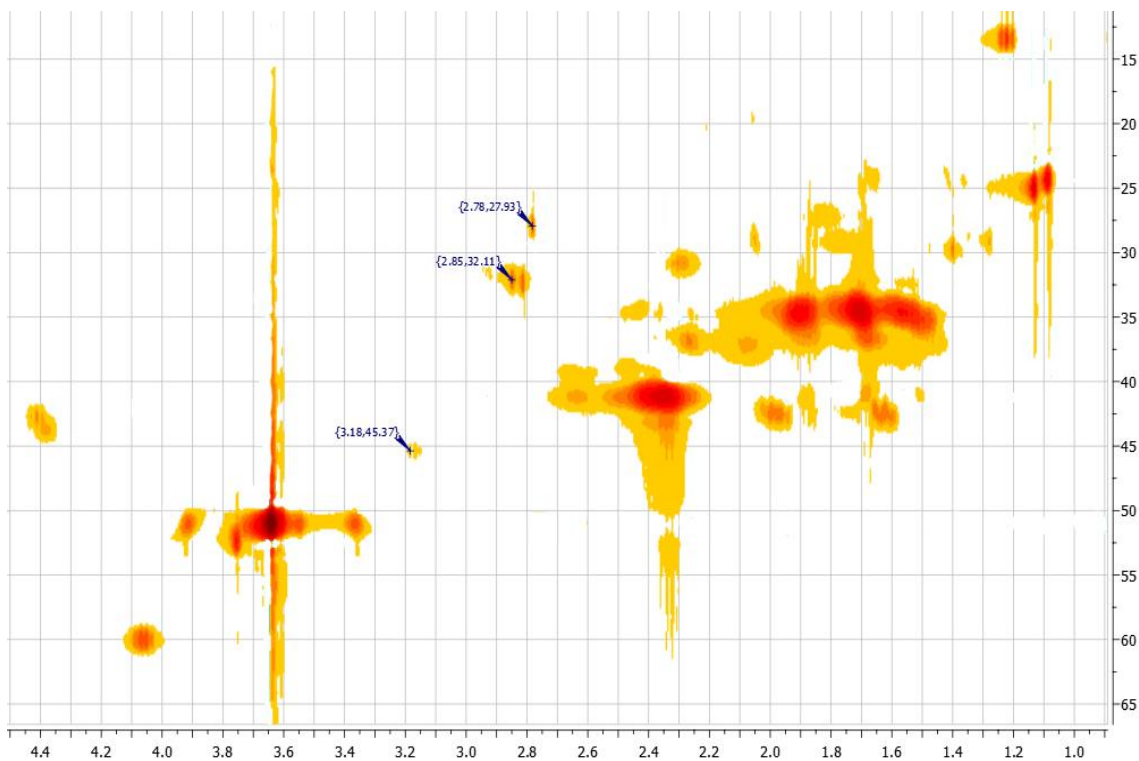


Figure 4-14. HSQC NMR of 102-3 PMA analysis following the grafting to cellulose acetate procedure

The area under the methine peak (**CH-S-**) in Figure 4-13 indicated that 26% of the chains may have contained at least one ethylene sulfide unit. The area under the methylene peaks may include the water signal; therefore the integration value was not considered to be indicative of the number of ethylene sulfide units attached. It may be coincidental, but the sum of the integration values under both methine peaks (next to sulfide and bromide) nearly added up to the initial chain-end functionality of PMA (82%). Hence, different chain loss mechanisms (102-2 versus 102-3) may have been caused by the different reaction conditions present in the one-pot and two-pot experiments.

Similar experiments (Table 4-5) and analyses were performed for the grafting of PMA *to* microcrystalline cellulose (MCC) under heterogeneous conditions. Since MCC is insoluble in organic solvents, this procedure did not require the use of soxhlet purification with methanol, and unattached polymer were removed by filtration with THF.

**Table 4-5. List of experimental conditions of grafting *to* microcrystalline cellulose**

#	ES	Solvent	BF <sub>3</sub> ·Et <sub>2</sub> O	Grafts
<b>201-0</b>	18 μL	Dioxane	-	PMA#31
<b>202-0</b>	18 μL	Dioxane	-	PMA#32
<b>201-1</b>	37 μL	Dioxane	0.1 mL	PMA#33
<b>201-2</b>	74 μL	DMF	0.1 mL	PMA#33 (Cu removed)
<b>201-3 (2 pot)</b>	0.3 mL	1.Dioxane 2. Acetonitrile	0.1 mL	PMA#33 (Cu removed)
<b>202-1 (2 pot)</b>	0.3 mL	1.Dioxane 2. Acetonitrile	0.1 mL	PMA#34 (Cu removed)

Gravimetric analysis (Table 4-6) following the grafting *to* procedure showed that the grafting of PMA to MCC was unsuccessful, as the weight of the cellulose substrate remained below 0.5 g. In case of even low DS of 0.02 with PMA the weight of MCC following the filtration with THF should have been at least 1 g.



**Table 4-6. Gravimetric analysis of MCC and PMA following the grafting *to* procedure**

#, DS	Sample	Used [g]	Obtained [g]	Expected* [g]
201-0, DS = 0.1	CELL	0.5	0.46	2.12
	PMA	2.8	2.31	1.17
202-0, DS = 0.1	CELL	0.5	0.48	1.36
	PMA	3.19	2.53	2.33
201-1, DS = 0.2	CELL	0.5	0.47	4.12
	PMA	5.0	4.53	1.36
201-2, DS = 0.2	CELL	0.5	0.47	4.12
	PMA	4.3	3.7	0.66
201-3, DS = 0.5	CELL	0.5	0.48	4.89
	PMA	5.28	4.79	0.86
202-1, DS. = 0.5	CELL	0.5	0.48	4.84
	PMA	5.2	4.6	0.78

\*Expected values are calculated based on the assumption of DS indicated next to the entry number

The PMA obtained was analyzed using GPC and NMR with the results summarized in Table 4-7, and molecular weight distribution displayed in Figure 4-15. Loss of chain-end functionality was noted, but was not as high as that observed in the grafting *to* cellulose acetate, which suggests that some loss of functionality occurred during the grafting procedure and some during the purification step (soxhlet extraction).

**Table 4-7. Results of GPC and NMR analysis of PMA following the grafting procedure *to* MCC**

Sample #	M <sub>w</sub>	M <sub>n</sub>	Đ	%f
<b>31FN</b>	<b>5,100</b>	<b>4,781</b>	<b>1.07</b>	87%
201-0	5,001	4,645	1.08	79%
<b>32FN</b>	<b>2,709</b>	<b>2,516</b>	<b>1.08</b>	88%
202-0	2,604	2,391	1.09	77%
<b>33 FN</b>	<b>5,940</b>	<b>5,540</b>	<b>1.07</b>	78%
201-1	5,778	5,392	1.07	77%
201-2	5,793	5,407	1.07	72%
201-3	5,848	5,465	1.07	72%
<b>34 FN</b>	<b>2,934</b>	<b>2,713</b>	<b>1.08</b>	82%
202-1	2,934	2,673	1.10	72%

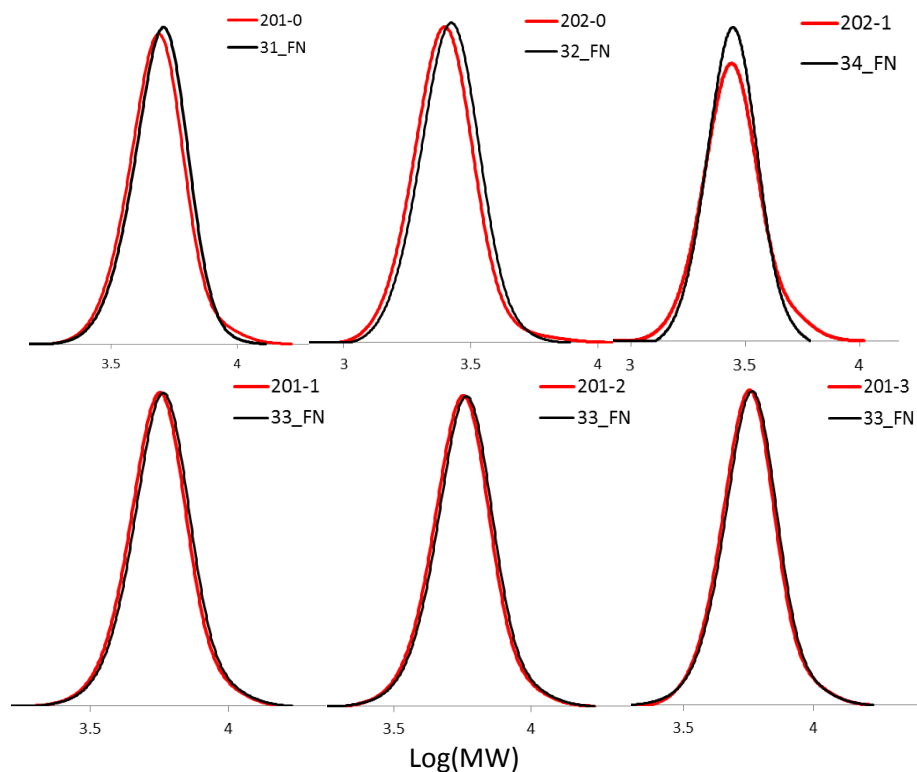


**Figure 4-15. Molecular weight distribution of PMA following the grafting procedure to MCC**

Bimolecular termination may have occurred in the 202-1 experiment, but it was not evident in other samples, which may have been the result of using excess ethylene sulfide and lower molecular weight grafts. More chain-end functionality was expected to be lost in polymer grafts of lower molecular weight (~2,500 g/mol versus ~5,500 g/mol), as the concentration of bromine chain-ends would increase.  $^1\text{H}$  and HSQC NMR analyses of PMA grafts performed after the attempted grafting procedure showed no changes (except a decrease in chain-end functionality) or new signals when compared to the initial spectra prior to grafting. It is peculiar that the attachment of ethylene sulfide to PMA was not observed in the experiments with MCC, even though the same conditions were used with the exception of the heterogeneity of the reaction.

#### 4.4 Conclusions & Recommendations

The grafting of polymer chains to cellulose substrates, cellulose acetate and microcrystalline cellulose, was attempted using thio-bromo click reaction. PMA grafts (~2,500 g/mol and 5,500 g/mol) with bromine chain functionality were synthesized using copper wire mediated CLRP. Cellulose substrates were functionalized with thiol groups using ethylene sulfide, used as accepting sites on the cellulose backbone. Grafting of EBiB was performed, where bromine was readily available, instead of being wrapped up in the polymer chains, however the degree of substitution was very low (DS = 0.026, 1 unit of EBiB per 39 AGU units). No other substantial evidence was obtained that functionalization was successful. Other more sensitive and accurate techniques for quantifying thiols, such as mass spectrometry or elemental analysis, should be utilized in the future work.

Gravimetric analysis following the experiments showed that grafting was unsuccessful, as all of the PMA polymer was removed from the cellulose acetate by soxhlet extraction with methanol and from microcrystalline cellulose by filtration with THF. It is possible that bromine end groups of the polymer were not reactive enough to graft to thiols with low DS or functionalization with ethylene sulfide was not an effective method of attaching thiol groups to cellulose. Ethylene sulfide may have autopolymerized, instead of reacting with hydroxyl group on the cellulose substrates. Reactions such as thiocarbonation<sup>81</sup> or esterification with mercaptoacetic acid<sup>82</sup> should be investigated in order to impart thiol functionality onto the cellulose substrates.

The polymer obtained following the grafting procedure was analyzed using NMR and GPC, which showed some loss of chain end functionality and an increase in dispersity. The evidence suggests that bimolecular termination of PMA had occurred during the reaction, and some chain end functionality was lost during the reaction and purification. Furthermore, <sup>1</sup>H and HSQC NMR of one of the samples appeared to indicate that ethylene sulfide may have attached

to PMA grafts instead of to cellulose, where several signals corresponding to ethylene sulfide units can be seen in the NMR spectra.

It is possible that grafting *to* was unsuccessful as a result of the ineffective reaction conditions and experimental set-up. In the one-pot system, the thio-bromo click reaction was performed in the same solution as the functionalization, which contained dioxane or DMF, ethylene sulfide and often a catalyst, which may not be favorable for this reaction. It is recommended that the thio-bromo reaction be performed in acetonitrile.<sup>11,29,75,76</sup> The two-pot system required purification of cellulose substrate after functionalization, which may have caused the loss of thiols by oxidation. Therefore, when thio-bromo click was attempted under favorable conditions, thiols may have already been lost. Further investigation is required to optimize the reaction conditions for both steps, and to minimize exposure of functionalized cellulose to oxygen.

## Chapter 5.

### Conclusion & Recommendations

Growing concern over limited resources and environmental deterioration has fueled interest in developing sustainable materials, implementing greener alternatives and utilizing renewable resources, such as polysaccharides and other naturally produced polymers. Recent progress in polymerization and post-polymerization modification methods has created new opportunities for developing high value copolymers containing polysaccharides. One example of such polymerization methods is copper wire mediated controlled radical polymerization (CLRP) that has been developed in the last decade, and is termed SET-LRP or SARA ATRP (Chapter 2). It provides precise control over degree of polymerization, molecular weight, dispersity ( $M_w/M_n$ ), composition, and polymer chain-end functionality. This exceptional control over macromolecular structure allows for tuning and designing materials with predefined characteristics. An example of post-polymerization technique is graft copolymerization, such as grafting of precisely designed polymer chains *to* the chosen polysaccharide substrate, to form a new material with unprecedented properties.

In this thesis, both of these methods were examined. First, solvent effects on the kinetics of copper wire mediated (CLRP) and characteristics of a resulting polymer were investigated by switching from typically used organic volatile solvents (e.g.. DMSO) to greener solvents systems (Chapter 3). The polymerization kinetics of methyl acrylate (MA) initiated with ethyl 2-bromoisobutyrate were examined in polyethylene glycol (PEG) and polypropylene glycol (PPG), and their binary mixtures with ethanol and DMSO. Two new green solvent systems were established, consisting of 75% PEG or PPG and 25% ethanol, where total volume of solvent to monomer is 33%. Both were found to support good control, narrow dispersity, and well-preserved chain-end functionality for molecular weights of PMA ranging from 4,000 to 25,000 g/mol. It

was also confirmed that removal of the residual copper catalyst is easier from PEG and PPG than from DMSO, reducing the required number of purification steps. For future work, optimization of time and temperature can be performed to increase conversion, without decreasing chain-end functionality. The recyclability potential of both solvents should also be investigated, further contributing to the greenness of these systems and potentially cutting cost for large scale processes. Furthermore, polymerization of broader range of monomers, such as methyl methacrylate (MMA), N-dimethylacrylamide (DMA), N-isopropylacrylamide (NIPAM) etc., can be studied in these greener solvent systems. Lastly, other solvents from the Kamlet-Taft plot in Figure 3-2 should be studied to expand the list of effective green solvent systems for such valuable polymerization technique.

In Chapter 4, the grafting of bromine capped low molecular weight PMA (synthesized via copper wire mediated CLRP) *to* cellulosic substrate was investigated. The goal was to utilize the obtained bromine chain-end functionality of PMA for grafting *to* cellulose using thio-bromo click reaction, where cellulose substrate was required to contain thiol functionality. Cellulose acetate and microcrystalline cellulose were functionalized with ring opening reaction with ethylene sulfide. Grafting via thio-bromo click reaction was attempted in one-pot and two-pot reaction systems. In the one-pot reaction, polymer chains were added to the solution following functionalization of cellulose, which was intended to reduce exposure of thiols to oxygen. Whereas, in the two-pot reaction, functionalized cellulose substrate was purified prior to the grafting step. Grafting was however not successful in either system. There are several possible reasons for unsuccessful grafting: 1) functionalization with ethylene sulfide may have been ineffective; 2) the one-pot reaction condition may be unfavorable for subsequent thio-bromo reaction; 3) in the two-pot system thiols may have been lost during purification step; 4) bromine chain-ends may not be reactive enough for accepting sites on the cellulose substrate.

Nevertheless, attachment of the initiator (ethyl 2-bromoisobutyrate) to cellulose acetate containing thiols showed some potential, but with low degree of substitution (DS of 0.026). Therefore, further investigation can be performed to optimize reaction conditions, maximizing number of thiol groups, minimizing exposure to oxygen and increasing number of active bromine units by synthesizing polymer grafts from  $\alpha$ -bromoisobutyryl bromide instead of ethyl 2-bromoisobutyrate. It was found that NMR analysis is insufficient for determining if cellulose acetate was functionalized with ethylene sulfide, as intensity of signals may be low and expected peaks are overlapping with signals corresponding to AGU units. Therefore, for future investigation other more sensitive techniques should be used to determine thiol content, such as mass spectrometry or elemental analysis.

## References

1. Matyjaszewski, K.; Gaynor, S.; Greszta, D.; Mardare, D.; Shigemoto, T. 'Living' and Controlled Radical Polymerization. *Journal of Physical Organic Chemistry* **1995**, *8*, 306-315.
2. Kato, M.; Kamigaito, M.; Sawamoto, M.; Higashimura, T. Polymerization of Methyl Methacrylate with the Carbon Tetrachloride/Dichlorotris-(triphenylphosphine)ruthenium(II)/Methylaluminum Bis(2,6-di-tert-butylphenoxide) Initiating System: Possibility of Living Radical Polymerization. *Macromolecules* **1995**, 1721-1723.
3. Percec, V.; Popov, A. V.; Ramirez-Castillo, E.; Monteiro, M.; Barboiu, B.; Weichold, O.; Asandei, A. D.; Mitchell, C. M. Aqueous Room Temperature Metal-Catalyzed Living Radical Polymerization of Vinyl Chloride. *Journal of American Chemical Society* **2002**, *124*, 4940-4941.
4. Percec, V.; Popov, A. V.; Ramirez-Castillo, E.; Weichold, O. Living Radical Polymerization of Vinyl Chloride Initiated with Iodoform and Catalyzed by Nascent Cu<sup>0</sup>/Tris(2-aminoethyl)amine or Polyethyleneimine in Water at 25°C Proceeds by a New Competing Pathways Mechanism. *Journal of Polymer Science* **2003**, *41*, 3283-3299.
5. Percec, V.; Guliashvili, T.; Ladislaw, J. S.; Wistrand, A.; Stjern Dahl, A.; Sienkowska, M. J.; Monteiro, M. J.; Sahoo, S. Ultrafast Synthesis of Ultrahigh Molar Mass Polymers by Metal-Catalyzed Living Radical Polymerization of Acrylates, Methacrylates, and Vinyl Chloride Mediated by SET at 25°C. *Journal of the American Chemical Society* **2006**, *128*, 14156-14165.
6. Rosen, B. M.; Percec, V. Single-Electron Transfer and Single-Electron Transfer Degenerative Chain Transfer Living Radical Polymerization. *Chemical Reviews* **2009**, *109*, 5069-5119.
7. Zhang, Y.; Wang, Y.; Matyjaszewski, K. ATRP of methyl acrylate with metallic zinc, magnesium, and iron as reducing agents and supplemental activators. *Macromolecules* **2011**, *44*, 683-685.
8. Zhang, Y.; Wang, Y.; Peng, C.-h.; Zhong, M.; Zhu, W.; Konkolewicz, D.; Matyjaszewski, K. Copper-Mediated CRP of Methyl Acrylate in the Presence of Metallic Copper: Effect of Ligand Structure on Reaction Kinetics. *Macromolecules* **2012**, *45*, 78-86.
9. Jessop, P. G. Searching for green solvents. *Green Chemistry* **2011**, *13*, 1391-1398.
10. Hansson, S.; Trouillet, V.; Tischer, T.; Goldmann, A. S.; Carlmark, A.; Barner-Kowollik, C.; Malmstrom, E. Grafting Efficiency of Synthetic Polymers onto Biomaterials: Comparative Study of Grafting-from versus Grafting-to. *Biomacromolecules* **2013**, *14*, 64-74.
11. Rosen, B. M.; Lligadas, G.; Hahn, C.; Percec, V. Synthesis of dendrimers through divergent iterative thio-bromo "Click" chemistry. *Journal of Polymer Science: Part A: Polymer*



- Chemistry* **2009**, *47*, 3931-3939.
12. Braunecker, W. A.; Matyjaszewski, K. Controlled/living radical polymerization: Features, developments, and perspectives. *Progress in Polymer Science* **2007**, *32*, 93-146.
  13. Ouchi, M.; Terashima, T.; Sawamoto, M. Transition Metal-Catalyzed Living Radical Polymerization: Toward Perfection in Catalysis and Precision Polymer Synthesis. *Chemistry Reviews* **2009**, *109*, 4963-5050.
  14. Jakubowski, W.; Min, K.; Matyjaszewski, K. Activators Regenerated by Electron Transfer for Atom Transfer Radical Polymerization of Styrene. *Macromolecules* **2006**, *39*, 39-45.
  15. Matyjaszewski, K.; Jakubowski, W.; Min, K.; Tang, W.; Huang, J.; Braunecker, W. A.; Tsarevsky, N. V. Diminishing catalyst concentration in atom transfer radical polymerization with reducing agents. *Proceedings of the National Academy of Sciences of the United States of America* **2006**, *103* (42), 15309-15314.
  16. Konkolewicz, D.; Wang, Y.; Zhong, M.; Kryszewski, P.; Isse, A. A.; Gennaro, A.; Matyjaszewski, K. Reversible-Deactivation Radical Polymerization in the Presence of Metallic Copper. A Critical Assessment of the SARA ATRP and SET-LRP Mechanisms. *Macromolecules* **2013**, *46*, 8749-8772.
  17. Matyjaszewski, K. Atom Transfer Radical Polymerization (ATRP): Current Status and Future Perspectives. *Macromolecules* **2012**, *45*, 4015-4039.
  18. Wang, Y.; Kwak, Y.; Buback, J.; Buback, M.; Matyjaszewski, K. Determination of ATRP Equilibrium Constants under Polymerization Conditions. *Macromolecules* **2012**, 1367-1370.
  19. Braunecker, W. A.; Tsarevsky, N. V.; Gennaro, A.; Matyjaszewski, K. Thermodynamic Components of the Atom Transfer Radical Polymerization Equilibrium: Quantifying Solvent Effects. *Macromolecules* **2009**, *42*, 6348-6360.
  20. Rosen, B. M.; Percec, V. A density functional theory computational study of the role of ligand on the stability of CuI and CuII species associated with ATRP and SET-LRP. *Journal of Polymer Science: Part A: Polymer Chemistry* **2007**, 4950-4964.
  21. Lligadas, G.; Percec, V. Ultrafast SET-LRP of Methyl Acrylate at 25C in Alcohols. *Journal of Polymer Science Part A: Polymer Chemistry* **2008**, *46*, 2745-2754.
  22. Jiang, X.; Fleischmann, S.; Nguyen, N. H.; Rosen, B. M.; Percec, V. Cooperative and synergistic solvent effects in SET-LRP of MA. *Journal of Polymer Science Part A: Polymer Chemistry* **2009**, *47*, 5591-5605.
  23. Nguyen, N. H.; Rosen, B. M.; Jiang, X.; Fleischmann, S.; Percec, V. New Efficient Reaction Media for SET-LRP Produced from Binary Mixtures of Organic Solvents and H<sub>2</sub>O. *Journal of Polymer Science* **2009**, *47*, 5577-5590.

24. Lligadas, G.; Percec, V. A Comparative Analysis of SET-LRP of MA in Solvents Mediating Different Degrees of Disproportionation of Cu(I)Br. *Journal of Polymer Science Part A: Polymer Chemistry* **2008**, *46*, 6880–6895.
25. Lligadas, G.; Rosen, B. M.; Monteiro, M. J.; Percec, V. Solvent Choice Differentiates SET-LRP and Cu-Mediated Radical Polymerization with Non-First-Order Kinetics. *Macromolecules* **2008**, *41*, 8360-8364.
26. Levere, M. E.; Nguyen, N. H.; Percec, V. No Reduction of CuBr<sub>2</sub> during Cu(0)-Catalyzed Living Radical Polymerization of Methyl Acrylate in DMSO at 25°C. *Macromolecules* **2012**, *45*, 8267-8274.
27. Nguyen, N. H.; Percec, V. Disproportionating versus nondisproportionating solvent effect in the SET-LRP of methyl acrylate during catalysis with nonactivated and activated Cu(0) wire. *Journal of Polymer Science Part A: Polymer Chemistry* **2011**, *49*, 4227–4240.
28. Nguyen, N. H.; Levere, M. E.; Percec, V. SET-LRP of methyl acrylate to complete conversion with zero termination. *Journal of Polymer Science Part A: Polymer Chemistry* **2012**, *50*, 860–873.
29. Nguyen, N. H.; Levere, M. E.; Kulis, J.; Monteiro, M. J.; Percec, V. Analysis of the Cu(0)-Catalyzed Polymerization of Methyl Acrylate in Disproportionating and Nondisproportionating Solvents. *Macromolecules* **2012**, *45*, 4606–4622.
30. Nyström, F.; Soeriyadi, A. H.; Boyer, C.; Zetterlund, P. B.; Whittaker, M. R. End-group fidelity of copper(0)-mediated radical polymerization at high monomer conversion: an ESI-MS investigation. *Journal of Polymer Science Part A: Polymer Chemistry* **2011**, *49*, 5313–5321.
31. Nguyen, N. H.; Sun, H.-J.; Levere, M. E.; Fleischmann, S.; Percec, V. Where is Cu(0) generated by disproportionation during SET-LRP? *Polymer Chemistry* **2013**, *4*, 1328-1332.
32. Levere, M. E.; Nguyen, N. H.; Xuefei, L.; Percec, V. Visualization of the crucial step in SET-LRP. *Polymer Chemistry* **2013**, *4*, 1635-1647.
33. Guliashvili, T.; Mendonca, P. V.; Serra, A. C.; Popov, A. V.; Coelho, J. F. J. Copper-Mediated Controlled/“Living” Radical Polymerization in Polar Solvents: Insights into Some Relevant Mechanistic Aspects. *Chemistry A European Journal* **2012**, *18*, 4607-4612.
34. Horn, M.; Matyjaszewski, K. Solvent effects on the activation rate constant in atom transfer radical polymerization. *Macromolecules* **2013**, *46*, 3350–3357.
35. Hornby, B. D.; West, A. G.; Tom, J. C.; Waterson, C.; Harrisson, S.; Perrier, S. Copper(0)-Mediated Living Radical Polymerization of Methyl Methacrylate in a Non-polar Solvent. *Macromolecular Rapid Communications* **2010**, No. 31, 1276–1280.

36. Magenau, A. J.; Kwak, Y.; Matyjaszewski, K. ATRP of Methacrylates Utilizing Cu II X 2 /L and Copper Wire. *Macromolecules* **2010**, *43*, 9682-9689.
37. Harrisson, S.; Couvreur, P.; Nicolas, J. Comproportionation versus Disproportionation in the Initiation Step of Cu (0)-Mediated Living Radical Polymerization. *Macromolecules* **2012**, *45*, 7388-7396.
38. Peng, C.-H.; Zhong, M.; Wang, Y.; Kwak, Y.; Zhang, Y.; Zhu, W.; Tonge, M.; Buback, J.; Park, S.; Krys, P.; Konkolewicz, D.; Gennaro, A.; Matyjaszewski, K. Reversible-Deactivation Radical Polymerization in the Presence of Metallic Copper. Activation of Alkyl Halides by Cu 0. *Macromolecules* **2013**, *46*, 3803–3815.
39. Wang, Y.; Soerensen, N.; Zhong, M.; Schroeder, H.; Buback, M.; Matyjaszewski, K. Improving the “Livingness” of ATRP by Reducing Cu Catalyst Concentration. *Macromolecules* **2013**, *46*, 683-691.
40. Konkolewicz, D.; Krys, P.; Góis, J. R.; Mendonça, P. V.; Zhong, M.; Wang, Y.; Gennaro, A.; Isse, A. A.; Fantin, M.; Matyjaszewski, K. Aqueous RDRP in the Presence of Cu 0 : The Exceptional Activity of Cu I Confirms the SARA ATRP Mechanism. *Macromolecules* **2014**, *47*, 560–570.
41. Anastas, P. T.; Zimmerman, J. B. Design through the 12 Principles of Green Engineering. *Environmental Science & Technology* **2003**, *37* (5), 94A-101A.
42. Mallakpour, S.; Rafiee, Z. Green Solvents Fundamental and Industrial Applications. In *Green Solvents I. Properties and Applications in Chemistry*; Springer, 2012; pp 1-66.
43. Mercer, S. M.; Andraos, J.; Jessop, P. G. Choosing the Greenest Synthesis: A Multivariate Metric Green Chemistry Exercise. *Journal of Chemical Education* **2012**, 215-220.
44. Ra, J. o.; Spear, S. K.; Huddleston, J. G.; Rogers, R. D. Polyethylene glycol and solutions of polyethylene glycol as green reaction media. *Green Chemistry* **2005**, *7*, 64-82.
45. Heldebrant, D. J.; Witt, H. N.; Walsh, S. M.; Ellis, T.; Rauscher, J.; Jessop, P. G. Liquid polymers as solvents for catalytic reductions. *Green Chemistry* **2006**, *8*, 807-815.
46. Perrier, S.; Gemici, H.; Li, S. Poly(ethylene glycol) as solvent for transition metal mediated living radical polymerisation. *Chemical Communications. The Royal Society of Chemistry* **2004**, 604-605.
47. Agency for Toxic Substances and Disease Registry. Toxicological Profiles: Propylene Glycol, 2014. Agency for Toxic Substances and Disease Registry. Toxic Substances Portal. <http://www.atsdr.cdc.gov> (accessed July 25, 2014).
48. Gruending, T.; Junkers, T.; Guilhaus, M.; Barner-Kowollik, C. Mark-Houwink parameters for the universal calibration of acrylate, methacrylate, and vinyl acetate polymers determined

- by online size-exclusion chromatography - mass spectrometry. *Macromolecular Chemistry and Physics* **2010**, *211* (5), 520-528.
49. Nguyen, N. H.; Rosen, B. M.; Lligadas, G.; Percec, V. Surface-Dependent Kinetics of Cu(0)-Wire-Catalyzed Single-Electron Transfer Living Radical Polymerization of Methyl Acrylate in DMSO at 25°C. *Macromolecules* **2009**, *42*, 2379-2386.
  50. Klemm, D.; Heublein, B.; Fink, H.-P.; Bohn, A. Cellulose: Fascinating Biopolymer and Sustainable Raw Material. *Angewandte Chemie International Edition* **2005**, *44*, 3358-3393.
  51. Roy, D.; Semsarilar, M.; Guthrie, J. T.; Perrier, S. Cellulose modification by polymer grafting: a review. *Chemical Society Reviews* **2009**, *38*, 2046-2064.
  52. Tizzotti, M.; Charlot, A.; Fleury, E.; Stenzel, M.; Bernand, J. Modification of Polysaccharides Through Controlled/Living Radical Polymerization Grafting-Towards the Generation of High Performance Hybrids. *Macromolecular Rapid Communications* **2010**, *31*, 1751-1772.
  53. Raus, V.; Štěpánek, M.; Uchman, M.; Šlouf, M.; Látalová, P.; Čadová, E.; Netopilík, M.; Kříž, J.; Dybal, J. Cellulose-based graft copolymers with controlled architecture prepared in a homogeneous phase. *Journal of Polymer Science Part A: Polymer Chemistry* **2011**, *49*, 4353-4367.
  54. Vlček, P.; Janata, M.; Látalová, P.; Kříž, J.; Čadová, E.; Toman, L. Controlled grafting of cellulose diacetate. *Polymer* **2006**, *47*, 2587-2595.
  55. Oestmark, E.; Harrison, S.; Wooley, K. L.; Malmström, E. E. Comb polymers prepared by ATRP from hydroxypropyl cellulose. *Biomacromolecules* **2007**, *8*, 1138-1148.
  56. Hiltunen, M.; Siirilä, J.; Maunu, S. Effect of catalyst systems and reaction conditions on the synthesis of cellulose-g-PDMAam copolymers by controlled radical polymerization. *Journal of Polymer Science Part A: Polymer Chemistry* **2012**, 3067-3076.
  57. Malmstrom, E.; Carlmark, A. Controlled grafting of cellulose fibres - an outlook beyond paper and cardboard. *Polymer Chemistry* **2012**, No. 3, 1702-1713.
  58. Carlmark, A.; Malmström, E. Atom transfer radical polymerization from cellulose fibers at ambient temperature. *Journal of the American Chemical Society* **2002**, *124*, 900-901.
  59. Roy, D.; Guthrie, J. T.; Perrier, S. Graft Polymerization: Grafting Poly(styrene) from Cellulose via Reversible Addition-Fragmentation Chain Transfer (RAFT) Polymerization. *Macromolecules* **2005**, *38*, 10363-10372.
  60. Carlmark, A.; Malmström, E. E. ATRP grafting from cellulose fibers to create block-copolymer grafts. *Biomacromolecules* **2003**, *4*, 1740-1745.
  61. Hansson, S.; Antoni, P.; Bergenudd, H.; Malmström, E. Selective cleavage of polymer grafts from solid surfaces: assessment of initiator content and polymer characteristics. *Polymer*

- Chemistry* **2011**, *2*, 556-558.
62. Zhao, G.-L.; Hafren, J.; Deiana, L.; Cordova, A. Heterogeneous “Organoclick” Derivatization of Polysaccharides: Photochemical Thiol-ene Click Modification of Solid Cellulose. *Macromolecular Rapid Communications* **2010**, *31* (8), 740-744.
  63. Hoyle, C. E.; Bowman, C. N. Thiol-ene click chemistry. *Angewandte Chemie* **2010**, *49*, 1540-1573.
  64. Kade, M. J.; Burke, D. J.; Hawker, C. J. The power of thiol-ene chemistry. *Journal of Polymer Science Part A: Polymer Chemistry* **2010**, *48*, 743-750.
  65. Lowe, A. B. Thiol-ene “click” reactions and recent applications in polymer and materials synthesis. *Polymer Chemistry* **2010**, *17*, 17-36.
  66. Goldmann, A. S.; Tischer, T.; Barner, L.; Bruns, M.; Barner-Kowollik, C. Mild and modular surface modification of cellulose via hetero Diels-Alder (HDA) cycloaddition. *Biomacromolecules* **2011**, *12*, 1137-1145.
  67. Tischer, T.; Goldmann, A. S.; Linkert, K.; Trouillet, V.; Börner, H. G.; Barner-Kowollik, C. Modular Ligation of Thioamide Functional Peptides onto Solid Cellulose Substrates. *Advanced Functional Materials* **2012**, *22*, 3853-3864.
  68. Chen, G.; Tao, L.; Mantovani, G.; Ladmiral, V.; Burt, D. P.; Macpherson, J. V.; Haddleton, D. M. Synthesis of azide/alkyne-terminal polymers and application for surface functionalization through a [2 + 3] Huisgen cycloaddition process, "click chemistry". *The Royal Society of Chemistry, Soft Matter* **2007**, *3*, 732-739.
  69. Filpponen, I.; Kontturi, E.; Nummelin, S.; Rosilo, H.; Kolehmainen, E.; Ikkala, O.; Laine, J. Generic method for modular surface modification of cellulosic materials in aqueous medium by sequential "click" reaction and adsorption. *Biomacromolecules* **2012**, *13*, 736-742.
  70. Krouit, M.; Bras, J.; Belgacem, M. Cellulose surface grafting with polycaprolactone by heterogeneous click-chemistry. *European Polymer Journal* **2008**, *44*, 4074-4081.
  71. Tsubokawa, N.; Iida, T.; Takayama, T. Modification of cellulose powder surface by grafting of polymers with controlled molecular weight and narrow molecular weight distribution. *Journal of Applied Polymer Science* **2000**, *75* (4), 515-522.
  72. Chaudhuri, R. D.; Hermans, J. J. Grafting onto Cellulosic Macromolecules Through Chain Transfer to Mercaptoethyl Side Chains. Experimental Procedure and Results. *Journal of Polymer Science* **1960**, *XLVIII*, 159-166.
  73. Chaudhuri, R. D.; Hermans, J. Grafting onto cellulosic macromolecules through chain transfer to mercaptoethyl side chains. II. Mechanism of the process. *Journal of Polymer Science* **1961**, 373-381.

74. Penn, B. G.; Stannett, V. T.; Gilbert, R. D. Biodegradable Cellulose Graft Copolymers. Vinyl Addition-Type Graft Reaction. *Journal of Macromolecular Science* **1981**, *A16* (2), 481-486.
75. Kolb, H.; Finn, M.; Sharpless, K. Click chemistry: diverse chemical function from a few good reactions. *Angewandte Chemie International Edition* **2001**, *40*, 2004-2021.
76. Rosen, B. M.; Lligadas, G.; Hahn, C.; Percec, V. Synthesis of dendritic macromolecules through divergent iterative thio-bromo "Click" chemistry and SET-LRP. *Journal of Polymer Science: Part A: Polymer Chemistry* **2009**, *47*, 3940-3948.
77. Heinze, T.; Liebert, T. Chemical characteristics of cellulose acetate. *Macromolecular Symposia* **2004**, *208*, 167-237.
78. Mitchell, T. N.; Costisella, B. *NMR - From Spectra to Structures. An Experimental Approach*, 2nd ed.; Springer-Verlag Berlin Heidelberg: New York, 2004.
79. Oyama, T.; Naka, K.; Chujo, Y. Polymer Homologue of DMSO: Synthesis of Poly(ethylene sulfoxide) by Selective Oxidation of Poly(ethylene sulfide). *Macromolecules* **1999**, *32* (16), 5240-5242.
80. Gobran, R.; Larsen, R. Poly (ethylene sulfide). I. Unique seed polymerization technique-growth of "immortal" polymer. *Journal of Polymer Science. Part C* **1970**, *31*, 77-86.
81. Zahran, M.; Morsy, M.; Mahmoud, R. Grafting of acrylic monomers onto cotton fabric using an activated cellulose thiocarbonate-azobisisobutyronitrile redox system. *Journal of Applied Polymer Science*. **2004**, 1261-1274.
82. Aoki, D.; Teramoto, Y.; Nishio, Y. SH-containing cellulose acetate derivatives: preparation and characterization as a shape memory-recovery material. *Biomacromolecules* **2007**, *8* (12), 3749-3757.